

Dissertation zur Erlangung des Doktorgrades  
der Fakultät für Chemie und Pharmazie  
der Ludwig-Maximilians-Universität München

# **PHYSICAL PROPERTIES OF PROTEIN FORMULATIONS**

**VIRGINIE LE BRUN**

aus

Le Mans (Frankreich)

2009

## **Erklärung**

Diese Dissertation wurde im Sinne von § 13 Abs. 3 bzw. 4 der Promotionsordnung vom 29. Januar 1998 von Herrn Prof. Dr. Wolfgang Frieß betreut.

## **Ehrenwörtliche Versicherung**

Diese Dissertation wurde selbständig, ohne unerlaubte Hilfe erarbeitet.

München, am 22. Juni 2009.



---

Virginie Le Brun

Dissertation eingereicht am 22. Juni 2009

1. Gutacher: Prof. Dr. Wolfgang Frieß

2. Gutachter: Prof. Dr. Gerhard Winter

Mündliche Prüfung am 27. Juli 2009

## **ACKNOWLEDGMENTS**

I wish to express my gratitude to my supervisor Prof. Dr. Wolfgang Frieß for his valuable advice and guidance through this study. I would also like to include my gratitude to Dr. Stefan Bassarab, Dr. Patrick Garidel, Dr. Silke Mühlau, Heidrun Schott and Torsten Schultz-Fademrecht at Boehringer Ingelheim Pharma GmbH & Co. KG for their fundamental support of this work.

Boehringer Ingelheim Pharma GmbH & Co. KG is acknowledged for the supplying of materials and for the financial support.

I am deeply indebted to Andrea Eiperle, Matthias Heggy and Inge Miller at Boehringer Ingelheim Pharma GmbH & Co. KG and Dr. Armin Giese and Tobias Högen at the Center for Neuropathology and Prion Research of the Ludwig-Maximilians-University for helping with the experimental studies.

I am extremely grateful to all members of our research group for the friendly atmosphere and the numerous French breakfasts, especially to: Cornelius Pompe, Miriam Printz, Johannes Mathes, Frank Schaubhut, Lars Schiefelbein, Katja Schmid and the members of the “Bubble lab” Klaus Freitag, Stephan Schultes and Steliyan Tinkov.

I would specially like to thank Magali Delais, Melanie Hübner, Claudia Lewerenz and Nantharat Pearnchob for their friendship and support.

Finally I want to thank my parents, my sister Hélène, and Matthias for their love, encouragement and continuous support in all circumstances.

# TABLE OF CONTENTS

## CHAPTER 1

### APPLICATIONS OF THE OSMOTIC SECOND VIRIAL COEFFICIENT IN PROTEIN FORMULATIONS..... 1

1. CHALLENGES IN LIQUID PROTEIN FORMULATIONS.....	1
2. PROTEIN SOLUBILITY .....	2
3. PROTEIN ASSOCIATION AND AGGREGATION .....	4
3.1. <i>Self-association</i> .....	4
3.2. <i>Aggregation</i> .....	5
3.3. <i>Factors inducing protein aggregation / association</i> .....	7
3.3.1 External factors in protein formulation inducing protein aggregation / association .....	7
3.3.2. Internal factors in protein formulation inducing protein aggregation / association.....	7
3.4. <i>Prevention of protein aggregation</i> .....	9
4. PROTEIN-PROTEIN INTERACTIONS .....	9
4.1. <i>Osmotic second virial coefficient</i> .....	9
4.2. <i>Nature of protein-protein interactions</i> .....	10
4.2.1. Excluded volume.....	10
4.2.2. Electrostatic interactions .....	11
4.2.3. Van der Waals forces.....	13
4.2.4. Hydrogen bonding.....	13
4.2.5. Solvation forces.....	14
4.3. <i>Analytical methods for the determination of protein-protein interactions</i> .....	15
4.3.1. Methods adapted to the determination of $B_{22}$ .....	15
4.3.1.1. Membrane osmometry.....	16
4.3.1.2. Scattering methods .....	17
4.3.1.3. Sedimentation equilibrium by analytical ultracentrifugation.....	18
4.3.1.4. Self-interaction chromatography .....	19
4.3.2. Other techniques adapted to the analysis of protein-protein interactions.....	21
4.3.2.1. Dynamic light scattering .....	21
4.3.2.2. Surface plasmon resonance .....	21
4.3.2.3. Ultrasonic storage modulus measurements .....	22
4.3.2.4. Concluding remarks .....	23
5. APPLICATIONS OF $B_{22}$ IN PROTEIN FORMULATIONS .....	23
5.1. <i>Protein crystallization</i> .....	23
5.2. <i>Protein solubility</i> .....	24
5.3. <i>Protein stability</i> .....	25
5.4. <i>Protein viscosity</i> .....	27
6. OBJECTIVES OF THE THESIS .....	29
7. REFERENCES .....	30

## CHAPTER 2

### INSIGHTS IN LYSOZYME-LYSOZYME SELF-INTERACTIONS AS ASSESSED BY THE OSMOTIC SECOND VIRIAL COEFFICIENT ..... 39

1. INTRODUCTION.....	39
2. MATERIALS AND METHODS .....	41
2.1. <i>Materials</i> .....	41
2.2. <i>Methods</i> .....	42
2.2.1. Lysozyme immobilization .....	42
2.2.2. ATR-FTIR adsorption spectra and second derivatives .....	42
2.2.3. Determination of the osmotic second virial coefficient $B_{22}$ .....	43
2.2.4. Determination of the net lysozyme charge .....	44
2.2.5. Determination of protein solubility .....	44
3. RESULTS AND DISCUSSION.....	44
3.1. <i>Establishment of <math>B_{22}</math> measurement via SIC for lysozyme</i> .....	44
3.1.1. Lysozyme characterization after binding on chromatography particles.....	44
3.1.2. Chromatogram analysis: retention volume determination .....	45
3.1.3. Influence of chromatography parameters on $B_{22}$ of lysozyme .....	46
3.1.3.1. Flow rate .....	46
3.1.3.2. Lysozyme concentration .....	47
3.1.3.3. Effect of temperature.....	49
3.1.3.4. Storage stability of the functionalized chromatography column .....	51
3.2. <i>Influence of formulation parameters on <math>B_{22}</math> of lysozyme</i> .....	51
3.2.1. Effect of the protonation degree .....	51
3.2.2. Effect of ionic strength and different salts of the Hofmeister series .....	52
3.2.3. Effect of sucrose and glycerol .....	54
3.2.4. Effect of PEG molecular weight.....	56
3.3. <i>Correlation between <math>B_{22}</math> and protein solubility</i> .....	57
4. CONCLUSIONS .....	58
5. REFERENCES .....	60

## CHAPTER 3

### LYSOZYME INTERACTIONS IN THE DENATURED STATE DETERMINED BY SELF-INTERACTION CHROMATOGRAPHY ..... 65

1. INTRODUCTION.....	65
2. MATERIALS AND METHODS .....	66
2.1. <i>Materials</i> .....	66
2.2. <i>Methods</i> .....	67
2.2.1. Self-interaction chromatography .....	67
2.2.2. Microcalorimetry.....	67
2.2.3. Lysozyme stability .....	67
2.2.3.1. Stirring stress.....	67
2.2.3.2. Thermal stress .....	67
3. RESULTS AND DISCUSSION.....	68
3.1. <i>Protein interactions: native versus unfolded state</i> .....	68
3.1.1. Lysozyme unfolding conditions .....	68

3.1.2. Characterization of the lysozyme interactions.....	69
3.2. <i>Lysozyme stability studies</i> .....	71
3.2.1. Stirring stress.....	71
3.2.2. Thermal stress.....	72
4. CONCLUSIONS.....	74
5. REFERENCES.....	75

## CHAPTER 4

### EVALUATION OF THE OSMOTIC SECOND VIRIAL COEFFICIENT IN PROTEIN FORMULATION: A CASE STUDY OF A MONOCLONAL ANTIBODY..... 77

1. INTRODUCTION.....	77
2. MATERIALS AND METHODS.....	79
2.1. <i>Materials</i> .....	79
2.2. <i>Methods</i> .....	80
2.2.1 IgG1 immobilization.....	80
2.2.2. ATR-FTIR adsorption spectra and second derivates.....	80
2.2.3. Fluorescence spectroscopy.....	81
2.2.4. Determination of the osmotic second virial coefficient.....	81
2.2.5. Determination of the IgG1 net charge.....	82
2.2.6. Turbidity.....	82
2.2.7. Size exclusion high performance liquid chromatography.....	82
2.2.8. Microcalorimetry.....	82
2.2.9. Lyophilization.....	83
2.2.10. Viscosity.....	83
3. RESULTS AND DISCUSSION.....	83
3.1. <i>Establishment of <math>B_{22}</math> measurement via SIC for the IgG1</i> .....	83
3.1.1. Protein characterization after binding on chromatography particles.....	83
3.1.2. Chromatogram analysis: retention volume determination.....	85
3.1.3. Influence of chromatography parameters on $B_{22}$ of IgG1.....	86
3.1.3.1. Flow rate.....	86
3.1.3.2. Protein concentration.....	87
3.1.3.3. Temperature.....	89
3.1.3.4. Column stability.....	89
3.2. <i>Influence of formulation parameters on <math>B_{22}</math> of IgG1</i> .....	90
3.2.1. IgG1 protonation degree.....	90
3.2.2. Buffer composition.....	91
3.2.3. Salt concentration.....	92
3.2.4. Influence of amino acids.....	93
3.2.5. Mannitol and sucrose addition.....	94
3.3. <i>Is <math>B_{22}</math> a relevant predictive tool in protein formulation?</i> .....	98
3.3.1. Comparison of $B_{22}$ to protein solubility.....	98
3.3.2. Comparison of $B_{22}$ to thermal stability.....	99
3.3.2.1. Stability of 20 mg/ml IgG1 solutions.....	99
3.3.2.2. Stability of 170 mg/ml IgG1 solutions.....	102
4. CONCLUSIONS.....	108
5. REFERENCES.....	110

## CHAPTER 5

<b>LIMITS OF THE PROTEIN SOLUBILITY DETERMINATION BY PRECIPITATION WITH POLYETHYLENE GLYCOL .....</b>	<b>115</b>
1. INTRODUCTION.....	115
2. MATERIALS AND METHODS .....	117
2.1. <i>Materials</i> .....	117
2.2. <i>Solubility determination by precipitation</i> .....	117
3. RESULTS AND DISCUSSION.....	118
3.1. <i>Method optimization</i> .....	118
3.1.1. Molecular weight of PEG.....	118
3.1.2. IgG1 concentration.....	119
3.2. <i>Comparison of different IgG1 formulations with the precipitation method</i> .....	120
3.2.1. Influence of pH.....	120
3.2.2. Influence of buffer composition .....	121
3.2.3. Influence of amino acids and salts.....	122
3.3. <i>Method interpretation: extrapolation versus ranking</i> .....	124
4. CONCLUSIONS .....	125
5. REFERENCES .....	126

## CHAPTER 6

<b>EVALUATION OF FLUORESCENCE CORRELATION SPECTROSCOPY FOR PROTEIN FORMULATION DEVELOPMENT .....</b>	<b>128</b>
1. INTRODUCTION.....	128
2. MATERIALS AND METHODS .....	130
2.1. <i>Materials</i> .....	130
2.2. <i>Methods</i> .....	130
2.2.1. Binding to Alexa <sup>®</sup> dyes.....	130
2.2.2. FCS and FIDA measurements and analysis.....	131
2.2.3. Size exclusion high performance liquid chromatography (SE-HPLC).....	132
2.2.4. Turbidity.....	132
2.2.5. Dynamic light scattering.....	132
2.2.6. Light obscuration.....	132
3. RESULTS AND DISCUSSION.....	132
3.1. <i>Optimization of protein binding to Alexa<sup>®</sup> dyes</i> .....	132
3.2. <i>Evaluation of the FIDA method for the screening of protein formulations</i> .....	134
3.2.1. Optimization of the spiking ratio.....	134
3.2.2. Comparison of FCS to other analytical methods .....	136
4. CONCLUSIONS .....	137
5. REFERENCES .....	138

## CHAPTER 7

<b>SUMMARY .....</b>	<b>139</b>
----------------------	------------

## LIST OF ABBREVIATIONS

ATR	attenuated total reflection
AUC	area under the curve
B <sub>22</sub>	osmotic second virial coefficient
BCA	bicinchoninic acid
Bis-ANS	4,4'-dianilino-1,1'-binaphthyl-5,5' disulfonic acid
BSA	bovine serum albumin
C <sub>p</sub>	heat capacity
d <sub>H</sub>	hydrodynamic diameter
DLS	dynamic light scattering
D <sub>m</sub>	mutual diffusion coefficient
D <sub>s</sub>	self-diffusion coefficient
DSC	differential scanning calorimetry
EDTA	ethylenediaminetetraacetic acid
FCS	fluorescence correlation spectroscopy
FIDA	fluorescence intensity distribution analysis
FNU	formazine nephelometric units
FTIR	Fourier transform infrared spectroscopy
G'	storage modulus
G''	loss modulus
H	enthalpy
IFN-tau	interferon-tau
ITC	isothermal titrating calorimetry
k	Boltzmann's constant
μ <sub>2</sub> (solution)	chemical potential of the protein in solution
MAb	monoclonal antibody
M <sub>w</sub>	molecular weight of the protein
MWCO	molecular weight cut off
η	solution viscosity
η <sub>0</sub>	solvent viscosity
N <sub>A</sub>	Avogadro's number
NMR	nuclear magnetic resonance
Π	osmotic pressure
PBS	phosphate buffered saline



PEG	polyethylene glycol
pl	isoelectric point
R	gas constant
rh-GCSF	recombinant human granulocyte colony-stimulating factor
rhIL-1ra	recombinant human interleukin-1 receptor antagonist
$R_{\theta}$	Rayleigh ratio
S	solubility
SANS	small angle neutron scattering
SAXS	small angle X-ray scattering
SE-HPLC	size exclusion high performance liquid chromatography
SIC	self-interaction chromatography
SLS	static light scattering
SPR	surface plasmon resonance
T	absolute temperature
$T_m$	melting temperature
$W_{22}$	potential of mean force

---

## CHAPTER 1

### APPLICATIONS OF THE OSMOTIC SECOND VIRIAL COEFFICIENT IN PROTEIN FORMULATIONS

#### 1. CHALLENGES IN LIQUID PROTEIN FORMULATIONS

During the last decades the interest in protein therapeutics drastically increased. Because of their poor bioavailability by most routes, protein drugs are usually delivered intravenously. The subcutaneous route of delivery presents an alternative for products requiring frequent and chronic administration. Furthermore it may provide the opportunity for self-administration. The subcutaneous route limits the volume and thus contributes to the new challenge of reaching high protein concentration. High protein concentrations imply to challenge the protein solubility, to control the solution viscosity and to maintain the protein function, structure and chemical and physical stabilities (Shire *et al.*, 2004). Enhancing protein solubility can be achieved by additives or by modification of protein structure (Trevino *et al.*, 2008). The most frequent chemical reactions involving deamidation, aspartate isomerization, oxidation and peptide bond hydrolysis (Wang, 2005), usually have kinetics of low order concentration dependency and should thus not be enhanced at higher protein concentration. The major protein instability lies in physical instability, namely protein aggregation, which generates loss of protein activity, changes in protein pharmacokinetics but also safety problems as inducing immunogenicity (Hermeling *et al.*, 2004). Protein aggregation is a major concern since it depends on protein concentration contrary to chemical instability. Given that aggregation results from the association of protein molecules, measuring protein-protein interactions in solution could be relevant for the protein aggregation prediction. Since the 1990s the osmotic second virial coefficient ( $B_{22}$ ) has been extensively studied to measure such protein interactions in solution in order to determine the protein phase behavior and thus to screen protein crystallization conditions.

This review aims first to define the concepts of protein solubility, protein aggregation and protein interactions. The analytical methods to measure protein-protein interactions

in solution will be further described. Finally, the potential applications of B<sub>22</sub> in protein formulation will be discussed.

## 2. PROTEIN SOLUBILITY

According to the measurement conditions, two different types of protein solubility are distinguished (Trevino *et al.*, 2008). True or thermodynamic solubility refers to the concentration of the protein in solution, which is in equilibrium with a crystalline solid phase of that protein (Arakawa and Timasheff, 1985). In contrast, apparent solubility corresponds to the concentration of protein in a solution, which is in equilibrium with a solid amorphous precipitate of the same protein. True solubility is a thermodynamic characteristic of a protein involving the chemical potential of the molecule. When the chemical potential of the protein molecule in solution becomes greater than its chemical potential in solid phase, protein precipitates. Given that solutions exhibit non ideal behavior in the presence of large macromolecular solutes, the chemical potential of the protein in solution  $\mu_2(\text{solution})$  is related to the protein activity (Arakawa and Timasheff, 1985, Guo *et al.*, 1999):

$$\mu_2(\text{solution}) = \mu_2^\circ(\text{solution}) + RT \ln (\gamma_2 c_2) \quad (1)$$

where R is the gas constant, T is the absolute temperature,  $\mu_2^\circ(\text{solution})$  is the standard chemical potential,  $\gamma_2$  is the activity coefficient and  $c_2$  is the protein concentration in  $\text{g}\cdot\text{ml}^{-1}$ . Considering that protein in a crystalline phase is in thermodynamic equilibrium with the same protein in solution, equation 1 gives:

$$\mu_2(\text{crystal}) = \mu_2^\circ(\text{solution}) + RT \ln (\gamma_2 S) \quad (2)$$

where  $\mu_2(\text{crystal})$  is the chemical potential of the protein crystal and  $c_2$  has been replaced by the protein solubility S ( $\text{g}\cdot\text{ml}^{-1}$ ). Defining  $\Delta\mu_2 = \mu_2^\circ(\text{solution}) - \mu_2(\text{crystal})$ , protein solubility can be expressed as follows:

$$\gamma_2 S = \exp (-\Delta\mu_2 / RT) \quad (3)$$

Since  $\Delta\mu_2$  can not be experimentally determined, absolute protein solubility can not be predicted. The hanging drop technique is one of the more common approaches to determine the solubility limits of crystalline protein. This screening method identifies buffer conditions reaching high protein concentration without inducing its precipitation (Bagby *et al.*, 1997, Lepre and Moore, 1998). The initial protein solution having a concentration near to its solubility limit will be concentrated using an osmotic gradient. The slower the protein precipitates, the higher is its solubility. This method requires an adjustment of the initial solution parameters to obtain a time controllable precipitation.

In addition, it does not enable the quantification of the protein solubility, only a solubility ranking is possible.

The determination of the apparent protein solubility is more convenient in protein formulation. However, both solubility data, true and apparent solubilities, can not be compared. It has been observed that, under the same conditions, the solubility of a protein solution with an amorphous solid phase will be higher than the solubility of a protein solution with a crystalline solid phase (Guilloteau *et al.*, 1992, Ries-Kautt and Ducruix, 1989). Apparent solubility is commonly determined by one of the following three empirical methods (Trevino *et al.*, 2008): addition of lyophilized protein, concentration by ultrafiltration or induction of amorphous precipitation.

The first method consists of the addition of lyophilized protein to a solution until it becomes saturated and its solubility limit is reached. The insoluble part of the drug is then removed by centrifugation and protein solubility has been defined as the maximum amount of protein in the presence of specified co-solutes that is not sedimented by 30,000 g centrifugation for 30 min (Schein, 1990). This simple method presents some drawbacks, since the protein can be damaged by the freeze drying process that is preferentially performed without excipient.

As an alternative, the protein solution of interest can be concentrated by ultrafiltration in a microconcentrator having a suitable molecular weight cut-off. However, reaching high protein concentration can induce the formation of viscous solutions reducing the passage through the membrane. As the lyophilized protein based technique, the concentration method consumes a substantial protein quantity in cases of highly soluble proteins. In addition, the buffer solution composition can be changed during the concentration process due to the Donnan effect (Stoner *et al.*, 2004), causing an unequal partitioning of electrolytes in solution. Charged particles near the semi-permeable membrane may be not distributed evenly across the two sides of the membrane, when a differently charged substance is unable to pass across the membrane and creates an uneven electrical charge. This effect is amplified with increasing protein concentration.

A third approach consists of reducing protein solubility in some regular and quantitatively definable manner and extrapolating to protein solubility (Middaugh *et al.*, 1979). For this purpose an inert macromolecule such as polyethylene glycol (PEG) (Middaugh *et al.*, 1979, Stevenson and Hageman, 1995) or a salting-out salt such as ammonium sulfate (Trevino *et al.*, 2007) is added to the protein solution which induces attraction between protein molecules and thus protein precipitation. Protein precipitation is proportional to the quantity of precipitating agent added. Thus, protein solubility is extrapolated to the theoretical protein quantity in solution in

the absence of precipitating agent. The precipitation region typically begins at high concentration of precipitating agent (10% PEG 6000 or 0.4 M ammonium sulfate). Because it is necessary to determine the protein precipitation profile over a broad range of precipitating agent concentrations, this method requires large amounts of protein material. Moreover, the obtained solubility values are questionable, as they are seldom comparable to other solubility data measured by other techniques. Even though protein solubility is a fundamental characteristic of protein solution, its determination remains extremely challenging and is based on laborious analytical methods.

### **3. PROTEIN ASSOCIATION AND AGGREGATION**

Protein solubility refers to the concentration of monomers in solution. But proteins interact to form higher molecular weight species. The term of protein aggregation is frequently used incorrectly to summarize two different phenomena, namely protein self-association and protein aggregation. Protein self-association denotes the formation of small, soluble oligomers from a native species that are reversible upon simple dilution with buffer, whereas protein aggregation depicts any formation of irreversible oligomers from non-native species (Saluja and Kalonia, 2008).

#### **3.1. Self-association**

Self-association corresponds to the formation of dimers or oligomers from a native species resulting from relative weak non covalent protein interactions (Cromwell *et al.*, 2006) as for example observed in a monoclonal antibody (MAb) (Liu *et al.*, 2005). The reversibility can be indicative for the presence of an equilibrium between monomer and oligomer species that is shifted by changing the formulation conditions such as pH or decrease in protein concentration. Although their formation is reversible, associated species may have further consequences. Indeed, the associate re-dissolution depends on their rate of dissociation, which can be too slow for clinical use. In addition, reversible associates can lead to the formation of irreversible aggregates during storage by formation of covalent link (Cromwell *et al.*, 2006, Saluja and Kalonia, 2008). Thus, they can act as precursors of protein aggregation. Exemplarily, self-associates of recombinant human interleukin-1 receptor antagonist prone to self-association and dimerization by increasing protein concentration (Alford *et al.*, 2008a) were involved in the formation of aggregates under accelerated stability studies. In addition, self-association can induce an increase in solution viscosity (Liu *et al.*, 2005), causing serious problems in manufacturing of the formulation and applying to the patients.

Self-association is favored by a protein concentration increase, since the presence of numerous adjacent protein molecules acts as crowding agent. Because of the high volume occupancy in concentrated protein solutions, the probability that protein molecules come closer increases, which enhances the possibility of self-association (Saluja and Kalonia, 2008).

## 3.2. Aggregation

In contrast to self-association, aggregation is irreversible. Two main pathways conduct to protein aggregation. On the one hand, physical aggregation results from the noncovalent association of protein molecules that do not present changes in primary structure (Wang, 2005). On the other hand, chemical association occurs by formation of new covalent bonds between protein molecules. The most common chemical pathway lies on the formation or the exchange of disulfide bonds. Many chemical reactions can directly crosslink protein chains or change protein hydrophobicity of a protein, indirectly changing its aggregation behavior. Overall, both physical and chemical mechanisms can occur simultaneously. We will focus in our study on physical aggregation, as this mechanism is more closely related to self-association.

Physical protein aggregation results from the association of unfolded proteins. According to the Lumry-Eyring model, the native protein is transformed in a transitional protein species that is prone to associate and to form protein aggregate (Lumry and Eyring, 1954). The protein aggregation pathway occurs in three steps: (1) protein unfolding; (2) association of unfolded monomers in oligomers; and (3) nucleation, growth and condensation in aggregates (Roberts, 2007, Weiss *et al.*, 2009). Precursors of protein aggregation are formed by protein folding intermediates.

As the hydrophobic side chains of completely folded proteins are either mostly out of contact with water or randomly scattered, those species can hardly aggregate (Wang, 2005). Under destabilizing conditions the free energy of the native folded state will be increased to that of the unfolded state or partially unfolded state. If protein reaches the free energy barrier for folding, a higher equilibrium population of the partially unfolded and completely unfolded states will be resulted. These transition forms do not necessarily induce protein associates. Indeed, a conformational state that is thermodynamically distinct from the native state, but structurally similar to it, may be reached directly from the native state through thermal fluctuations. Even though these conformational states have a higher energy than the native state, they are separated from it only by a low energy barrier. They present local unfolding sites, which are limited to local perturbations, and are named locally unfolded monomers or native-like

monomers. These limited unfolded areas facilitate the attractive interactions and native-like protein aggregates result from this process. This model has been described for numerous proteins such as human lysozyme or human superoxide dismutase or human  $\beta$ 2-microglobulin (Chiti and Dobson, 2009). Only small changes of the protein native state are sufficient to influence the protein aggregation behavior, as a 4% increase in molecular diameter of recombinant human interferon- $\gamma$  was found sufficient to form the aggregation prone intermediate state (Saluja and Kalonia, 2008). The difference in energy between folded and unfolded states is weak and corresponds to about 10 k·cal·mol<sup>-1</sup>, which is comparable with the formation of approximately 10 hydrogen bonds or a net hydrophobic interaction of 10 CH<sub>3</sub> groups (Gitlin *et al.*, 2006). Because of the minor protein unfolding, the protein species involved in aggregation could be described as native (Chiti and Dobson, 2009) or native-like or partial unfolded (Weiss *et al.*, 2009), depending on the authors, and the aggregation process is consequently considered as native or non-native respectively.

Some degrees of unfolding are needed to facilitate aggregation since the process is initiated by the patches of contiguous hydrophobic groups in the intermediates. In addition, unfolded intermediates might more rapidly aggregate because of their higher rate of diffusion relative to the folded state (Wang, 2005). The transition from folded to unfolded monomer is in principle reversible, but the two states are not necessarily at equilibrium. In addition, the soluble oligomers can undergo conformational changes or internal structural rearrangement because their constitutive monomer units are not tightly bound to one another. The structural rearrangement stage is important in the formation of strong inter-protein  $\beta$ -sheet contacts to help to stabilize aggregates and make them irreversible. Protein-protein interactions are often more pronounced if irreversible alterations in protein secondary structure are observed (Garidel and Schott, 2006a, Garidel and Schott, 2006b), with the transition from  $\alpha$ -helix to  $\beta$ -sheet structure being the most prominent change (Chi *et al.*, 2003b). This conversion of reversible oligomer species to the smallest irreversible species corresponds to the nucleation step. The growth of soluble aggregates to larger higher molecular weight species is described by the term of polymerization. The expansion of the aggregates results from the addition of monomers, which are assumed to be partially unfolded, to irreversible oligomers. Finally, during the condensation, one or more monomers assemble to nucleated aggregates to form larger aggregates that are soluble or insoluble. Soluble aggregates may also aggregate with one another to form larger aggregates being soluble or insoluble.

Different mechanisms of non-native aggregation are differentiated with regard to the rate limiting step of the aggregation process: (1) unfolding-limited aggregation;

(2) association-limited aggregation or downhill polymerization; (3) aggregation by nucleation and growth; and (4) aggregation with condensation (Roberts, 2007). The unfolding-limited aggregation is only controlled by the unfolding thermodynamics, while the three other aggregation processes depend on two contributions, namely the unfolding thermodynamics and the association dynamics.

### **3.3. Factors inducing protein aggregation / association**

#### **3.3.1 External factors in protein formulation inducing protein aggregation / association**

Stress factors are well known to generate protein instability. Different kinds of simulations are commonly tested to stress protein stability comprising shaking, stirring, pumping, freezing / thawing or heating. Each technique induces a different stress for the tested protein and different forms of aggregates (Kiese *et al.*, 2008). The different agitation stresses induce shearing, interfacial effects, local thermal effects, and rapid motion of solutes in solution. Cavitation, corresponding to the rapid formation of voids and bubbles within the solution, can be an important effect as well (Mahler *et al.*, 2009). Temperature is the most important stress factor. At a temperature close to its melting point ( $T_m$ ), which is generally between 40 °C and 80 °C, the protein becomes unfolded or partially unfolded and is more able to aggregate. In addition, temperature affects reaction kinetics as the frequencies of molecular collision and hydrophobic interactions are increased (Chi *et al.*, 2003b, Wang, 2005). Furthermore, heat enhances protein chemical degradation, which can amplify protein aggregation by modifying the amino acid sequences and distorting the protein conformation (Wang, 2005).

#### **3.3.2. Internal factors in protein formulation inducing protein aggregation / association**

An important factor affecting protein interactions is the protein concentration in solution. Protein aggregation is concentration dependent, as increasing the protein concentration increases the total volume occupancy by protein molecules. This phenomenon is described as “macromolecular crowding”, and results from the sum of two contributions: (i) the excluded volume that depends only on the protein itself and corresponds to the repulsive interaction due to mutual penetrability; and (ii) forces either attractive or repulsive between the molecules at distance greater than steric contact, which is conditional on the solution conditions (Ellis and Minton, 2006, Minton, 2005). Protein crowding generates two opposite effects on protein aggregation. On the one hand, the crowding effect protects protein from unfolding,



since its molecular motion is restricted by the presence of the other protein molecules. Protein is thermodynamically stabilized by increasing protein concentration, as its secondary structure stability is probably increased by the decrease in solvent exposed surface area (Harn *et al.*, 2007). On the other hand, the volume occupancy brings the protein molecules closer and thus favors their self-assembly.

Protein can be stabilized or destabilized according to the formulation parameters. The most important factor is the formulation pH, as the protein sequence bears different ionizable amino acids (Shaw *et al.*, 2001). Thus, a protein molecule carries a different net charge as a function of pH difference from pI, which theoretically should be as high as possible to increase electrostatic repulsions between protein molecules. However, increasing the protein net charge induces also an increase of charge repulsion within the protein, which destabilizes the folded protein conformation, as the charge density of the folded protein is greater than of the unfolded protein (Chi *et al.*, 2003b). Consequently, the pH value is optimal for protein stability from a colloidal point of view, if its value is balanced and adjusted in a narrow range such that the protein net charge is high enough to induce electrostatic repulsions between charged macromolecules in solution but does not perturb the folded protein conformation.

The second factor of importance is the ionic strength, as increasing the solution ionic strength modulates electrostatic interactions between the charged groups within the protein but also between protein molecules. The salt effect is strongly pH dependent. As the addition of low concentration of ions shields electrostatic repulsive forces between protein molecules, the colloidal stability is usually reduced. Nevertheless, at high concentration, certain salts present a second property, namely to preferentially bind to the protein surface which could decrease the protein conformational stability. The salt effect has been classified by the Hofmeister in a series according to their strength in salting-in or salting-out at high concentration (Curtis and Lue, 2005). However, this series is empirical and do not fit to all proteins.

Furthermore, protein stability can be improved by the use of some excipients including amino acids, polyols and sugars, or surfactants. Polyols and sugars have been reported to be preferentially excluded from the protein surface (Lee and Timasheff, 1981). As these excipients are depleted in the protein domain, the protein surface is enriched in water. Most amino acids are known to stabilize protein also by preferential exclusion, however, two of them, arginine and histidine, are reported to stabilize protein due to their weak binding capacity (Arakawa *et al.*, 2007, Katayama *et al.*, 2006). Nonionic surfactants are added to prevent aggregation, despite that they often cause a reduction in the protein thermodynamic stability (Chi *et al.*, 2003b). Surfactants, which generally do not directly interact with protein (Hoffmann *et al.*, 2009),

inhibit interface induced aggregation by limiting the extent of protein adsorption notably at air / water interfaces and container surfaces.

### 3.4. Prevention of protein aggregation

Protein aggregation can be prevented by two different mechanisms. The first one consists of stabilizing the protein native conformation by increasing its thermodynamic stability, shifting the equilibrium away from unfolded or partially unfolded protein, the latter being also more prone for aggregation. Cosolutes that enhance the stability of protein native conformation are effective in reducing protein aggregation (Chi *et al.*, 2003b). The second strategy is based on improving the protein's colloidal stability by reducing attractive protein-protein interactions, as the aggregation process requires the assembly of molecules that should be spatially near enough to interact. This problem could be circumvented by decreasing protein mobility to reduce the number of collisions (Shire *et al.*, 2004). Thus, the restriction of the protein conformational flexibility could be reached by the removal of water by e.g. lyophilization. Consequently, the prevention of protein association and aggregation requires the management of both thermodynamic and colloidal stabilities. The preponderant protein stabilizing mechanism depends on the aggregation rate limiting step and thus differs for each protein, or at least for each protein class.

## 4. PROTEIN-PROTEIN INTERACTIONS

### 4.1. Osmotic second virial coefficient

Protein molecules behave like charged colloid particles in solution. At concentration higher than infinite dilution, molecules in solution interact and thus have a non-ideal behavior. The interaction between two same protein molecules can be described by the osmotic second virial coefficient ( $B_{22}$ ) (Curtis *et al.*, 1998):

$$B_{22} = - \frac{1}{2} \frac{N_A}{M_w^2} \int_0^\infty (e^{-W_{22}/kT} - 1) 4 \Pi r^2 dr \quad (4)$$

where  $N_A$  is Avogadro's number,  $M_w$  is the molecular weight of the protein,  $k$  is Boltzmann's constant,  $W_{22}$  is the potential of mean force between two interacting molecules and  $r$  is the intermolecular center to center distance. The factor of  $1/2$  corrects for double counting of an identical pair of molecules. The potential of mean force expresses the strength of protein-protein interactions and its negative derivate shows

the force between two protein molecules averaged over all possible orientations and configurations of the solute and solvent molecules.  $W_{22}$  corresponds to:

$$W_{22}(r) = W_{hs}(r) + W_{charge}(r) + W_{disp}(r) + W_{osm}(r) + W_{dip}(r) + W_{ass}(r) \quad (5)$$

where  $W_{hs}$  represents the hard sphere (excluded volume) potential,  $W_{charge}$  is the energetic potential comprising of charge-charge interactions,  $W_{disp}$  is the dispersion (van der Waals) attractive potential,  $W_{osm}$  is the attractive potential due to the osmotic effect of high salt concentrations,  $W_{dip}$  is the interactions arising from permanent and induced dipole moment of the molecules and  $W_{ass}$  is the square-well interaction that accounts for protein self-association. The square-well potential results from strong short-range interactions such as hydrophobic bonds, hydrogen bonds and ionic bonds (Curtis *et al.*, 1998).

$B_{22}$  reflects the extent and direction of the non-ideal solution property by its value and its sign respectively, and thus the interaction between two same protein molecules in solution. Positive  $B_{22}$  values reflect predominant repulsive intermolecular interactions, while negative  $B_{22}$  values are indicative of prevailing attractive interactions. Protein interactions that dominate  $B_{22}$  have been shown to be short range in nature (Saluja and Kalonia, 2008), typically persisting over a distance less than the diameter of the protein molecule at moderate ionic strength.

## 4.2. Nature of protein-protein interactions

Kauzmann (1959) described that hydrogen bonding, electrostatic forces, van der Waals forces, conformational entropy and hydrophobic interactions are the thermodynamic forces responsible for protein folding and stability. Except for hydrogen bonding, all these interactions are weak. Excluded volume is the only repulsive force in nature while all other interactions are attractive. The role of the different forces depends on the protein concentration. Indeed, in dilute solutions and in the presence of folded molecules, electrostatic and hydrophobic interactions are the major forces while hydrogen bonding, van der Waals interactions and excluded volume are minor. Increasing the protein concentration enhances the importance of steric interactions as well as van der Waals forces.

### 4.2.1. Excluded volume

The excluded volume represents the repulsive interaction due to mutual impenetrability between two protein molecules. Modeling the protein molecule as a sphere, the excluded volume is usually described as representing approximately 4 times the volume of the protein molecule. However the sphere modeling probably underestimates

the real contribution of the excluded volume. This one has been calculated to correspond up to 6.7 times the volume of the protein molecule because of the roughness of the surface and of the non perfect spherical volume (Neal and Lenhoff, 1995). In addition, a hydration layer is sometimes assumed to surround the molecules and effectively represents an additional excluded volume (Neal *et al.*, 1998). Increasing the protein concentration reduces the intermolecular center to center distance between two protein molecules and consequently amplifies the role of excluded volume. For example, an IgG2 molecule having a hydrodynamic diameter of 11 nm and formulated at 20 mg/ml is separated from a second IgG2 molecule by 12 nm. Enhancing the IgG2 concentration to 120 mg/ml reduces the surface-surface distance to 1 nm. Thus, higher protein concentration favors short range interactions due to the protein crowding (Saluja and Kalonia, 2008).

#### **4.2.2. Electrostatic interactions**

Electrostatic interactions are long range interactions that occur between charged groups separated by a distance comparable to the dimension of the protein (Gitlin *et al.*, 2006). A protein molecule reflects a network of interdependent charges that are involved in electrostatic interactions. The average charge density of native proteins is estimated to be 1.4 charged groups per 100 Å<sup>2</sup> of protein surface (Xu *et al.*, 1997). The calculation of electrostatic forces must consider the following protein features: (1) pK's of ionizable groups are shifted due to the desolvation and interactions with other charged groups; (2) charges are not uniformly distributed on the protein surface but are rather grouped in patches and consequently electric dipole and higher multipole moments may be large, so that their effects on interparticle interactions may be rather strong (Piazza, 2004); (3) solvent molecules and ions can be adsorbed; (4) because of the irregularity of the molecular surface, the potential profiles at boundaries of differing dielectric permitivities are amplified (Leckband and Sivasankar, 1999); and (5) the protein dielectric constant is not constant, since it depends on the specific region of high and low polarizability in the protein (Warshel *et al.*, 2006). The intrinsic dielectric constants of model proteins have been calculated using the Fröhlich-Kirkwood theory (Dominy *et al.*, 2004, Simonson and Brooks, 1996). Schematically, three protein regions are distinguished (Gitlin *et al.*, 2006). The core of the protein that regroups the hydrophobic regions of the protein has a low dielectric constant (between 2 and 4). The bulk solvent formed of water and buffer presents a high dielectric constant (about 80), whereas the surface of the protein with the surrounding layer possesses an intermediate value (between 10 and 20).

Whereas the pH determines the total charge of the protein, electrostatic interactions are supplemented by ion effects. Increasing the net charge favors electrostatic forces since the electrostatic free energy depends on the square of the net charge (Dill, 1990). The diminution of protein net charge is usually characterized by a decrease of repulsive interactions measured by  $B_{22}$  (Dumetz *et al.*, 2008, Tessier *et al.*, 2002). *Pseudomonas* amylase was particularly sensitive to the diminution of protein net charge. Approaching the pH value from its pI dramatically decreased  $B_{22}$  to reach strong negative values reflecting the lack of repulsive interactions (Valente *et al.*, 2006). Consequently, electrostatic contribution can not or only weakly influence protein stability near the pI. In a solution containing dissolved ions, a charge tends to repel ions of the same charge and to attract ions of the opposite charge. In the vicinity of the charge, ions of opposite charge are consequently highly concentrated as compared to the bulk solution. Thus, the electrostatic potential of the charge is weakened. Increasing the ionic strength enhances the number of counter-ions in solution, causing the diminution of the zeta potential. Obviously, electrostatic interactions usually decrease with addition of salt ions. It is reflected by a decrease of  $B_{22}$  values for many proteins. This decrease can be important in the case of lysozyme (Ahamed *et al.*, 2005, Tessier *et al.*, 2002) or moderate for IgG (Saluja *et al.*, 2007). Piazza and co-workers (2002) reported no salt influence on  $B_{22}$  of  $\beta$ -lactoglobulin. Nevertheless, the addition of high concentration of salt often raises the attractive potential. Indeed, at high concentration, the excluded volume of the salt ions is significant and the osmotic effect of salt can not be anymore neglected. This effect occurs when the intermolecular distance between solute molecules is reduced to the order of the salt ion size. Consequently, the salt ions are squeezed out of the region between the solute molecule (Wu *et al.*, 1998). Increasing ionic strength does not necessary diminish intermolecular charge-charge interactions especially if salt ions bind to the protein, changing the effective protein charge (Saluja and Kalonia, 2008). The ion binding effect can be manifested by increasing  $B_{22}$  values, but only at salt concentrations above 1 M (Piazza *et al.*, 2002). In addition, the presence of salt can diminish the pH effect. Indeed, increasing the sodium chloride concentration to 0.3 M neutralized the pH effect on chymotrypsinogen (Neal *et al.*, 1999). Above a solution ionic strength of 40 mM, the pH value did not influence the strength of protein-protein interactions of an IgG2 anymore (Saluja *et al.*, 2007). Obviously, the effect of pH and salt on electrostatic forces can not be systematically rationalized.

### 4.2.3. Van der Waals forces

Van der Waals as well as solvation and hydrogen bonding interactions belong to the class of short range effects that are less well understood than electrostatic forces. Van der Waals forces, including Keesom, Debye, and London contributions, arise from interactions among fixed or induced dipoles. They are generally attractive and active at relatively shorter distances as compared to charge-charge interactions. Because of their short range of action, van der Waals forces depend strongly on the shape of the interacting surfaces (Lenhoff, 2003). At the atomic level, the van der Waals potential is usually described by a relation of Lennard-Jones form or by the Lifshitz-Hamaker equation (Neal *et al.*, 1998). The magnitude of the van der Waals interactions can be characterized by the Hamaker constant. In both approaches, the van der Waals potential varies with the inverse of the sixth power of the intermolecular center to center distance (Saluja and Kalonia, 2008). Thus, the van der Waals contribution becomes more important by increasing protein concentration. Indeed, it becomes effective when the protein concentration is high enough to reduce the intermolecular center to center distance between two protein molecules to a value significantly less than the molecular diameter.

### 4.2.4. Hydrogen bonding

A hydrogen bond is a polar attractive interaction that occurs when a hydrogen atom is shared between generally two electronegative atoms (Jones and Thornton, 1996). The hydrogen attached to one electronegative atom of one molecule interacts with another electronegative atom of the same or different molecule. In proteins, hydrogen bonds are formed between the backbone oxygens and amide hydrogens. Hydrogen bonds are strong forces. They produce interatomic distances shorter than those induced by van der Waals forces and involve a limited number of interaction partners. They occur typically at a distance of 3 Å (Gitlin *et al.*, 2006). Hydrogen bonds have an important impact on protein structure, by stabilizing the protein secondary structure. They are involved in the formation of helix-coil as well as of intramolecular sheets. While a  $\beta$ -sheet can be expanded across the binding interface, an  $\alpha$ -helix can only be formed by a single continuous chain. Hydrogen bonding is very frequent in native proteins as only 11 % of all C=O groups and 12 % of all NH groups have no hydrogen bonds (Dill, 1990). Of all the hydrogen bonds involving the C=O groups, 43 % are to water, 11 % are to side chains and 46 % are to main chain NH groups. Of all the hydrogen bonds involving the NH groups, 21 % are to water, 11 % are to side chains and 68 % are to main chain C=O groups. Hydrogen bonds seem to be also important in the stabilization of the core structure of fibrils (Dobson, 2003).

However, interfacial hydrogen bonds are weaker than the intra-chain ones because of the hydrophilic surface of proteins and the rigid protein body binding. More water molecules mediate hydrogen bonds at the interfaces and thus control protein-protein interactions (Xu *et al.*, 1997).

#### 4.2.5. Solvation forces

Solvation forces arise from the ordering of solvent molecules around the protein molecule and act over 1 to 5 solvent molecule diameters (Rosenbaum and Zukoski, 1996). Thus, hydration forces refer to the solvation interaction of surfaces containing polar or charged groups (Curtis and Lue, 2005). The characteristics of the bulk water are only preserved at relatively large distances from the protein surface. The first hydration layer refers to the solvent layer that is directly in contact with the protein surface. Many water molecules of the first hydration layer form hydrogen bonds to polar protein atoms (Eisenhaber, 1999). The hydrogen bonds made with water have an energy similar to those between protein regions (Janin *et al.*, 2008). The second and next few layers in the hydration zone result from cooperative interaction between the solvent molecules and the first hydration layer (Yousef *et al.*, 1998a). The energy of protein surface group solvation is determined by the first hydration layer. A preferential interaction with salt and water is associated with a repulsive solvation potential of mean force, while preferential exclusion is associated with an attractive solvation potential of mean force (Curtis *et al.*, 2002b). Osmolyte effects that are known to stabilize proteins against denaturing stresses originate from their unfavorable interaction with protein. They are preferentially excluded from the immediate vicinity of the protein resulting in an increase in the Gibbs energy of the protein species, improving protein stability (Bolen and Baskakov, 2001). Stabilization by preferential exclusion by addition of sugars, polyols or amino acids is more efficient in the presence of salt for most model proteins. The presence of salt reduces repulsive electrostatic interactions. Under those primary unfavorable conditions,  $B_{22}$  of lysozyme has been reported to increase by addition of one of those previous excipients (Valente *et al.*, 2005b). This increase is probably due to the improvement of the protein compactness induced by the preferential exclusion phenomenon. As a consequence, the protein hydrophobicity could be reduced (Valente *et al.*, 2005a).

Hydrophobic interactions are considered as a type of solvation force. They arise from the interaction between two or more non polar molecules in a solvent and describe the tendency of two non polar solute molecules to come together in aqueous solutions (Jancso *et al.*, 1994). They are attractive in nature since the surface energy of non polar group in contact with solvent is greater than zero (Curtis *et al.*, 2002a).

In proteins, hydrophobic interactions are due to the presence of apolar amino acids, namely alanine, isoleucine, leucine, methionine, phenylalanine, proline, tryptophan and valine. Side chains containing apolar amino acids tend to associate and to be sequestered into a core, avoiding contact with water (Dill, 1990). Changing a polar amino acid of lysozyme with an apolar amino acid increases the attractive protein-protein interactions (Curtis *et al.*, 2002a). However, hydrophobic interactions at protein-protein interfaces have been described to be weaker than those in the protein interior (Tsai *et al.*, 1997) because of the higher frequency of apolar groups. The protein interface interactions should be mainly governed by hydrogen bonds and electrostatic interactions as higher proportions of charged and polar groups are located at the protein surface.

Hydrophobicity plays a dominant role in fixing protein tertiary and quaternary structures (Piazza, 2004) and hydrophobic interactions are considered as the main force driving protein folding. According to computer simulations, incorrectly folded proteins originate, apart from inappropriate burial of charge, from the interior/ exterior misdistribution of non polar residues (Dill, 1990). Protein aggregation is also driven to a large extent by hydrophobic forces similar to those driving protein folding in aqueous solution (Roberts, 2003, Chiti *et al.*, 2003). Protein aggregation comes with substantial changes in the tertiary structure. Partially unfolded protein molecules are in a more expanded state, which is more apolar and results in an increase in the exposure of hydrophobic sites at the subunit interface (Grillo *et al.*, 2001). The impact of physicochemical perturbations depends on the protein region on which changes occur (Chiti *et al.*, 2003). Aggregate formation should rather result from perturbation of physicochemical properties of the main chains than from alterations of specific interactions involving the side chains within the resulting aggregates.

### **4.3. Analytical methods for the determination of protein-protein interactions**

#### **4.3.1. Methods adapted to the determination of $B_{22}$**

Measuring  $B_{22}$  reflects the interactions between molecules in solution and thus the association dynamic of the solutes. During these last decades, different analytical methods have been developed to investigate protein-protein interactions. A part of these techniques are mathematically modeled to determine  $B_{22}$ . This mathematical modeling is only possible for protein solution having a restricted concentration, as the probability that interactions only occur between two same molecules goes down by increasing protein concentration. Even though  $B_{22}$  has been



historically first determined by membrane osmometry, it is currently most of the time measured by other analytical methods. Static light scattering (SLS) is the method mostly described in the literature and is considered as reference method. New methods have recently been developed to improve drawbacks of the traditional SLS method.

#### 4.3.1.1. Membrane osmometry

Zimm (1946) analyzed the dependency of the solute concentration with regard to the osmotic pressure. For the measurement of the osmotic pressure, the protein solution is separated from the protein-free solvent by a semi-permeable membrane. The external pressure that is applied to the protein side to suppress any mass transfer between the protein solution and the solvent corresponds to the osmotic pressure. William McMillan and Joseph Mayer (1945) derived a series of expansion for the osmotic pressure ( $\Pi$ ) in terms of concentration. Under the consideration that the higher order terms can be neglected, the non-ideality of  $\Pi$  is given as:

$$\Pi = R \cdot T \cdot c_p (1/M_w + B_{22} \cdot c_p) \quad (6)$$

where  $R$  is the gas constant,  $T$  is the absolute temperature,  $c_p$  is the protein concentration in mass units,  $M_w$  is the molecular weight of the protein. Supposing that the protein concentration is maintained at low range, plotting  $\Pi/RTc_p$  versus  $c_p$  gives a linear function, with a slope equal to  $B_{22}$  and an intercept at  $1/M_w$ .

The osmotic pressure of IgG and bovine serum albumin solutions has been measured at high concentration up to 400 mg/ml (Yousef *et al.*, 1998a, Yousef *et al.*, 1998b). Both protein solutions showed a linear increase of their osmotic pressure by increasing concentration up to 150 mg/ml. Above this concentration, their osmotic pressures were strongly enhanced showing changes in protein solution behavior that were not correlated to  $B_{22}$ . This different behavior was attributed and modeled to changes in protein hydration by increasing protein concentration.

The application of the osmotic pressure technique can be problematic at high protein concentration. Increasing protein concentration may induce the Donnan effect (Stoner *et al.*, 2004) and favor an unequal electrolyte partitioning across the two sides of the membrane. In addition, the membrane osmometry technique is time consuming and has a poor accuracy at low protein concentrations. Indeed, increasing protein concentration prolongs the time needed to reach pressure equilibrium. The inherent inaccuracy of  $B_{22}$  values measured by membrane osmometry comes from the inaccuracy in the osmotic pressure measurement, usually of about 1 % or in  $B_{22}$  of  $\pm 1 \cdot 10^{-4} \text{ mol} \cdot \text{ml} \cdot \text{g}^{-2}$  (Ahamed *et al.*, 2005).

### 4.3.1.2. Scattering methods

#### 4.3.1.2.1. Static light scattering

Macromolecular solutions that are irradiated with a light source scatter, diffract, reflect and absorb the light due to the presence of particles. The light scattering varies with regard to the nature and the size of macromolecules in solution and reflects interactions between individual macromolecule species. The measurement of  $B_{22}$  relies on the determination of the intensity of light scattered as a function of the protein concentration. Since protein molecules are usually much smaller than the wavelength of the incident light ( $< \lambda/20$ ), their scattering intensity is independent of the scattering angle. The Rayleigh ratio  $R_\theta$ , which is proportional to the scattered light intensity, is defined as follow (George and Wilson, 1994):

$$\frac{Kc_p}{R_\theta} = \frac{1}{M_w} + 2 B_{22} c_p \quad (7)$$

where  $c_p$  is the protein concentration,  $M_w$  is the molecular weight of the protein and  $K$  is an optical constant as defined below.

$$K = \frac{4 \Pi^2 n_0^2}{N_A \lambda^4} \left( \frac{dn}{dc_p} \right)^2 \quad (8)$$

and  $N_A$  is Avogadro's number,  $\lambda$  is the laser wavelength,  $n_0$  is the solvent refractive index and  $dn/dc_p$  is the refractive index increment of the protein. The Debye plot represents graphically  $Kc_p / R_\theta$  versus  $c_p$ . The slope of the graph corresponds to  $B_{22}$  while the intercept is equal to  $1/M_w$ . SLS is usually used at dilute protein concentrations, below 10 mg/ml, where the Rayleigh scattering theory for solutions is most applicable. SLS is considered as the reference method in  $B_{22}$  determination, even though it presents some disadvantages: (i) macromolecules and peptides can not be measured; (ii) large amounts of protein are required, since the ratio  $Kc_p / R_\theta$  should be determined over a large concentration range (typically between 1 and 10 mg/ml); and (iii) the data acquisition is slow. The classical equipment does not allow a systematic screening of protein interactions in solution. To remedy for these two last drawbacks, miniaturization of the measurement cell and a coupling to pump systems have been developed. The coupling of size exclusion high performance liquid chromatography (SE-HPLC) to SLS offers as advantages to separate the protein monomer from other species in solution and to simultaneously measure the protein concentration and its light scattering (Bajaj *et al.*, 2004). An alternative consists of the use of a programmable dual-syringe infusion pump to introduce into parallel flow cells a

protein solution of variable concentration and measure directly its concentration and light scattering (Attri and Minton, 2005).

By studies with concentrated protein solutions, information on molecular weights and assembly states can be obtained. In the absence of protein association, light scattering is proportional to the protein concentration. In the presence of weak reversible dimerization, the observed scattering is altered, causing the curvature characteristic of concentration dependent self-association. The presence of dimers in solution reduces significantly the  $Kc_p / R_\theta$  signal (Alford *et al.*, 2008b). Increasing curvature reflects the predominance of protein self-association, which influences the calculated molecular weight, since the species molecular weight becomes higher as the protein concentration rises (Minton, 2007).

#### 4.3.1.2.2. Other scattering methods

Small angle X-ray scattering (SAXS) and small angle neutron scattering (SANS) are both techniques of small angle scattering where the elastic scattering of X-ray and neutron respectively are recorded at very low angles (typically  $0.1^\circ$  to  $10^\circ$ ). SAXS and SANS studies have been carried out in a similar way as those with SLS,  $B_{22}$  calculation relying on the same principle. SAXS (Bonnete and Vivares, 2002) and SANS (Velev *et al.*, 1998) data have been consistent with SLS data. Interactions at high protein concentration (up to 500 mg/ml) can be also studied by SAXS (Tardieu *et al.*, 1999, Zhang *et al.*, 2007). SANS could be advantageous, as it allows the use of isotope substitution in the solvent as well as in the solute (Gripon *et al.*, 1997, Jancso *et al.*, 1994), which allows to gain information on the changes brought by the solute in the solvent structure in its neighborhood.

#### 4.3.1.3. Sedimentation equilibrium by analytical ultracentrifugation

The centrifugal force of the analytical ultracentrifuge produces a gradient in protein concentration across the centrifuge cell, where sedimentation is balanced by diffusion opposing the concentration gradients. The equilibrium concentration distribution across the cell is detected either by absorbance or refractive index. Thus, the sample concentration is characterized as a function of the axis of rotation and the apparent weight average molecular weight ( $M_{w,app}$ ) is determined according to the following equation (Liu *et al.*, 2005):

$$c(r) = c_0 \exp \left[ \frac{M_{w,app} (1 - \bar{V} \rho) \omega^2}{R T} \xi \right] \quad (9)$$

where  $c(r)$  is the protein concentration at the radial position  $r$ ,  $c_0$  is the initial loading protein concentration,  $\bar{v}$  is the partial specific volume,  $\rho$  is the buffer density,  $\omega$  is the angular velocity,  $\xi = (r^2 - r_0^2) / 2$ ,  $r_0$  is the reference radial position,  $R$  is the gas constant and  $T$  is the absolute temperature.  $B_{22}$  can be obtained using the following equation (10), where  $M_w$  is the weight average molecular weight and  $c_p$  the protein concentration.

$$\frac{1}{M_{w,app}} = \frac{1}{M_w} + 2 B_{22} c_p \quad (10)$$

Sedimentation equilibrium can be conducted at low protein concentration for the determination of  $B_{22}$  but also directly at high concentration (Alford *et al.*, 2008b). This second option is however more difficult to analyze because of the increasing non-ideality character. Different mathematical models have been proposed for the data interpretation. The method developed by Zorilla and co-workers (2004) is commonly accepted and is based on the integration of two components, because of the possibility of both types of interactions in solution (association and repulsive interactions).

#### 4.3.1.4. Self-interaction chromatography

Different chromatographic methods have been proposed for the determination of protein interactions based, for example, on size exclusion chromatography (Bloustine *et al.*, 2003) or hydrophobic chromatography (Gagnon *et al.*, 1997). Self-interaction chromatography (SIC) is the chromatographic method that is the most developed in the literature (Ahamed *et al.*, 2007, Ahamed *et al.*, 2005, Katayama *et al.*, 2006, Payne *et al.*, 2006, Tessier *et al.*, 2003, Tessier *et al.*, 2002, Valente *et al.*, 2006). SIC is based on the principle of weak affinity chromatography. First, the protein of interest is covalently immobilized on chromatography particles. Then, a pulse of the protein of interest, free in solution, is injected and passed through the chromatography column filled with the chromatography beads carrying the protein on their surface. The obtained elution profile reflects the interaction of immobilized protein with protein that is free in solution, under the assumption that the immobilized protein retains its native three-dimensional and secondary structure. The smaller the protein retention, the more repulsive are the protein-protein interactions. Furthermore, it is assumed that the protein is immobilized to the chromatography particles in a broad range of orientations, avoiding a side specific interaction, which would not be representative of the interaction between two protein molecules, both free in solution. Under these conditions the measured protein-protein interaction reflects the ensemble average interaction energy between two protein molecules under the investigated solution conditions.

The retention measurements are used to calculate the retention factor  $k'$  (equation 11) that measures the strength of interaction between the mobile phase protein and non-interacting species:

$$k' = \frac{V_o - V_r}{V_o} \quad (11)$$

where  $V_r$  is the volume required to elute the protein in the mobile phase and  $V_o$  is the retention volume of non-interacting species (e.g. acetone).  $B_{22}$  is related to the retention factor as follow (Tessier *et al.*, 2002, Zimm, 1946):

$$B_{22} = B_{HS} - \frac{k'}{\rho_s \Phi} \quad (12) \quad B_{HS} = \frac{16}{3} r^3 \frac{N_A}{M_w^2} \quad (13)$$

$\rho_s$  is the number of immobilized molecules per unit area and  $\Phi$  is the phase ratio, which is the total surface available to the mobile phase protein. The phase ratio can be interpreted using the work of DePhillips and Lenhoff (2000). This method uses a chromatographic system that can be equipped with an autosampler, allowing automation and thus a throughput screening. In addition, the quantity injected is reduced, limiting the protein consumption.

Even though  $B_{22}$  was historically first measured by membrane osmometry, SLS became rapidly the method of reference. Edsall and co-workers (1950) compared both methods with serum albumin and found comparable results. More recently, some studies demonstrated that SLS and SIC deliver equivalent results for different proteins such as lysozyme (Tessier *et al.*, 2002, Ahamed *et al.*, 2005) or BSA (Tessier *et al.*, 2004). However, Winzor *et al.* pointed out discrepancies between SLS and sedimentation equilibrium (Winzor *et al.*, 2007), which would arise from the measurements of different parameters. As SLS, membrane osmometry and SIC measurements provide only a single assessment of thermodynamic non-ideality, the  $B_{22}$  measurements includes the effects of nonideality arising from protein interactions with small molecules. Those methods consequently reflect the combined contributions of protein-protein and protein-buffer interactions, while sedimentation equilibrium would only determine protein-protein interactions. In addition, SLS and sedimentation equilibrium conveniently measure protein interactions at low as well as at high concentration.

### 4.3.2. Other techniques adapted to the analysis of protein-protein interactions

The previously described methods, membrane osmometry, SLS and sedimentation equilibrium, can characterize protein-protein interactions at low concentration as well as at high concentration. Few other methods, such as dynamic light scattering (DLS), surface plasmon resonance or ultrasonic storage modulus measurements can analyze protein-protein interactions especially at high concentration, even though they do not quantify  $B_{22}$ .

#### 4.3.2.1. Dynamic light scattering

DLS measures the diffusion coefficient of a solute molecule in solution that depends on its hydrodynamic diameter and interparticle repulsive and attractive forces (Saluja *et al.*, 2007). Solutions, in which interparticle forces are too weak to influence the diffusion of the solute, can be considered as ideal. The diffusion coefficient of molecules is then independent on the protein concentration and is named self-diffusion coefficient ( $D_s$ ) (Zhang and Liu, 2003). For non ideal solution, where protein interactions occur, DLS measures the mutual diffusion coefficient  $D_m$ .  $D_m$ , which varies with the protein concentration, can be represented by the following relationship:

$$D_m = D_s (1 + k_D c_p) \quad (14) \qquad D_m = \frac{k T}{3 \Pi \eta d_H} \quad (15)$$

where  $k_D$  is a measure of interparticle interaction,  $c_p$  is the protein concentration,  $k$  is Boltzmann's constant,  $T$  is the absolute temperature,  $\eta$  is the solution viscosity and  $d_H$  is the hydrodynamic diameter. The nature of protein interactions can be determined according to the value and the sign of  $k_D$ . A positive value of  $k_D$  reflects an increase in  $D_m$  over  $D_s$ , indicating a facilitation of the diffusion of the solute and thus repulsive interparticle interactions. On the contrary, a negative value of  $k_D$  corresponds to a decrease in  $D_m$  below  $D_s$ , revealing an inhibition of the solute diffusion and thus attractive interparticle interactions. The use of DLS presents some restrictions, as the method is only accurate to resolve size differences of fivefold or greater (Mahler *et al.*, 2009).

#### 4.3.2.2. Surface plasmon resonance

The surface plasmon resonance (SPR) technique measures any change in the resonance angle of light on a gold surface arising from changes in the refractive index of the surface up to 300 nm away (Phizicky and Fields, 1995). In practice, the interactions between immobilized protein molecules on a gold surface and free

protein molecules in solution are measured. When both protein species interact, the free protein is retained on the gold surface, modifying the refractive index and thus the resonance angle of impinging light. Since all proteins have the same refractive index, changes in signal can be linearly correlated to changes in protein concentration near the surface. Consequently, SPR is currently used to determine the specificity, the kinetics or the affinity of an interaction between two different molecules.

Tessier and co-workers (2008) have described a method derived from SPR called self-interaction nanoparticle spectroscopy. Protein molecules were adsorbed on the surface of gold nanoparticles and added to the solution of interest. Since the optical properties of gold nanoparticles depend on the interparticle distance, the detection of any changes in color of the gold suspensions, which can be followed by spectrophotometry, is correlated to the distance between the coated particles and consequently reflects the strength of protein-protein interactions. This shift in wavelength has been shown to correspond to solution conditions favorable to protein crystallization or weak attractive interactions. However, this method was only possible with acidic proteins at pH values above their pI. Since gold particles are negatively charged, the addition of positively charged protein, such as lysozyme at neutral pH, induces a non specific aggregation between the oppositely charged particles. This promising method needs first to be optimized to overcome the limitations of method sensitivity and protein species.

#### **4.3.2.3. Ultrasonic storage modulus measurements**

The flow properties of a solution result from the solution composition and the molecule properties in solution. Most of protein solutions exhibit non-Newtonian behavior caused by protein-protein interactions in solution; and their rheological properties depend on stress conditions applied. Studying the viscoelasticity of protein solutions by oscillatory experiments gives information on the nature of intermolecular interactions. Applying a sinusoidal oscillatory strain with an angular frequency ( $\omega$ ), the system undergoes changes in its structure that result in both loss and storage of the applied mechanical energy. If strong interactions between the structural elements occur in solution, some processes are unable to relax or rearrange on the timescale of the applied oscillation causing energy storage. Any movement of solvent or solute molecules or interactions between them is associated with a relaxation process characterized by a relaxation time ( $\tau$ ). Ultrasonic rheometer measures the storage ( $G'$ ) and loss ( $G''$ ) moduli of a solution, which characterize elastic storage and viscous loss of energy of the studied solution respectively, in relation to the angular frequency and the relaxation time (Saluja and Kalonia, 2008).

$$G' \propto \frac{\omega^2 \tau^2}{1 + \omega^2 \tau^2} \quad (16)$$

$$G'' \propto \frac{\omega \tau}{1 + \omega^2 \tau^2} \quad (17)$$

Since molecules can not relax within a single strain cycle at high frequency, the applied energy is stored and  $G'$  has a finite value. Macromolecules are in solution dynamic molecules whose conformation changes continuously and randomly. Since the rapidity of conformational changes depends on the interactions between solvent and solute molecules, the relaxation process usually exhibits a spectrum of relaxation times in concentrated macromolecule solutions. Thus, changes in  $G'$  can be measured and compared at a same and unique frequency with regard to solution conditions. An increase in storage modulus was shown to go with a diminution of repulsive interactions in solution (Saluja *et al.*, 2007).

#### 4.3.2.4. Concluding remarks

These alternative techniques characterize protein-protein interactions at high concentration. Except for the ultrasonic storage modulus, these methods consume a huge amount of protein. In addition, DLS is limited in resolution. Self-interaction nanoparticle spectroscopy is to date only possible with acidic protein and not sensitive enough to measure small differences in protein-protein interactions. Thus, ultrasonic storage modulus appears to be a more promising method characterizing protein interactions in solution. It is competitive to the other standard methods able to measure  $B_{22}$  as it reduces significantly the protein consumption.

## 5. APPLICATIONS OF $B_{22}$ IN PROTEIN FORMULATIONS

### 5.1. Protein crystallization

Conditions promoting protein crystallization are often found by trial and error screening methods. George and Wilson (1994) observed that for protein solutions which are suitable for crystallization growth,  $B_{22}$  falls in a narrow range between  $-1 \cdot 10^{-4}$  and  $-8 \cdot 10^{-4} \text{ mol} \cdot \text{ml} \cdot \text{g}^{-2}$ , corresponding to weak protein-protein attractive conditions. The solvent conditions can be designated as being “moderate poor” as they favor more protein-protein interactions than protein-solvent interactions. This narrow range that is referred as crystallization slot defines conditions favorable to post-nucleation protein crystal growth. If a  $B_{22}$  value is more negative than  $-8 \cdot 10^{-4} \text{ mol} \cdot \text{ml} \cdot \text{g}^{-2}$ , amorphous precipitation is induced. This crystallization slot has been confirmed with various proteins and many different crystallization solvent conditions (Berger *et al.*, 2005,



Bonnete and Vivares, 2002, Tessier *et al.*, 2003). Recently, Ahamed and co-workers (2007) successfully applied this technique to compare the phase behavior of a MAb to its  $B_{22}$  values in the presence of NaCl,  $(\text{NH}_4)_2\text{SO}_4$  and PEG. The MAb crystallization was found difficult, since very few  $B_{22}$  values were found to be negative under a large range of conditions. Adding high concentration of excipients induced a drastic decrease of  $B_{22}$ , leaving an extremely small window of crystallization.

However, the crystallization slot may vary with the protein size, as increasing the macromolecule size shifts the range of  $B_{22}$  values to the smallest  $B_{22}$  values of the crystallization slot (Bonnete and Vivares, 2002). Crystallization occurs in the presence of different chemicals such as salt or polyethylene glycol at high concentrations. The protein phase behavior predicted by  $B_{22}$  measurements was demonstrated to be in agreement with the adhesive hard sphere potential (Rosenbaum and Zukoski, 1996). This model describes protein interactions regarding two parameters, namely the effective size and the measure of the attractive interaction strength. Obviously, this result emphasizes the importance of short range attractive interactions in the protein phase behavior and the ability of  $B_{22}$  to describe them. Consequently,  $B_{22}$  can be used to identify solution conditions favorable to protein crystallization.

## 5.2. Protein solubility

Solubility and  $B_{22}$  data of various proteins have been compared in the literature experimentally as well as theoretically in order to establish the proper supersaturation conditions for protein crystal growth experiments. George and Wilson (1994) first pointed out that lysozyme solubility and  $B_{22}$  data depended in a similar manner on salt concentration and temperature. Guo and co-workers (1999) have shown that lysozyme  $B_{22}$  data were highly correlated to crystal lysozyme solubility values. Changes in  $B_{22}$  were reflected by changes in solubility for numerous variables such as salt type and concentration, pH or temperature. Plotting solubility versus  $B_{22}$  pointed to a linear correlation especially for the moderate to the higher solubilities, whereas non linearity was evident for the lower solubility data. A theoretical relation was established between  $B_{22}$  and the solubility  $S$  from a thermodynamic point of view (Guo *et al.*, 1999, Haas *et al.*, 1999):

$$B_{22} = (-\Delta\mu_2 / RT) \cdot (1 / 2M_2S) - (\ln S / 2M_2S) \quad (18)$$

where  $\Delta\mu_2 = \mu_2^0$  (solution) -  $\mu_2^0$  (solid),  $\mu_2^0$  (solution) is the chemical potential of the protein in solution,  $\mu_2^0$  (solid) is the chemical potential of the protein in a solid form (e.g. crystal),  $R$  is the gas constant,  $T$  is the absolute temperature,  $M_2$  is the molecular weight of the protein (denoted as 2) and  $S$  is the solubility expressed in  $\text{g}\cdot\text{ml}^{-1}$ .

The correlation between protein solubility and  $B_{22}$  was confirmed by other authors working with different protein models including ovalbumin (Ruppert *et al.*, 2001), equine serum albumin (Demoruelle *et al.*, 2002) and a 36 amino acid therapeutic peptide (Payne *et al.*, 2006).

### 5.3. Protein stability

Measuring  $B_{22}$  could be relevant for the prediction of protein aggregation as protein-protein interactions interfere in the aggregation process. The effect of pH, NaCl, sucrose and sorbitol on  $B_{22}$  of a *Pseudomonas* amylase was compared to the protein solubility and activity (Valente *et al.*, 2006). While  $B_{22}$  was strongly negative at pH 4.5, shifting the pH solution to 6 or adding NaCl, sorbitol or sucrose significantly improved  $B_{22}$  values with  $B_{22}$  becoming close to zero. Solution conditions enhancing  $B_{22}$  favored protein solubility and activity, except at conditions near the pI of amylase. For example, the addition of 20% sucrose in the presence of 1 % NaCl at pH 4.53 increased  $B_{22}$  from approx.  $-50$  to  $-5 \cdot 10^{-4} \text{ mol} \cdot \text{ml} \cdot \text{g}^{-2}$  and the amylase activity by a factor of 6. The enhancement of the amylase activity was probably related to the concentration increase.

The effect of buffer species on the stability of interferon-tau (IFN-tau) was compared to  $B_{22}$  determined by SIC (Katayama *et al.*, 2006). At pH 7 and 20 mM buffer, IFN-tau formulated at 1 mg/ml aggregated under thermal stress quicker in phosphate buffer than in Tris or histidine buffers. Histidine, which gave the better stabilization, improved the repulsive interactions between protein molecules. Even though histidine slightly improved  $B_{22}$  as compared to the other buffer species, its effect on IFN-tau was reported to be minor on the colloidal stability. Indeed, according to the complementary studies based on intrinsic tryptophan fluorescence monitoring and isothermal calorimetry, histidine additively appeared to weakly bind to the native state of IFN-tau, thereby shifting the equilibrium towards the native state of the protein and thus stabilizing it.

In another study, two different protein species, ovalbumin and an IgG2, prepared at a concentration of 7.5 mg/ml were incubated during 3 months at 37°C under various solution conditions to monitor the extent of protein aggregation (Bajaj *et al.*, 2006). Both proteins were pH sensitive. They aggregated at pH 4.0 but remained stable at pH 7.4.  $B_{22}$  of ovalbumin, measured by a derivative SLS method, was similar for all solution conditions tested, reflecting moderate protein attractive interactions.  $B_{22}$  of IgG2 was slightly negative at pH 7.4, showing moderate attractive interactions. No linear Debye plots could be obtained at pH 4.0 indicating self-association. Complementary circular dichroism studies revealed that both proteins were partially

unfolded at pH 4.0. As the initial step inducing protein aggregation was protein unfolding,  $B_{22}$  of native species could not be correlated to protein stability in this study. Similarly, the stability of recombinant human granulocyte colony-stimulating factor (rh-GCSF) was compared to the free energy of protein unfolding and  $B_{22}$  measured by SLS (Chi *et al.*, 2003a), representing the protein conformational and colloidal stability respectively. rh-GCSF formulated at 1.5 mg/ml was prone to aggregate at pH 7.0 when  $B_{22}$  of the native state was negative. At the opposite, it did not aggregate at pH 3.5 when  $B_{22}$  was positive. Under solution conditions where the rh-GCSF conformational stability dominated, the protein aggregation involved first the perturbation of the protein native structure. Controlling the free energy of protein unfolding could diminish protein aggregation. On the other hand, in solutions where colloidal stability was high, solution conditions favoring repulsive interactions reduced the rh-GCSF aggregation. Thus, protein aggregation was pointed out dependent on both colloidal and conformational stabilities.

Lastly, rhIL-1ra was investigated by sedimentation equilibrium and SLS studies demonstrated that the protein is prone to self-associate at high protein concentration (Alford *et al.*, 2008b). rhIL-1ra dimerization, which was controlled by solution ionic strength, was studied by sedimentation equilibrium to measure the dimer dissociation constants as a function of ionic strength. An expanded virial coefficient model based on membrane osmometry and SLS measurements was developed to differentiate the interactions in solution between monomer-monomer ( $B_{22}$ ), monomer-dimer ( $B_{23}$ ) and dimer-dimer ( $B_{33}$ ) regarding the calculated dimer dissociation constants.  $B_{22}$  and  $B_{33}$  were both positive over the ionic strength range tested. Only  $B_{23}$  had a negative coefficient, corresponding to attractive interactions between monomer-dimer in solution, and could be responsible for the self-association phenomenon. Even though the native state of rhIL-1ra was thermodynamically favored at high protein concentration (100 mg/ml) and low ionic strength, self-association accelerated the aggregate formation at 37°C (Alford *et al.*, 2008a). Indeed, seeding aggregates into the initial protein solution did not enhance the aggregate formation. Consequently, the colloidal stability was reduced due to the self-association phenomenon whose importance rises with increasing protein concentration.

Thus, measuring protein-protein interactions contributes to elucidate the mechanism of protein aggregation. As protein aggregation can occur via different pathways controlled either by protein unfolding or protein association,  $B_{22}$  can not systematically predict protein stability. Because of the variability of the aggregation rate limiting step, the study of protein unfolding thermodynamic parameters completes the information required to the comprehension of the aggregation phenomenon.

## 5.4. Protein viscosity

Higher protein concentration may induce an increase of solution viscosity (Shire *et al.*, 2004, Matheus, 2006, Harris *et al.*, 2004) and consequently disturb the protein application and delivery. The Mooney equation (Kanai *et al.*, 2008), which is an empirical model for non-interacting hard spheres, describes the viscosity of a concentrated protein solution as follows:

$$\eta = \eta_0 \cdot \exp \left( \frac{c [\eta]}{1 - (k/v) c [\eta]} \right) \quad (19)$$

where  $\eta$  is the solution viscosity,  $\eta_0$  is the solvent viscosity,  $c$  is the protein concentration,  $[\eta]$  is the intrinsic viscosity of the protein,  $k$  is the crowding factor and  $v$  is the Simha parameter that is a shape determining factor (being 2.5 for spherical particles and exceeding 2.5 for non-spherical particles). Thus, according to the equation 19, the protein solution viscosity increases with the protein concentration and is dependent on the macromolecular crowding effect through the impact of the excluded volume.

Obviously, solution viscosity is not only protein concentration dependent but also formulation and protein dependent. Indeed, some proteins including MAbs present low viscosity solutions at concentrations higher than 100 mg/ml (Dani *et al.*, 2007), enabling the solution syringeability for subcutaneous administration. Manipulating the solution conditions, such as ionic strength, buffer species or pH values, may reduce the viscosity of high concentrated MAb solutions (Liu and Shire, 2002 and 2004). In the presence of positively charged protein molecules, the addition of anions has been reported more efficient in viscosity reduction than the addition of cations (Kanai *et al.*, 2008, Matheus, 2006). The addition of electrostatic charges to a multiple charged protein affects its intrinsic viscosity, which could be described by the following relationship:

$$[\eta] = \frac{v (V_h N_A)}{M} \quad (20)$$

where  $V_h$  is the hydrated volume of the protein molecule,  $N_A$  is Avogadro's number and  $M$  is the protein molecular weight (Harding, 1997). The protein intrinsic viscosity is basically influenced by its shape and hydration. The addition of charges modifies the protein hydration by affecting the diffuse double layer surrounding the protein molecule and consequently the repulsion between the double layer of different molecules and the intermolecular repulsions.

Three different MAbs constructed from the same IgG1 human framework with  $\kappa$  light chain were compared regarding their solution viscosity, self-association and  $B_{22}$  both measured by sedimentation equilibrium (Liu *et al.*, 2005). Two of the MAbs presented similar properties, namely low solution viscosity and weak repulsive interactions independently of the solution conditions. The third MAb behaved differently. Its viscosity was highly dependent on protein concentration, pH and ionic strength. Self-association of the third MAb was so important that no  $B_{22}$  value could be extrapolated from the sedimentation equilibrium analysis. The higher solution viscosity and self-association phenomenon were caused by Fab-Fab interaction (Kanai *et al.*, 2008). The addition of salt to the third MAb formulation could reduce both viscosity and self-association.  $B_{22}$  became positive and comparable to the  $B_{22}$  values of the two other MAb (Liu *et al.*, 2005). Consequently, the reversible association of the third MAb was mediated mainly by electrostatic interactions of charged residues. Thus, positive  $B_{22}$  values corresponded to favorable conditions to reduce viscosity.

The viscosity of a macromolecule in solution can be expressed as a virial expansion, where the viscosity  $\eta$  can be related to the solvent viscosity  $\eta_0$  and protein concentration  $C$  ( $\text{g}\cdot\text{ml}^{-1}$ ) (Liu *et al.*, 2005, Shire *et al.*, 2004):

$$\eta = \eta_0 (1 + k_1 C + k_2 C^2 + \dots) \quad (21)$$

where  $k_1$  is related to the contribution from individual solute molecules,  $k_2$  and higher order are related to effects from interactions of two or more protein molecules and  $(k_1 C)$  is related to the intrinsic viscosity whereas  $(k_2 C^2 + k_3 C^3 + \dots)$  reflects the pairwise interactions or protein-protein interactions meaning charge-charge electrostatics, hydrophobic interactions and other weaker interactions including van der Waals and dipole-dipole interactions. Consequently,  $B_{22}$  could reflect the influence of  $k_2$  on viscosity and correlate to protein solution viscosity.

Thus,  $B_{22}$  is a potential multiple predictive tool in protein formulations. The description of protein-protein interactions has been shown to be relevant in the determination of protein crystallization, solubility and viscosity as well as in the control of protein stability.  $B_{22}$  can predict the protein phase behavior in a comparable manner as the hard sphere model, as both describe protein-protein interactions lying on the effective size and the short attractive interactions between molecules in solution. Obviously, the prediction of protein stability for example can not be managed with  $B_{22}$  only, as it depends as well very much on protein unfolding thermodynamic, which cannot be derived from  $B_{22}$  under the presented conditions.

## 6. OBJECTIVES OF THE THESIS

The development of protein formulations notably requires the control of protein solubility and protein association / aggregation. Managing protein interactions could help to predict the best conditions improving protein solubility and avoiding protein association. This work aimed to develop new analytical tools adapted to liquid protein formulation screening. These methods should be time saving and protein consumption reducing.

The first objective was to develop an analytical method characterizing protein interactions in solution.  $B_{22}$  was established with the self-interaction chromatography method. This method was attractive as it allowed a high through put screening with the possible automation of the apparatus. The measure of protein interactions may deliver substantial information on protein solubility, solution viscosity and risk of protein aggregation for a given solution composition. This method was implemented with (i) lysozyme as protein model, whose results were compared to those published in the literature; and (ii) a model therapeutic protein of type IgG1. Pharmaceutical excipients used in protein formulations were screened according to  $B_{22}$ . After the method implementation, the correlation of  $B_{22}$  to protein solubility and to protein aggregation was studied. Moreover, as physical protein aggregation involves partially unfolded protein molecules, a virial coefficient model under denaturing conditions was presented.

Alternative methods to  $B_{22}$  were evaluated to measure protein solubility and protein aggregation. For this purpose, the PEG precipitation method was explored as it was described in the literature as a relevant method for the quantification of protein solubility. This method was first optimized and subsequently evaluated for the protein solubility determination.

Furthermore, the monitoring of protein association / aggregation with fluorescence correlation spectroscopy (FCS) was tested. FCS is commonly used at low protein concentration to detect and to follow the formation of aggregates or amyloid fibrils. This method presented an interesting potential in protein formulation development as it is very sensitive and requires low amount of material. However, any sample dilution should be avoided to better reflect the protein association status in solution. The study of undiluted protein solution sample represented a challenge. The potential of FCS in protein formulation screening was finally explored.

## 7. REFERENCES

Ahamed, T., Esteban, B. N. A., Ottens, M., Van Dedem, G. W. K., Van Der Wielen, L. A. M., Bisschops, M. A. T., Lee, A., Pham, C., and Thommes, J. Phase behavior of an intact monoclonal antibody. *Biophysical Journal*, 93, 610-619 (2007).

Ahamed, T., Ottens, M., Van Dedem, G. W., and Van Der Wielen, L. A. Design of self-interaction chromatography as an analytical tool for predicting protein phase behavior. *Journal of Chromatography A*, 1089, 111-124 (2005).

Alford, J. R., Kendrick, B. S., Carpenter, J. F., and Randolph, T. W. High concentration formulations of recombinant human interleukin-1 receptor antagonist: II. Aggregation kinetics. *Journal of Pharmaceutical Sciences*, 97, 3005-3021 (2008a).

Alford, J. R., Kwok, S. C., Roberts, J. N., Wuttke, D. S., Kendrick, B. S., Carpenter, J. F., and Randolph, T. W. High concentration formulations of recombinant human interleukin-1 receptor antagonist: I. Physical characterization. *Journal of Pharmaceutical Sciences*, 97, 3035-3050 (2008b).

Arakawa, T., Ejima, D., Tsumoto, K., Obeyama, N., Tanaka, Y., Kita, Y., and Timasheff, S. N. Suppression of protein interactions by arginine: a proposed mechanism of the arginine effects. *Biophysical Chemistry*, 127, 1-8 (2007).

Arakawa, T., and Timasheff, S. N. Theory of protein solubility. *Methods in Enzymology*, 114, 49-77 (1985).

Attri, A. K., and Minton, A. P. New methods for measuring macromolecular interactions in solution via static light scattering: basic methodology and application to nonassociating and self-associating proteins. *Analytical Biochemistry*, 337, 103-110 (2005).

Bagby, S., Tong, K. I., Liu, D. J., Alattia, J. R., and Ikura, M. The button test: A small scale method using microdialysis cells for assessing protein solubility at concentrations suitable for NMR. *Journal of Biomolecular NMR*, 10, 279-282 (1997).

Bajaj, H., Sharma, V. K., Badkar, A., Zeng, D., Nema, S., and Kalonia, D. S. Protein structural conformation and not second virial coefficient relates to long-term irreversible aggregation of a monoclonal antibody and ovalbumin in solution. *Pharmaceutical Research*, 23, 1382-1394 (2006).

Bajaj, H., Sharma, V. K., and Kalonia, D. S. Determination of second virial coefficient of proteins using a dual-detector cell for simultaneous measurement of scattered light intensity and concentration in SEC-HPLC. *Biophysical Journal*, 87, 4048-4055 (2004).

Berger, B. W., Blamey, C. J., Naik, U. P., Bahnson, B. J., and Lenhoff, A. M. Roles of additives and precipitants in crystallization of calcium- and integrin- binding protein. *Crystal Growth and Design*, 5, 1499-1507 (2005).

Bloustine, J., Berejnov, V., and Fraden, S. Measurements of protein-protein interactions by size exclusion chromatography. *Biophysical Journal*, 85, 2619-2623 (2003).

Bolen, D. W., and Baskakov, I. V. The osmophobic effect: natural selection of a thermodynamic force in protein folding. *Journal of Molecular Biology*, 310, 955-963 (2001).

Bonnete, F., and Vivares, D. Interest of the normalized second virial coefficient and interaction potentials for crystallizing large macromolecules. *Acta Crystallographica Section D-Biological Crystallography*, 58, 1571-1575 (2002).

Chi, E. Y., Krishnan, S., Kendrick, B. S., Chang, B. S., Carpenter, J. F., and Randolph, T. W. Roles of conformational stability and colloidal stability in the aggregation of recombinant human granulocyte colony-stimulating factor. *Protein Science*, 12, 903-913 (2003a).

Chi, E. Y., Krishnan, S., Randolph, T. W., and Carpenter, J. F. Physical stability of proteins in aqueous solution: Mechanism and driving forces in nonnative protein aggregation. *Pharmaceutical Research*, 20, 1325-1336 (2003b).

Chiti, F., and Dobson, C. M. Amyloid formation by globular proteins under native conditions. *Nature Chemical Biology*, 5, 15-22 (2009).

Chiti, F., Stefani, M., Taddei, N., Ramponi, G., and Dobson, C. M. Rationalization of the effects of mutations on peptide and protein aggregation rates. *Nature* 424, 805-808 (2003).

Cromwell, M. E. M., Hilario, E., and Jacobson, F. Protein aggregation and bioprocessing. *AAPS Journal*, 8, E572-E579 (2006).

Curtis, R. A., and Lue, L. A molecular approach to bioseparations: Protein-protein and protein-salt interactions. *Chemical Engineering Science*, pp. 907-923, (2005).

Curtis, R. A., Prausnitz, J. M., and Blanch, H. W. Protein-protein and protein-salt interactions in aqueous protein solutions containing concentrated electrolytes. *Biotechnology and Bioengineering*, 57, 11-21 (1998).

Curtis, R. A., Steinbrecher, C., Heinemann, M., Blanch, H. W., and Prausnitz, J. M. Hydrophobic forces between protein molecules in aqueous solutions of concentrated electrolyte. *Biophysical Chemistry*, 98, 249-265 (2002a).

Curtis, R. A., Ulrich, J., Montaser, A., Prausnitz, J. M., and Blanch, H. W. Protein-protein interactions in concentrated electrolyte solutions. *Biotechnology Bioengineering*, 79, 367-380 (2002b).

Dani, B., Platz, R., and Tzannis, S. T. High concentration formulation feasibility of human immunoglobulin G for subcutaneous administration. *Journal of Pharmaceutical Sciences*, 96, 1504-1517 (2007).



Demoruelle, K., Guo, B., Kao, S. M., McDonald, H. M., Nikic, D. B., Holman, S. C., and Wilson, W. W. Correlation between the osmotic second virial coefficient and solubility for equine serum albumin and ovalbumin. *Acta Crystallographica Section D-Biological Crystallography*, 58, 1544-1548 (2002).

Dephillips, P., and Lenhoff, A. M. Pore size distributions of cation-exchange adsorbents determined by inverse size-exclusion chromatography. *Journal of Chromatography A*, 883, 39-54 (2000).

Dill, K. A. Dominant forces in protein folding. *Biochemistry*, 29, 7133-7155 (1990).

Dobson, C. M. Protein folding and misfolding. *Nature*, 426, 884-890 (2003).

Dominy, B. N., Minoux, H. and Brooks III, C. L. An electrostatic basis for the stability of thermophilic proteins. *Proteins: Structure, Function and Bioinformatics*, 57, 128-141 (2004).

Dumetz, A. C., Chockla, A. M., Kaler, E. W., and Lenhoff, A. M. Effects of pH on protein-protein interactions and implications for protein phase behavior. *Biochimica et Biophysica Acta*, 1784, 600-610 (2008).

Edsall, J. T., Edelhoch, H., Lontie, R., and Morrison, P. R. Light scattering in solutions of serum albumin: Effects of charge and ionic strength. *Journal of American Chemical Society*, 72, 4641-4656 (1950).

Eisenhaber, F. Hydrophobic regions on protein surfaces. *Perspectives in Drug Discovery and Design*, 17, 27-42 (1999).

Ellis, R. J., and Minton, A. P. Protein aggregation in crowded environments. *Biological Chemistry*, 387, 485-497 (2006).

Gagnon, P., Mayes, T., and Danielsson, A. An adaptation of hydrophobic interaction chromatography for estimation of protein solubility optima. *Journal of Pharmaceutical and Biopharmaceutical Analysis*, 16, 587-592 (1997).

Garidel, P., and Schott, H. Fourier-transform midinfrared spectroscopy for analysis and screening of liquid protein formulations, part 1: understanding infrared spectroscopy of protein. *BioProcess International*, 4, 40-46 (2006a).

Garidel, P., and Schott, H. Fourier-transform midinfrared spectroscopy for analysis and screening of liquid protein formulations. Part 2: detailed analysis and applications. *BioProcess International*, 4, 48-54 (2006b).

George, A., and Wilson, W. W. Predicting protein crystallization from a dilute solution property. *Acta Crystallographica D-Biological Crystallography*, 50, 361-365 (1994).

Gitlin, I., Carbeck, J. D., and Whitesides, G. M. Why are proteins charged? Networks of charge-charge interactions in proteins measured by charge ladders and capillary electrophoresis. *Angewandte Chemie*, 45, 3022-3060 (2006).

Grillo, A. O., Edwards, K. T., Kashi, R. M., Shipley, K. M., Hu, L., Besman, M. J., and Middaugh, C. R. Conformational origin of the aggregation of recombinant human factor VIII. *Biochemistry*, 40, 586-595 (2001).

Gripon, C., Legrand, L., Rosenman, I., Vidal, O., Robert, M. C., and Boue, F. Lysozyme-lysozyme interactions in under- and super-saturated solutions: a simple relation between the second virial coefficients in H<sub>2</sub>O and D<sub>2</sub>O. *Journal of Crystal Growth*, 178, 575-584 (1997).

Guilloteau, J., Ries-Kautt, M. M., and Ducruix, A. F. Variation of lysozyme solubility as a function of temperature in the presence of organic and inorganic salts. *Journal of Crystal Growth*, 122, 223-230 (1992).

Guo, B., Kao, S., McDonald, H., Asanov, A., Combs, L. L., and Wilson, W. W. Correlation of second virial coefficients and solubilities useful in protein crystal growth. *Journal of Crystal Growth*, 196, 424-433 (1999).

Haas, C., Drenth, J., and Wilson, W. W. Relation between the solubility of proteins in aqueous solutions and the second virial coefficient of the solution. *Journal of Physical Chemistry B*, 103, 2808-2811 (1999).

Harding, S. E. The intrinsic viscosity of biological macromolecules. Progress in measurement, interpretation and application to structure in dilute solution. *Progress in Biophysics & Molecular Biology*, 68, 207-262 (1997).

Harn, N., Allan, C., Oliver, C., and Middaugh, C. R. Highly concentrated monoclonal antibody solutions: Direct analysis of physical structure and thermal stability. *Journal of Pharmaceutical Sciences*, 96, 532-546 (2007).

Harris, R. J., Shire, S. J., and Winter, C. Commercial manufacturing scale formulation and analytical characterization of therapeutic recombinant antibodies. *Drug Development Research*, 61, 137-154 (2004).

Hermeling, S., Crommelin, D. J. A., Schellekens, H., and Jiskoot, W. Structure-immunogenicity relationships of therapeutics proteins. *Pharmaceutical Research*, 21, 897-903 (2004).

Hoffmann, C., Blume, A., Miller, I. and Garidel, P. Insights into protein-polysorbate interactions analyses by means of isothermal titration and differential scanning calorimetry. *European Biophysics Journal*, 38, 557-568 (2009).

Jancso, G., Cser, L., Grosz, T., and Ostanevich, Y. M. Hydrophobic interactions and small-angle neutron-scattering in aqueous-solutions. *Pure and Applied Chemistry*, 66, 515-520 (1994).

Janin, J., Bahadur, R. P., and Chakrabarti, P. Protein-protein interaction and quaternary structure. *Quarterly Reviews of Biophysics*, 41, 133-180 (2008).

Jones, S., and Thornton, J. M. Principles of protein-protein interactions. *Proceedings of the National Academy of Sciences*, 93, 13-20 (1996).

Kanai, S., Liu, J., Patapoff, T. W., and Shire, S. J. Reversible self-association of a concentrated monoclonal antibody solution mediated by Fab-Fab interaction that impacts solution viscosity. *Journal of Pharmaceutical Sciences*, 97, 4219-4227 (2008).

Katayama, D. S., Nayar, R., Chou, D. K., Valente, J. J., Cooper, J., Henry, C. S., Vander Velde, D. G., Villarete, L., Liu, C. P., and Manning, M. C. Effect of buffer species on the thermally induced aggregation of interferon-tau. *Journal of Pharmaceutical Sciences*, 95, 1212-1226 (2006).

Kauzmann, W. Factors in interpretation of protein denaturation. *Advances in Protein Chemistry*, 14, 1-63 (1959).

Kiese, S., Pappenberger, A., Friess, W., and Mahler, H. C. Shaken, not stirred: Mechanical stress testing of an IgG1 antibody. *Journal of Pharmaceutical Sciences*, 97, 4347-4366 (2008).

Leckband, D., and Sivasankar, S. Forces controlling protein interactions: theory and experiment. *Colloids and Surfaces B-Biointerfaces*, 14, 83-97 (1999).

Lee, J. C., and Timasheff, S. N. The stabilization of proteins by sucrose. *Journal of Biological Chemistry*, 256, 7193-7201 (1981).

Lenhoff, A. M. A natural interaction: Chemical engineering and molecular biophysics. *AiChE Journal*, 49, 806-812 (2003).

Lepre, C. A., and Moore, J. M. Microdrop screening: a rapid method to optimize solvent conditions for NMR spectroscopy of proteins. *Journal of Biomolecular NMR*, 12, 493-499 (1998).

Liu, J., Nguyen, M. D., Andya, J. D., and Shire, S. J. Reversible self-association increases the viscosity of a concentrated monoclonal antibody in aqueous solution. *Journal of Pharmaceutical Sciences*, 94, 1928-1940 (2005).

Liu, J., and Shire, S. J. Reduced-viscosity concentrated protein formulations. *WO Patent*, 30463A2 (2002).

Liu, J., and Shire, S. J. High concentration antibody and protein formulations. *US Patent*, 0197324A1 (2004).

Lumry, R., and Eyring, H. Conformation changes of proteins. *Journal of Physical Chemistry*, 58, 110-120 (1954).

Mahler, H. C., Friess, W., Grauschopf, U., and Kiese, S. Protein aggregation: Pathways, induction factors and analysis. *Journal of Pharmaceutical Sciences*, DOI 10.1002/jps.21566 (2009).

Matheus, S. Development of high concentration cetuximab formulations using ultrafiltration and precipitation techniques. Ludwig-Maximilians-University, Munich, (2006).

McMillan, W. G., and Mayer, J. E. The statistical thermodynamics of multicomponent systems. *Journal of Chemical Physics*, 13, 276-305 (1945).

Middaugh, C. R., Tisel, W. A., Haire, R. N., and Rosenberg, A. Determination of the apparent thermodynamic activities of saturated protein solutions. *Journal of Biological Chemistry*, 254, 367-370 (1979).

Minton, A. P. Influence of macromolecular crowding upon the stability and state of association of proteins: Predictions and observations. *Journal of Pharmaceutical Sciences*, 94, 1668-1675 (2005).

Minton, A. P. Static light scattering from concentrated protein solutions, I: General theory for protein mixtures and application to self-associating proteins. *Biophysical Journal*, 93, 1321-1328 (2007).

Neal, B. L., Asthagiri, D., Delev, O. D., Lenhoff, A. M., and Kaler, E. W. Why is the osmotic second virial coefficient related to protein crystallization? *Journal of Crystal Growth*, 196, 377-387 (1999).

Neal, B. L., Asthagiri, D., and Lenhoff, A. M. Molecular origins of osmotic virial coefficients of proteins. *Biophysical Journal*, 75, 2469-2477 (1998).

Neal, B. L., and Lenhoff, A. M. Excluded-volume contribution to the osmotic second-virial-coefficient for proteins. *AIChE Journal*, 41, 1010-1014 (1995).

Payne, R. W., Nayar, R., Tarantino, R., Del Terzo, S., Moschera, J., Di, J., Heilman, D., Bray, B., Manning, M. C., and Henry, C. S. Second virial coefficient determination of a therapeutic peptide by self-interaction chromatography. *Biopolymers*, 84, 527-533 (2006).

Phizicky, E. M., and Fields, S. Protein-protein interactions - methods for detection and analysis. *Microbiological Reviews*, 59, 94-123 (1995).

Piazza, R. Protein interactions and association: an open challenge for colloid science. *Current Opinion in Colloid & Interface Science*, 8, 515-522 (2004).

Piazza, R., Iacopini, S., and Galliano, M. BLGA protein solutions at high ionic strength: Vanishing attractive interactions and "frustrated" aggregation. *Europhysics Letters*, 59, 149-154 (2002).

Ries-Kautt, M. M., and Ducruix, A. F. Relative effectiveness of various ions on the solubility and crystal growth of lysozyme. *Journal of Biological Chemistry*, 264, 745-748 (1989).

Roberts, C. J. Kinetics of irreversible protein aggregation: Analysis of extended Lumry-Eyring models and implications for predicting protein shelf life. *Journal of Physical Chemistry B*, 107, 1194-1207 (2003).

Roberts, C. J. Non-native protein aggregation kinetics. *Biotechnology and Bioengineering*, 98, 927-938 (2007).

Rosenbaum, D. F., and Zukoski, C. F. Protein interactions and crystallization. *Journal of Crystal Growth*, 169, 752-758 (1996).

Ruppert, S., Sandler, S. I., and Lenhoff, A. M. Correlation between the osmotic second virial coefficient and the solubility of proteins. *Biotechnology Progress*, 17, 182-187 (2001).

Saluja, A., Badkar, A. V., Zeng, D. L., Nema, S., and Kalonia, D. S. Ultrasonic storage modulus as a novel parameter for analyzing protein-protein interactions in high protein concentration solutions: Correlation with static and dynamic light scattering measurements. *Biophysical Journal*, 92, 234-244 (2007).

Saluja, A., and Kalonia, D. S. Nature and consequences of protein-protein interactions in high protein concentration solutions. *International Journal of Pharmaceutics*, 358, 1-15 (2008).

Schein, C. H. Solubility as a function of protein-structure and solvent components. *Bio-Technology*, 8, 308-315 (1990).

Shaw, K. L., Grimsley, G. R., Yakovlev, G. I., Makarov, A. A., and Pace, C. N. The effect of net charge on the solubility, activity, and stability of ribonuclease Sa. *Protein Science*, 10, 1206-1215 (2001).

Shire, S. J., Shahrokh, Z., and Liu, J. Challenges in the development of high protein concentration formulations. *Journal of Pharmaceutical Sciences*, 93, 1390-1402 (2004).

Simonson, T. and Brooks III, C. L. Charge screening and the dielectric constant of proteins: Insights from molecular dynamics. *Journal of American Chemical Society*, 118, 8452-8458 (1996).

Stevenson, C. L., and Hageman, M. J. Estimation of recombinant bovine somatotropin solubility by excluded-volume interaction with polyethylene glycols. *Pharmaceutical Research*, 12, 1671-1676 (1995).

Stoner, M. R., Fischer, N., Nixon, L., Buckel, S., Benke, M., Austin, F., Randolph, T. W., and Kendrick, B. S. Protein-solute interactions affect the outcome of ultrafiltration/diafiltration operations. *Journal of Pharmaceutical Sciences*, 93, 2332-2342 (2004).

Tardieu, A., Le Verge, A., Malfois, M., Bonnete, F., Finet, S., Ries-Kautt, M. M., and Belloni, L. Proteins in solution: From X-ray scattering intensities to interaction potentials. *Journal of Crystal Growth*, 196, 193-203 (1999).

Tessier, P. M., Jinkoji, J., Cheng, Y. C., Prentice, J. L., and Lenhoff, A. M. Self-interaction nanoparticle spectroscopy: A nanoparticle-based protein interaction assay. *Journal of the American Chemical Society*, 130, 3106-3112 (2008).

Tessier, P. M., Johnson, H. R., Pazhianur, R., Berger, B. W., Prentice, J. L., Bahnson, B. J., Sandler, S. I., and Lenhoff, A. M. Predictive crystallization of ribonuclease A via rapid screening of osmotic second virial coefficients. *Proteins: Structure, Function, and Genetics*, 50, 303-311 (2003).

Tessier, P. M., Lenhoff, A. M., and Sandler, S. I. Rapid measurement of protein osmotic second virial coefficients by self-interaction chromatography. *Biophysical Journal*, 82, 1620-1631 (2002).

Tessier, P. M., Sandler, S. I., and Lenhoff, A. M. Direct measurement of protein osmotic second virial cross coefficients by cross-interaction chromatography. *Protein Science*, 13, 1379-1390 (2004).

Trevino, S. R., Scholtz, J. M., and Pace, C. N. Amino acid contribution to protein solubility: Asp, Glu, and Ser contribute more favorably than the other hydrophilic amino acids in RNase Sa. *Journal of Molecular Biology*, 366, 449-460 (2007).

Trevino, S. R., Scholtz, J. M., and Pace, C. N. Measuring and increasing protein solubility. *Journal of Pharmaceutical Sciences*, 97, 4155-4166 (2008).

Tsai, C. J., Lin, S. L., Wolfson, H. J., and Nussinov, R. Studies of protein-protein interfaces: a statistical analysis of the hydrophobic effect. *Protein Science*, 6 (1997).

Valente, J. J., Fryksdale, B. G., Dale, D. A., Gaertner, A. L., and Henry, C. S. Screening for physical stability of a *Pseudomonas* amylase using self-interaction chromatography. *Analytical Biochemistry*, 357, 35-42 (2006).

Valente, J. J., Payne, R. W., Manning, M. C., Wilson, W. W., and Henry, C. S. Colloidal behavior of proteins: effects of the second virial coefficient on solubility, crystallization and aggregation of proteins in aqueous solution. *Current Pharmaceutical Biotechnology*, 6, 427-436 (2005a).

Valente, J. J., Verma, K. S., Manning, M. C., Wilson, W. W., and Henry, C. S. Second virial coefficient studies of cosolvent-induced protein self-interaction. *Biophysical Journal*, 89, 4211-4218 (2005b).

Velev, O. D., Kaler, E. W., and Lenhoff, A. M. Protein interactions in solution characterized by light and neutron scattering: comparison of lysozyme and chymotrypsinogen. *Biophysical Journal*, 75, 2682-2697 (1998).

Wang, W. Protein aggregation and its inhibition in biopharmaceutics. *International Journal of Pharmaceutics*, 289, 1-30 (2005).

Warshel, A., Sharma, P. K., Kato, M., and Parson, W. W. Modeling electrostatic effects in proteins. *Biochimica et Biophysica Acta-Proteins and Proteomics*, 1764, 1647-1676 (2006).

---

Weiss, W. F., Young, T. M., and Roberts, C. J. Principles, approaches, and challenges for predicting protein aggregation rates and shelf life. *Journal of Pharmaceutical Sciences*, DOI 10.1002/jps21521 (2009).

Winzor, D. J., Deszczynski, M., Harding, S. E., and Wills, P. R. Nonequivalence of second virial coefficients from sedimentation equilibrium and static light scattering studies in protein solutions. *Biophysical Chemistry*, 128, 46-55 (2007).

Wu, J., Bratko, D., and Prausnitz, J. M. Interactions between like-charged colloidal spheres in electrolyte solutions. *Proceedings of the National Academy of Sciences*, 95, 15169-15172 (1998).

Xu, D., Tsai, C. J., and Nussinov, R. Hydrogen bonds and salt bridges across protein-protein interfaces. *Protein Engineering*, 10, 999-1012 (1997).

Yousef, M. A., Datta, R., and Rodgers, V. G. J. Free-solvent model of osmotic pressure revisited: Application to concentrated IgG solution under physiological conditions. *Journal of Colloid and Interface Science*, 197, 108-118 (1998a).

Yousef, M. A., Datta, R., and Rodgers, V. G. J. Understanding nonidealities of the osmotic pressure of concentrated bovine serum albumin. *Journal of Colloid and Interface Science*, 207, 273-282 (1998b).

Zhang, F., Skoda, M. W. A., Jacobs, R. M. J., Martin, R. A., Martin, C. M., and Schreiber, F. Protein interactions studied by SAXS: Effect of ionic strength and protein concentration for BSA in aqueous solutions. *Journal of Physical Chemistry B*, 111, 251-259 (2007).

Zhang, J., and Liu, X. Y. Effect of protein-protein interactions on protein aggregation kinetics. *Journal of Chemical Physics*, 119, 10972-10976 (2003).

Zimm, B. H. Application of the methods of molecular distribution to solutions of large molecules. *Journal of Chemical Physics*, 14, 164-179 (1946).

Zorrilla, S., Jimenez, M., Lillo, P., Rivas, G. N., and Minton, A. R. Sedimentation equilibrium in a solution containing an arbitrary number of solute species at arbitrary concentrations: theory and application to concentrated solutions of ribonuclease. *Biophysical Chemistry*, 108, 89-100 (2004).

## CHAPTER 2

# INSIGHTS IN LYSOZYME-LYSOZYME SELF-INTERACTIONS AS ASSESSED BY THE OSMOTIC SECOND VIRIAL COEFFICIENT

## 1. INTRODUCTION

Lysozyme is a compact globular protein presenting a catalytic enzymatic activity that has been extensively studied under its native as well denatured states. This model protein has been used to determine protein solubility, aggregation pathway or crystallization. Lysozyme crystallization has been particularly widely described by measuring protein interactions in solution that were reflected in the osmotic second virial coefficient ( $B_{22}$ ).

Various chromatography based techniques have emerged in the last years in order to characterize protein-protein interactions (Bajaj *et al.*, 2004, Beeckmans, 1999, Gripon *et al.*, 1997a, Patro and Przybycien, 1996). The concept behind this approach is related to studies and observations made many years ago. Zimm (1946) published a paper entitled “application of the methods of molecular distribution to solutions of large molecules”, where he stated that the objective of statistical mechanics was to link the knowledge of solution thermodynamics to the properties of the molecules that composed the solution. It was recognized that the large deviations from Raoult’s law, which were especially observed for “large” solutes like polymers and proteins, were related to non-ideal properties of the solutes and this could be accounted for by means of methods using continuous molecular distributions functions. The outcome of this investigation was the ability to interpret and better understand thermodynamic data derived from protein solutions. The thermodynamic property examined by Zimm was the osmotic pressure, and the different molecular interactions between the solutes in solution were considered. The dependency of the concentration with regard to the osmotic pressure was analyzed. McMillan and Mayer (1945) derived a series of expansion for the osmotic pressure ( $\Pi$ ) in terms of concentration. Under the consideration that the higher order terms can be neglected, the non-ideality of  $\Pi$  is given as:

$$\Pi = R \cdot T \cdot c_p (1/M_w + B_{22} \cdot c_p) \quad (1)$$



where  $R$  is the gas constant,  $T$  is the absolute temperature,  $c_p$  is the protein concentration in mass units,  $M_w$  is the molecular weight of the protein and  $B_{22}$  is the osmotic second virial coefficient. The parameter  $B_{22}$  reflects the extent and direction of the non-ideal solution property, and thus protein-protein interactions.

Various molecular theories of fluids can be used to develop a mean force expression for describing protein-protein interactions. The application of chromatography methods like self-interaction chromatography (SIC) (Payne *et al.*, 2006, Tessier *et al.*, 2002, Winzor *et al.*, 2007) requires the correlation of the osmotic coefficient of diluted to concentrated aqueous solution conditions (Haynes *et al.*, 1992). Rosenberger and co-workers have shown by means of static and dynamic light scattering for undersaturated and supersaturated lysozyme solutions that  $B_{22}$  values measured at low solution concentrations, which are prone for the formation of crystals, are indicative for supersaturated solution conditions (Muschol and Rosenberger, 1995, 1996 and 1997, Rosenberger *et al.*, 1996). Using the adhesive sphere potential along with  $B_{22}$  data for modeling protein interactions, the group of Rosenbaum and co-workers could construct the lysozyme phase boundary (Rosenbaum *et al.*, 1996, Rosenbaum *et al.*, 1999, Rosenbaum and Zukoski, 1996). These results showed, using simple fluid theory, that  $B_{22}$  is a reliable parameter for the prediction of solution conditions favorable for protein crystallization.

In contrast to the typical  $B_{22}$  target, i.e. the optimization of protein crystallization solution conditions, in the presented study, solution conditions that minimize attractive protein-protein interactions have to be identified, in order to avoid protein precipitation and aggregation. The procedure for the determination of the osmotic second virial coefficients as derived from SIC can be briefly summarized as follow. First, the protein of interest is covalently immobilized on chromatography particles. Then, a pulse of the protein of interest, free in solution, is injected and passed through the chromatography column filled with the chromatography beads carrying the protein on their surface. The obtained elution profile reflects the interaction of immobilized protein with protein that is free in solution, under the assumption that the immobilized protein retains its native three-dimensional and secondary structure. Furthermore, it is assumed that the protein is immobilized to the chromatography particles in a broad range of orientations, avoiding a side specific interaction, which will not be representative for the interaction between two protein molecules, both free in solution. Under these conditions the measured protein-protein interaction reflects the ensemble average interaction energy between two protein molecules under the investigated solution conditions.

The influence of various excipients with regard to protein-protein interactions can be screened using an automated chromatography system. Thus, the effectiveness of

formulation solutions, containing e.g. different excipients at varying concentrations, can easily be assessed. Solution conditions reducing attractive protein-protein interactions are characterized by a reduction of the retention volume, whereas the opposite is the case for solution conditions favoring attractive protein-protein interactions.

The following solution conditions were investigated with regard to lysozyme-lysozyme interactions: (i) pH-value (protonation degree); (ii) ionic strength and differences between various salts of the Hofmeister series; (iii) pharmaceutical excipients (sucrose, glycerol); and (iv) PEG qualities of different molecular weight. In addition, the effect of chromatography bead surface coverage and temperature on the osmotic second virial coefficient was studied. Furthermore, the storage stability of the functionalized chromatography particles was investigated. In addition,  $B_{22}$  a correlation to protein solubility was tested.

## **2. MATERIALS AND METHODS**

### **2.1. Materials**

Lysozyme from chicken egg white (135500 U/mg cryst.) was obtained from Serva (Heidelberg, Germany), Toyopearl AF Formyl 650M from Tosoh Bioscience (Stuttgart, Germany), potassium phosphate, sodium chloride, magnesium chloride, ammonium chloride, glacial acetic acid and sodium cyanoborohydride from Merck (Darmstadt, Germany), PEG 4000 and PEG 6000 from Merck-Schuhardt (Hohenbrunn, Germany), potassium chloride from Caelo (Hilden, Germany), PEG 400 from Fluka (Buchs, Switzerland), ethanolamine from VWR Prolabo (Fontenay sous bois, France), citric acid monohydrate from Roth (Karlsruhe, Germany), ammonium sulfate and glycerol from Grüssing Diagnostika Analytika (Filsum, Germany), sodium sulfate from Riedel-de-Häen, Seelze, Germany), potassium sulfate from J.T. Baker (Deventer, Netherlands) and BCA-assay Uptima from Interchim (Montluçon, France).

The pH of the solutions was adjusted using hydrochloric acid or sodium hydroxide and measured with a pH meter Inolab level 1 from WTW (Weilheim, Germany). The protein concentrations were evaluated with an UV-photometer UV1 from Thermo Spectronic (Dreieich, Germany).

## 2.2. Methods

### 2.2.1. Lysozyme immobilization

3 ml Toyopearl AF-Formyl 650M particles were washed on a glass frit with a 0.2  $\mu\text{m}$  hydrophilic polyethersulfone membrane filter with first 250 ml de-ionized water and secondly with 50 ml of 0.1 M potassium phosphate buffer pH 7.5. The washed particles were recovered and mixed to 10 ml lysozyme solution (6.5 mg/ml in 0.1 M potassium phosphate buffer pH 7.5) and 90 mg sodium cyanoborohydride used as activator of protein binding. The suspension was mixed over night ( $\approx 12$  h) on a rotary mixer. At the end of the coupling reaction the particles were washed with 200 ml of 0.1 M potassium phosphate buffer. After recovery they were added to 15 ml of 1 M ethanolamine pH 8.0 and 20 mg sodium cyanoborohydride to cap the remaining matrix reactive groups. The suspension was mixed on a rotary mixer during 4 h. At the end of the reaction the particles were washed with 200 ml of 1 M sodium chloride solution pH 7.0 to remove any unbound material. The amount of bound protein was determined by analyzing the absorbance of the initial protein solution and the wash solutions (A280), and by determining the protein quantity immobilized on the matrix by bicinchoninic acid (BCA) assay.

The chromatography particles were prepared in the form of a 50 % slurry in 1 M NaCl, 5 mM acetic acid solution pH 4.5. Approximately 2.5 ml slurry was packed in a Tricorn<sup>®</sup> 5/50 column (GE Healthcare, Uppsala, Sweden) with the same buffer 1 M NaCl, 5 mM acetic acid buffer pH 4.5 at a flow rate of 3 ml/min during 15 min using a FPLC system (Äkta Purifier, GE Healthcare, Uppsala, Sweden). At the end of the packing procedure the flow-rate was maintained at 0.75 ml/min during at least 30 min. The column integrity was tested by injecting 50  $\mu\text{l}$  of 1 % acetone solution. Columns were stored at 4 °C in a 5 mM sodium phosphate buffer pH 7.0 containing 0.05 % sodium azide.

### 2.2.2. ATR-FTIR adsorption spectra and second derivatives

Fourier Transform Infrared (FTIR) spectroscopy measurements were conducted with a Tensor 37 spectrometer (Bruker Optics, Ettlingen, Germany). Filtered samples were dried overnight at room temperature and measured by the attenuated total reflection (ATR) technique with the MVP unit at 20 °C. Each sample measurement was the average of 120 scans and was measured 3 times. The spectra were collected from 4000 to 1000  $\text{cm}^{-1}$  with a 4  $\text{cm}^{-1}$  resolution. The particle spectrum was manually subtracted from the bound protein particle spectrum and the protein spectra were further processed by vector normalization on the amide I band.

### 2.2.3. Determination of the osmotic second virial coefficient $B_{22}$

All mobile phase solutions were buffered with 5 mM acetic acid at pH 3.0 and 4.5 or 5 mM sodium phosphate at pH 6-8. Lysozyme was dissolved in the studied solutions at 20 mg/ml.  $B_{22}$  measurements were realized with a FPLC Äkta Purifier system equipped with an UV detector (A280). Before each run the column was equilibrated with 10 ml of protein free mobile phase. The column dead volume was determined with the 1 % acetone solution injection. All experiments were carried out at 25 °C and at a flow rate of 0.75 ml/min. 10  $\mu$ l sample was injected; each sample was measured 6 times. Chromatogram peaks were analyzed with the UNICORN<sup>®</sup> software (GE Healthcare, Uppsala, Sweden). The retention volume was determined at the peak maximum. The retention measurements were used to calculate the retention factor  $k'$  (equation 2) that measures the strength of interaction between the mobile phase protein and non-interacting species:

$$k' = \frac{V_o - V_r}{V_o} \quad (2)$$

$V_r$  is the volume required to elute the protein in the mobile phase and  $V_o$  the retention volume of non-interacting species (e.g. acetone).  $B_{22}$  is related to the retention factor as follows (Tessier *et al.*, 2002, Zimm, 1946):

$$B_{22} = B_{HS} - \frac{k'}{\rho_s \cdot \Phi} \quad (3) \quad B_{HS} = \frac{16}{3} \cdot r^3 \cdot \frac{N_A}{M_2^2} \quad (4)$$

$\rho_s$  is the number of immobilized molecules per unit area,  $\Phi$  is the phase ratio, which is the total available surface available to the mobile phase protein,  $r$  is the protein radius,  $N_A$  is the Avogadro's number and  $M_2$  is the protein (index 2) molecular weight.  $\rho_s$  was calculated by dividing the immobilized concentration by the porosity (0.811 for Toyopearl AF Formyl 650M) and the phase ratio of one lysozyme molecule. As lysozyme has a radius of 1.55 nm, the following phase ratios of lysozyme were taken: 20.9 m<sup>2</sup>/ml for  $\Phi$  (1.55 nm) and 16.9 m<sup>2</sup>/ml for  $\Phi$  (4.65 nm) (DePhillips and Lenhoff, 2000). The first value corresponds to the phase ratio of one lysozyme molecule that was used to determine  $\rho_s$ , whereas the second value represents the phase ratio of three molecules, which reflects two molecules immobilized and one free molecule and corresponds to the  $\Phi$  value in the equation 3.

### 2.2.4. Determination of the net lysozyme charge

The net lysozyme molecule charge was calculated for the amino acid sequence of lysozyme from white chicken egg (EC 3.2.1.17) with the EMBOSS-software (Rice *et al.*, 2000) based on single chain and 4 disulfide bonds.

### 2.2.5. Determination of protein solubility

350  $\mu$ l of buffer solution were added to 100 mg lysozyme powder. The samples were first continually stirred during 24 h at 25 °C to facilitate the powder dissolution and then centrifuged at 20,000 g during 1 h. After correction of the pH shift, the samples were stirred a second time 12 h at 25 °C and finally centrifuged at 20,000 g during 1 h. Lysozyme concentration was measured by UV spectroscopy at 280 nm with an extinction coefficient of 2.63 ml  $\cdot$  mg<sup>-1</sup>  $\cdot$  cm<sup>-1</sup>. Each determination was carried out in triplicate.

## 3. RESULTS AND DISCUSSION

### 3.1. Establishment of B<sub>22</sub> measurement via SIC for lysozyme

#### 3.1.1. Lysozyme characterization after binding on chromatography particles

The SIC method consists of the immobilization of the studied protein on chromatography particles and of the injection of the same initial protein to measure free protein – immobilized protein interactions. As the protein immobilization should not disrupt the protein structure and activity,  $\alpha$ -amino and  $\epsilon$ -lysyl amino residues are the main targets in bioconjugation. This amino acid is present with high frequencies in proteins (up to 10 %) and only a few of its residues are involved in the protein active site (Veronese and Morpurgo, 1999). Carboxyl amino acids constitute a second choice in bioconjugation as it is difficult to avoid cross-linking with the same protein's amino groups. Toyopearl<sup>®</sup> AF Formyl 650M that is a resin functionalized with a chemical reactive aldehyde group was chosen to immobilize lysozyme, since ligands bearing amine group, e.g. protein, can be coupled by reductive alkylation in the neutral pH region to form a stable secondary amine linkage between lysozyme and the resin. This chemistry should only slightly damage lysozyme molecules. Indeed, lysozyme, which was coupled to Cyanogen Bromide activated Sepharose 4 B, retained 27 % of its activity toward *M. lysodeikticus* after 6 weeks of storage at 4 °C (Patro and Przybycien, 1996). In addition, the immobilized lysozyme molecules are assumed to be oriented

randomly with no preference to a single orientation, as the lysine side chains and N-terminus are well distributed over the surface of the lysozyme molecule.

FTIR was performed to characterize the secondary structure of lysozyme after binding to chromatography particles. The second derivative spectrum of the amide I band of the native lysozyme measured in transmission (Fig. II-1) was characterized by three peaks at 1630, 1656 and 1679  $\text{cm}^{-1}$ . The absorbance maximum at 1656  $\text{cm}^{-1}$  indicated the predominance of the  $\alpha$ -helical structure, whereas the bands at 1630 and 1679  $\text{cm}^{-1}$  corresponded to intra-molecular  $\beta$ -sheet structure elements and turn structures respectively. Those bands were characteristics of lysozyme and were comparable to those reported by X-ray crystallographic analysis (Robertson and Murphy, 1997) and further FTIR investigations (Byler and Susi, 1986, van de Weert *et al.*, 2001). Lysozyme that was immobilized to the chromatographic particles had a comparable derivative spectrum, as two main peaks were detectable at 1656 and 1681  $\text{cm}^{-1}$ . Nevertheless the minor structural loss could be confirmed by comparison to the spectrum of immobilized lysozyme after thermal stress (95  $^{\circ}\text{C}$  / 1 h), which revealed the presence of the two peaks at 1656 and 1679  $\text{cm}^{-1}$ , but also a broadening of the peak at 1656  $\text{cm}^{-1}$  and a reduction of its intensity, both characteristic of structural differences (Pelton and Mclean, 2000). Consequently, the binding process did not induce major detectable structural change of lysozyme.

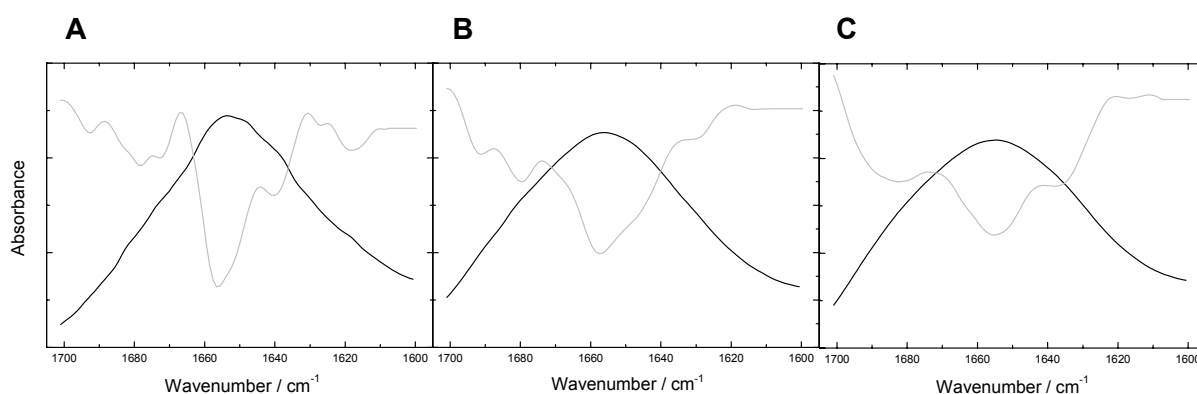


Fig. II-1: ATR-FTIR adsorption spectra (black) and second derivatives (light gray) of lysozyme (A), immobilized lysozyme (B) and immobilized lysozyme after thermal stress (95  $^{\circ}\text{C}$ , 1h) (C) measured at 20  $^{\circ}\text{C}$ .

### 3.1.2. Chromatogram analysis: retention volume determination

The retention volume is usually determined at the peak maximum of the chromatogram, as a suitable chromatographic method is supposed to deliver symmetric peaks. However, SIC did not systematically deliver symmetric peaks. Two different calculation methods were compared, namely the determination of the retention volume at the peak maximum and the analysis at 50 % of the total area under the curve (AUC).

Both methods delivered  $B_{22}$  values presenting the same trend, e.g. increasing the NaCl concentration reduced  $B_{22}$  of lysozyme (Fig. II-2). Determining  $B_{22}$  at the peak maximum tended to results in slightly higher  $B_{22}$  because of the asymmetry of the peak. This effect was more pronounced at high salt concentration, as the peak asymmetry increased. The asymmetry factor took the values of 1.4 between 0 and 0.3 M NaCl and 1.8 at 0.8 M NaCl. Since the two calculation methods delivered convergent results at low salt concentration, which is of interest in protein formulation, the retention volume was determined at the peak maximum in the following experiments.

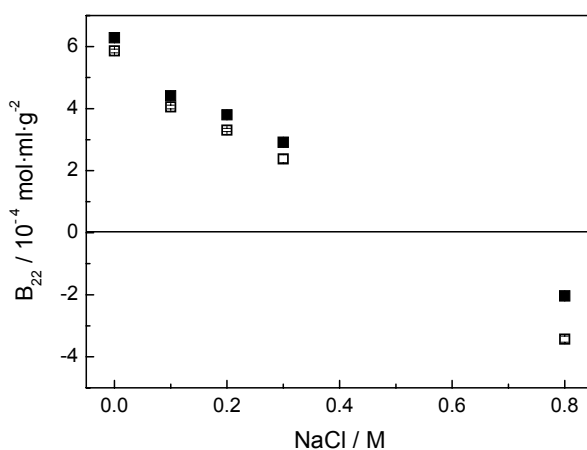


Fig. II-2: Effect of retention volume determination on  $B_{22}$  value of lysozyme with regard to NaCl concentration (5 mM acetic acid, pH 4.5) at a loading of 18 mg/g: retention volume at the peak maximum (■) and retention volume at 50 % of the total area under the curve (□).

### 3.1.3. Influence of chromatography parameters on $B_{22}$ of lysozyme

#### 3.1.3.1. Flow rate

Since the measurement of  $B_{22}$  should be performed at solution equilibrium, the retention volume of free protein could be influenced by the flow rate that also determines the analysis run time and thus the throughput of the screening method. The flow rate influence was tested in the presence of 300 mM NaCl pH 4.5. Three flow rates were selected: 0.25, 0.50 and 0.75 ml/min. Increasing the flow rate lowered the retention volume, but did not perturb the scatter of the results and the standard deviations and did not affect the  $B_{22}$  value (Table II-1). Even though decreasing the flow rate was expected to improve the interaction time between immobilized and free lysozyme molecules, no significant effect was observed. It was found that the retention volume of the non-interacting species was changed in a similar way as the retention volume of lysozyme. As flow rate influenced the analysis run time and thus the speed of the method, the high flow rate of 0.75 ml/min was preferred in order to shorten analysis.

Flow rate (ml·min <sup>-1</sup> )	Retention volume (ml)	B <sub>22</sub> (10 <sup>-4</sup> mol·ml·g <sup>-2</sup> )
0.25	1.49 ± 0.02	3.50 ± 0.24
0.50	1.48 ± 0.01	3.42 ± 0.16
0.75	1.44 ± 0.01	3.70 ± 0.15

Table II-1: Effect of flow rate on retention volume and B<sub>22</sub> value of lysozyme in the presence of 300 mM NaCl and 5 mM acetic acid pH 4.5 at a loading of 22 mg/g (injection of 0.2 mg lysozyme).

### 3.1.3.2. Lysozyme concentration

As described previously, the approach using SIC for the determination of B<sub>22</sub> based on the consideration of Zimm (1946) takes account of an anisotropy interaction energy of a two-body interaction (i.e. interaction of two protein molecules). This means that the potential mean force for the description of the interaction depends on the separation of the two bodies and is a function of all orientations. Therefore, the concept just considers the interaction of a free protein molecule in solution with only one protein molecule immobilized on the chromatography particles. The interaction of e.g. a free protein molecule in solution with two immobilized protein molecules, i.e. a three-body interaction, is not considered (see equation 1). Therefore, the validity of the applied method depends on the chromatography particle surface coverage of the immobilized protein (Tessier *et al.*, 2002). This has also to be considered for the interaction in solution of the free protein molecules, namely interactions of free protein molecules with each other in solution should be strongly reduced. This can easily be realized using relatively diluted protein solutions. Thus, the free protein in solution interacts just with one immobilized protein molecule.

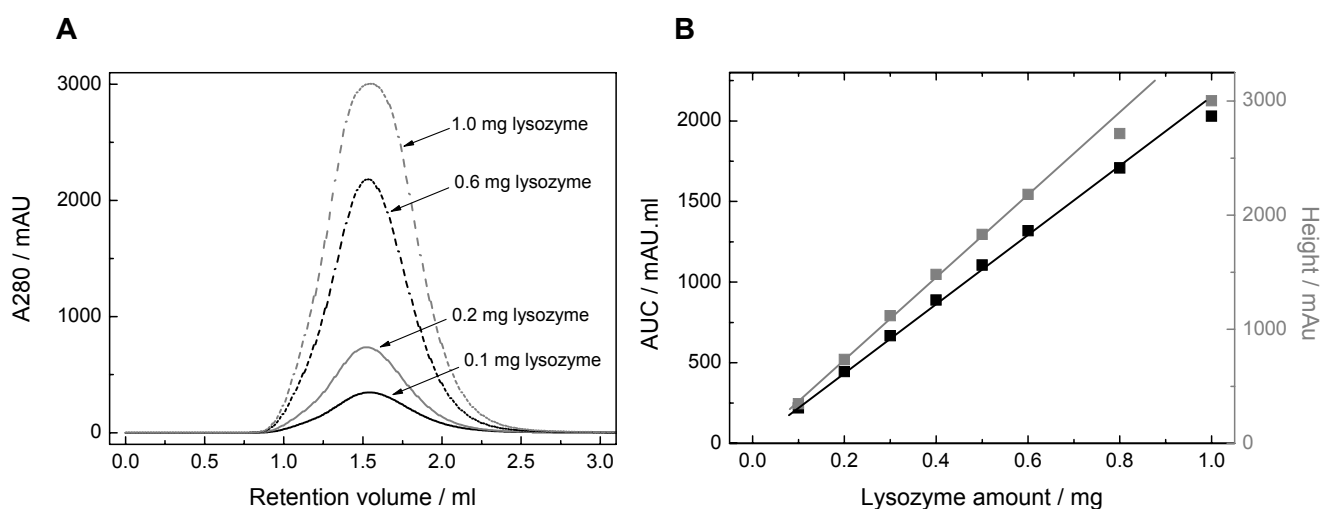


Fig. II-3: Effect of lysozyme quantity injected on (A) peak shape and peak position and (B) AUC (■) and peak height (■) in the presence of 300 mM NaCl and 5 mM acetic acid pH 4.5 (column loading of 22 mg/g).



### 3.1.3.2.1. Quantity of lysozyme injected

The influence of the lysozyme quantity injected was tested in the presence of 300 mM NaCl at pH 4.5 (Fig. II-3) under constant surface coverage (22 mg/g), flow rate (0.75 ml/min) and temperature (25 °C) conditions. Increasing the injected lysozyme amount did not modify the chromatogram peak maximum and consequently did not influence  $B_{22}$ . However when 1 mg lysozyme was injected on the SIC column, the chromatogram showed a plateau at the peak maximum meaning that the detection system was saturated (Fig. II-3A). This phenomenon was confirmed by plotting the lysozyme quantity injected versus AUC and peak height (Fig. II-3B). Indeed, the AUC and height were both proportional to the quantity injected up to 0.6 mg lysozyme. Therefore, the injection of 0.2 mg lysozyme was chosen for the next experiments in order to reduce the lysozyme consumption and avoid any potential overloading.

### 3.1.3.2.2. Correlation between protein surface coverage and $B_{22}$

Three different degrees of protein surface coverage were tested: 18 mg/g, 21 mg/g and 56 mg/g (mg protein per g chromatography particles). The experiment with 21 mg/g was repeated with a similar surface coverage of 22 mg/g.  $B_{22}$  was measured, for a constant protein surface coverage at constant temperature  $T = 25$  °C, 5 mM acetic acid pH = 4.5, as a function of ionic strength. The NaCl concentration was varied between 0 M and 0.8 M. Figure II-4A shows exemplarily elution profiles of lysozyme at four different ionic strengths. A small retention volume and a sharper peak indicated predominant repulsive intermolecular interactions, whereas a higher retention volume and a wider peak characterized the gain in attractive intermolecular interactions. The AUC remained mainly unchanged. The retention volume increased with increasing ionic strength, reflecting changes in  $B_{22}$ .

The data reported in Figure II-4B represent the average data of 6 independent experiments with their standard error of deviations. As can be seen from Figure II-5, an increase of the ionic strength induced a decrease of  $B_{22}$ . At low ionic strength  $B_{22}$  values were positive, and a change in sign was observed at a NaCl concentration of approximately 0.6 M. Above 0.6 M NaCl,  $B_{22}$  data were negative. Thus, at higher NaCl concentrations attractive protein-protein interactions were favored, because the protein charges became strongly screened with higher amounts of present NaCl (Retailleau *et al.*, 2002, Retailleau *et al.*, 1997).

With regard to the protein surface coverage (Fig. II-4B) between 18-56 mg/g the obtained  $B_{22}$  data were quite similar with a slight trend of decreasing values for 56 mg/g. The comparison of two independent preparations of protein immobilization to the chromatography particles (21 and 22 mg lysozyme / g chromatography particles)

showed a rather good reproducibility of  $B_{22}$  values of  $\pm 0.1 \cdot 10^{-4} \text{ mol} \cdot \text{ml} \cdot \text{g}^{-2}$  at different NaCl concentrations. This observation is in accordance with the work from Tessier and co-workers (2002), which showed that low surface coverage was ineffective in the measurement of  $B_{22}$  by SIC as compared to higher surface coverages (above 33 %). Teske and co-workers (2004) also reported  $B_{22}$  values obtained by SIC were comparable to  $B_{22}$  values measured by static light scattering only at low surface coverage because of the increasing risk of multiple body interaction at higher protein immobilization. Obviously, the lysozyme immobilization conditions tested in combination with the previously described injection conditions (0.2 mg lysozyme) results in  $B_{22}$  measurements which are reproducible and comparable to the results reported in the literature.

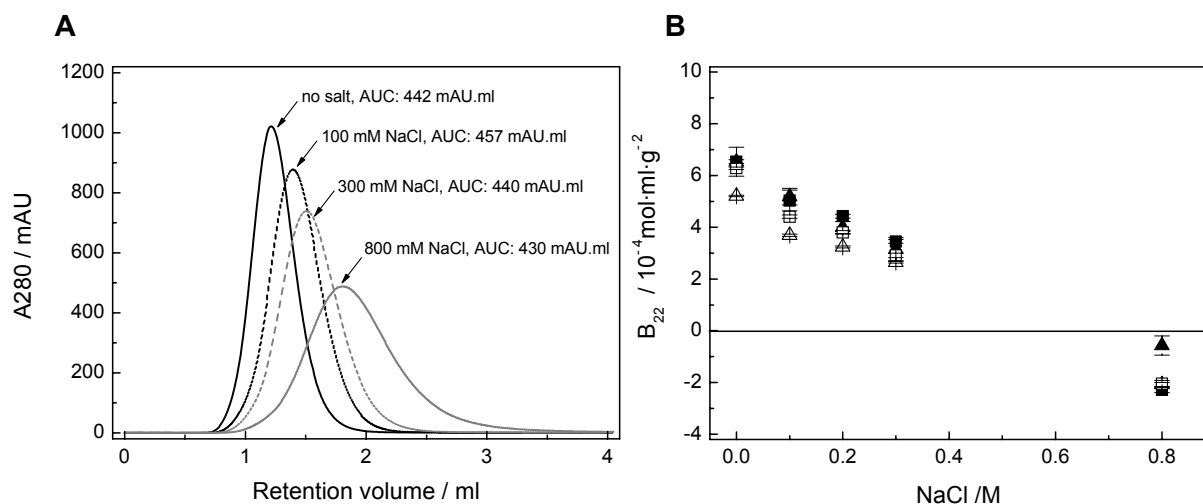


Fig. II-4: (A) Elution profiles of lysozyme as a function of NaCl concentration in the presence of 5 mM acetic acid at pH 4.5 at a loading of 18 mg/g: no salt (—), 100 mM NaCl (- -), 300 mM NaCl (- · -) and 800 mM NaCl (— · —) (Injection of 0.2 mg).

(B) Effect of surface coverage (mg lysozyme / g particles) on lysozyme  $B_{22}$  value as a function of NaCl concentration in the presence of 5 mM acetic acid at pH 4.5: 18 mg/g (■), 21 mg/g (□), 22 mg/g (▲), 56 mg/g (△).

### 3.1.3.3. Effect of temperature

The effect of temperature with regard to  $B_{22}$  depends on the overall solution condition properties. Figure II-5A shows the variation of  $B_{22}$  as a function of temperature in the range between 5 °C and 35 °C at a NaCl concentration of 800 mM (pH = 4.5). The investigated temperature interval was well below the denaturation temperature of lysozyme (Garidel and Schott, 2006). Thus the interactions between native structures were investigated. Under these solution conditions and in the investigated temperature interval all data were negative and lied between  $-7$  and  $-1 \cdot 10^{-4} \text{ mol} \cdot \text{ml} \cdot \text{g}^{-2}$ . These are solution conditions favoring crystallization (Cheng *et al.*, 2008, Dumetz *et al.*, 2008b, Dumetz *et al.*, 2008a, Dumetz *et al.*, 2007, Zhang *et al.*, 2006). With increasing temperature repulsive interactions intensified. However, this trend depended on the

overall solution conditions. Reducing the ionic strength from 0.8 M NaCl to 0.3 M NaCl, the temperature effect was rather small (Fig. II-5B) with a slight decrease in  $B_{22}$ . Under these solution conditions  $B_{22}$  was positive with values between 2.5 and  $3.5 \cdot 10^{-4} \text{ mol} \cdot \text{ml} \cdot \text{g}^{-2}$ .

Gripon and co-workers first described the dependence of lysozyme solubility (Gripon *et al.*, 1997b) and lysozyme  $B_{22}$  (Gripon *et al.*, 1997a) on temperature. Increasing temperature enhanced solubility and  $B_{22}$  of lysozyme in the NaCl concentration range tested (0.2 to 0.6M NaCl at pH 4.45). This temperature effect was in agreement with the work of Valente and co-workers (2005a) on  $B_{22}$  of lysozyme. In addition, the temperature variation was shown to be dependent on the ion type and the ionic strength (Bonnete *et al.*, 1999). For example, NaCl had a more pronounced effect than sodium acetate on lysozyme. The variations of lysozyme  $B_{22}$  with regard to temperature matched to the variations of lysozyme solubility (George *et al.*, 1997, Guo *et al.*, 1999, Ruppert *et al.*, 2001). However, increasing the temperature has also been displayed to decrease  $B_{22}$  of ovalbumin (Antipova *et al.*, 1999), as it favored aggregate formation by initiating partial unfolding and exposing hydrophobic regions that led to more attractive interactions. This temperature dependence probably derives from hydrophobic interactions, which are known to depend strongly on temperature and mediate very short-ranged interparticle forces (Piazza, 2004). Solvation forces are modified in concentrated salt solutions as compared to dilute electrolyte solutions, as hydrophobic interactions between non-polar residues increase with addition of salt (Curtis *et al.*, 2002). Consequently, the temperature effect was accentuated in the presence of high salt concentration.

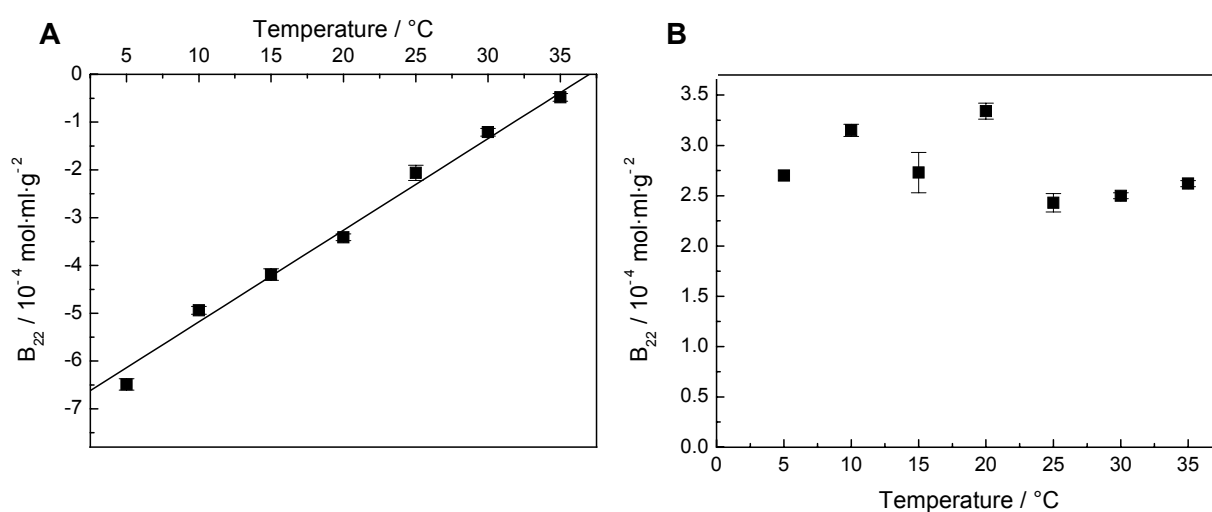


Fig. II-5: Effect of temperature from 5 to 35 °C on lysozyme  $B_{22}$  value as a function of NaCl concentration in the presence of 5 mM acetic acid at pH 4.5 at a loading of 22 mg/g.

(A) NaCl concentration = 800 mM,

(B) NaCl concentration = 300 mM.

### 3.1.3.4. Storage stability of the functionalized chromatography column

Using the presented method as a screening assay, it is crucial that the column shows certain stability in order to be able to perform and evaluate various solution conditions with regard to  $B_{22}$ . Therefore, the storage stability at 4 °C of the functionalized column was investigated (Fig. II-6). The column was stored in a 5 mM sodium phosphate buffer at pH 7.0 containing 0.05 % sodium azide at 4 °C up to 307 days. Figure II-6A showed that the obtained  $B_{22}$  data were very similar showing that the column still remained its functionality. However, analysis of the chromatograms (Fig. II-6B) showed the appearance of a shoulder at about 2.3 ml. This was especially observed after the column has been stored for 161 days. Based on the obtained data, stability of the lysozyme functionalized column, under the chosen storage conditions, is given for 3 months. This allows SIC as being used as a high throughput screening method for the evaluation of a large number of solution conditions.

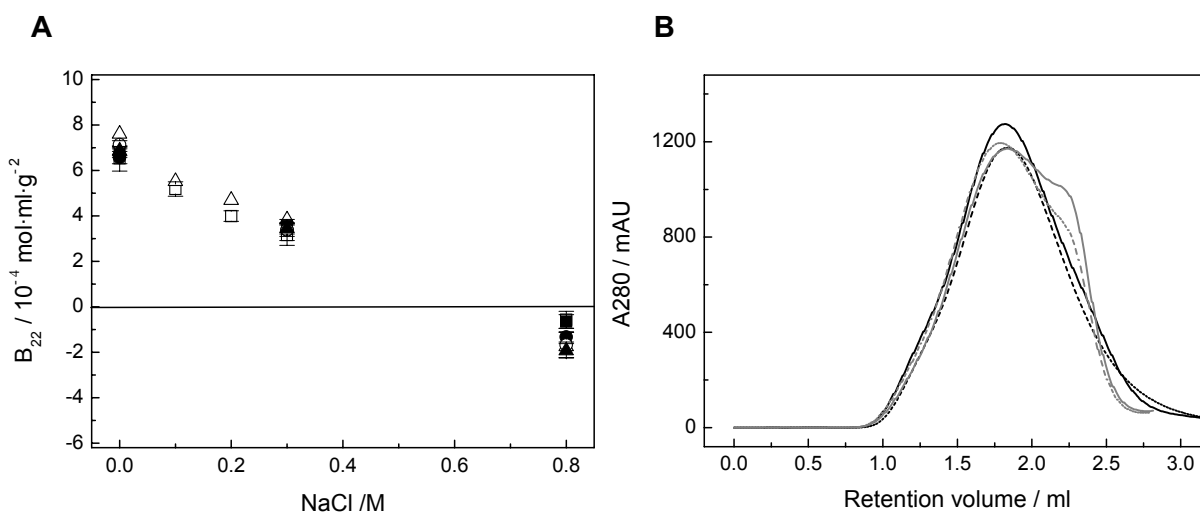


Fig. II-6: Column stability at a loading of 22 mg/g:

(A) lysozyme  $B_{22}$  value as a function of NaCl concentration in the presence of 5 mM acetic acid at pH 4.5 after 21 days (■), 30 days (□), 45 days (●), 86 days (○), 161 days (▲), and 307 days (△),

(B) Elution profile of lysozyme with 800 mM NaCl and 5 mM acetic acid at pH 4.5 after 21 days (—), 45 days (---), 86 days (- -), and 161 days (—).

(Injection of 20  $\mu\text{l}$  lysozyme solution at 20 mg/ml, storage at 4 °C in 5 mM sodium phosphate buffer pH 7.0 containing 0.05 % sodium azide).

## 3.2. Influence of formulation parameters on $B_{22}$ of lysozyme

### 3.2.1. Effect of the protonation degree

The surface charge of a protein, and related effects e.g. protein hydration, have a strong influence on protein-protein interactions. Lysozyme is a protein with an extremely basic pI (pI  $\approx$  11) (Alderton *et al.*, 1945, Wetter and Deutsch, 1951, Zschornig *et al.*, 2005). Its titration curve (in absence of any excipient, i.e. ion binding is not considered that may affect the surface charge in solution) was calculated using the

EMBOSS-software (Rice *et al.*, 2000) (Fig. II-7). At pH 4.5 lysozyme is positively charged, with 11 positive elementary charges. At pH 7.5 lysozyme is still positively charged, with 8 positive elementary charges. Charge neutralization is given for pH 11. Choosing pH conditions close to the pI would reduce protein solubility and thus favor protein precipitation, as protein solubility changes with the square of the protein net charge (Shaw *et al.*, 2001). Increasing the pH substantially decreased  $B_{22}$  (Fig. II-7). Under acidic pH conditions  $B_{22}$  was positive, whereas  $B_{22}$  became negative at pH 7. Experiments for pH > 8 were not followed, because strongly alkaline solution conditions would damage the chromatography particles. In the presented case the dependency on pH with regard to  $B_{22}$  was linear. At pH 11 one would obtain a  $B_{22}$  of  $-3 \cdot 10^{-4} \text{ mol} \cdot \text{ml} \cdot \text{g}^{-2}$  (data derived from extrapolation), reflecting conditions prone for precipitation. The explanation for the pH dependency with regard to  $B_{22}$  is the change in protonation degree of lysozyme accompanied by changes of protein hydration. With decreasing pH the positive surface charge increases, i.e. the zeta potential and thus the solubility (Arakawa and Timasheff, 1985, Ruppert *et al.*, 2001).

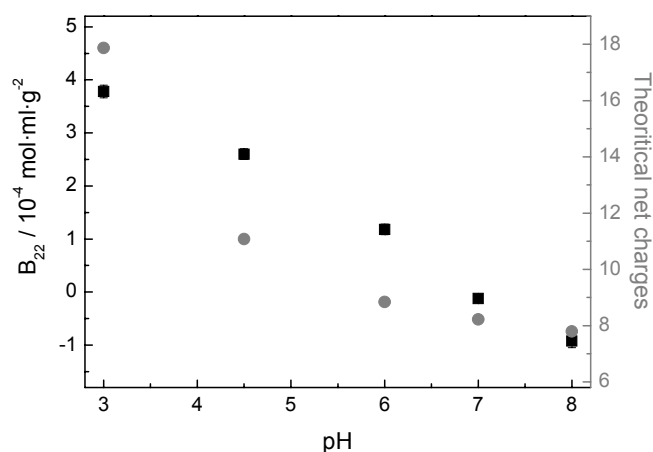


Fig. II-7: Effect of pH on lysozyme theoretical net charges (●) and lysozyme  $B_{22}$  value (■) at a loading of 51 mg/g in the presence of 300 mM NaCl and 5 mM acetic acid at pH 3.0 and 4.5, and 5 mM sodium phosphate at pH 6.0, 7.0 and 8.0.

### 3.2.2. Effect of ionic strength and different salts of the Hofmeister series

It has been known from the pioneering work of Hofmeister (1888) that the presence of some salts is able to precipitate proteins, whereas other salts exert a salting-in effect. The Hofmeister series ranks the salting-out effectiveness of various ions for globular proteins. The effectiveness of anions is much stronger than that of cations. The series for anions and cations follow this decreasing orders in salting out capacity:  $\text{SO}_4^{2-} > \text{HPO}_4^{2-} > \text{CH}_3\text{COO}^- > \text{Cl}^- > \text{Br}^- > \text{I}^- > \text{SCN}^-$  and  $\text{Li}^+ > \text{Na}^+ \sim \text{K}^+ > \text{NH}_4^+ > \text{Mg}^{2+}$  (Benas *et al.*, 2002). The salt concentrations applied for e.g. protein precipitation by  $(\text{NH}_4)_2\text{SO}_4$

are often very high (up to 3 M). Especially at these high salt concentrations the effects and trends of the Hofmeister series become relevant (Curtis *et al.*, 2002). However, for pharmaceutical applications such high salt concentrations are of minor importance. Therefore, the presented investigations are focused on the presence of lower salt concentrations. A parameter not further considered by Hofmeister was the pH of the solution, as the concept of pH was not known at that time. The concept of pH was introduced about 20 years later by Sørensen (1909). However, the solution pH and thus the overall surface charge of a particle have a strong impact on its interaction characteristics, and have to be considered. As ammonium sulfate has the property of being kosmotropic at high salt concentration (4 M), which favors protein precipitation (Cacace *et al.*, 1997), increasing the  $(\text{NH}_4)_2\text{SO}_4$  concentration should decrease  $B_{22}$ . Figure II-8A shows the variation of  $B_{22}$  as a function of  $(\text{NH}_4)_2\text{SO}_4$  concentration between 0 and 0.8 M. Even if  $B_{22}$  decreased by increasing salt concentration,  $B_{22}$  data were still positive for the investigated  $(\text{NH}_4)_2\text{SO}_4$  salt concentrations. Negative  $B_{22}$  could only be obtained when the  $(\text{NH}_4)_2\text{SO}_4$  concentration exceeded concentration of at least 3 M.

Considering the  $B_{22}$  data of two additional sulfate salts, namely  $\text{K}_2\text{SO}_4$  and  $\text{Na}_2\text{SO}_4$ , it could be seen that the  $B_{22}$  data were very similar for salt concentrations between 0 and 0.3 M. Differences were observed for salt concentrations higher than 0.6 M, with the sodium salt resulting in more negative  $B_{22}$  values. As seen for the sulfate salts, the chloride salts of  $\text{Na}^+$ ,  $\text{K}^+$  and  $\text{Mg}^{2+}$  exhibited a more pronounced effect at high salt concentration, with  $\text{MgCl}_2$  having the strongest salting-in effect (Fig. II-8B). At 0.8 M salt concentration the  $B_{22}$  values ranked:  $B_{22}(\text{MgCl}_2) > B_{22}(\text{KCl}) > B_{22}(\text{NaCl})$ . At high ionic strength, the observed cation effect followed the trend of the Hofmeister series. In addition, the influence of the cation species was studied at two different pH values: at pH 4.5 in the presence of sulfate salts and at pH 7.4 in the presence of chloride salts. Under both pH conditions, the salting-out by  $\text{Na}^+$  was stronger than the effect of  $\text{NH}_4^+$  (Fig. II-8A and II-8D), corresponding to the Hofmeister series.

As described above, the effect of salts on the protein interaction characteristics depends on the overall solution conditions. Yamasaki and co-workers (1991) have shown for BSA with regard to thermally induced denaturation, that in the presence of kosmotrope salts, the protein structure is stabilized, whereas it becomes destabilized in the presence of chaotrope salts. This is especially the case at high ionic strength, but a reversal of the stability effect is observed at low ionic strength (0.01-0.1 M). The reason for such a behavior lies in the screening of the electrostatic repulsions via the close interaction/binding of the anion to the protein, and this effect is stronger with chaotrope than with kosmotrope ions.

In this study, it was shown that the effect of different salts/ions does not necessarily correlate with the Hofmeister series. In some cases a reverse effect is observed. This was also described by Riès-Kautt and Ducruix (1989). The reason for this phenomenon was attributed to the effectiveness of anions to promote protein crystallization, which is dependent on the net charge of the protein. Therefore, for acidic proteins the salting-in/salting-out behavior of ions follows the Hofmeister series, whereas the effect and order are reversed for basic proteins like lysozyme.

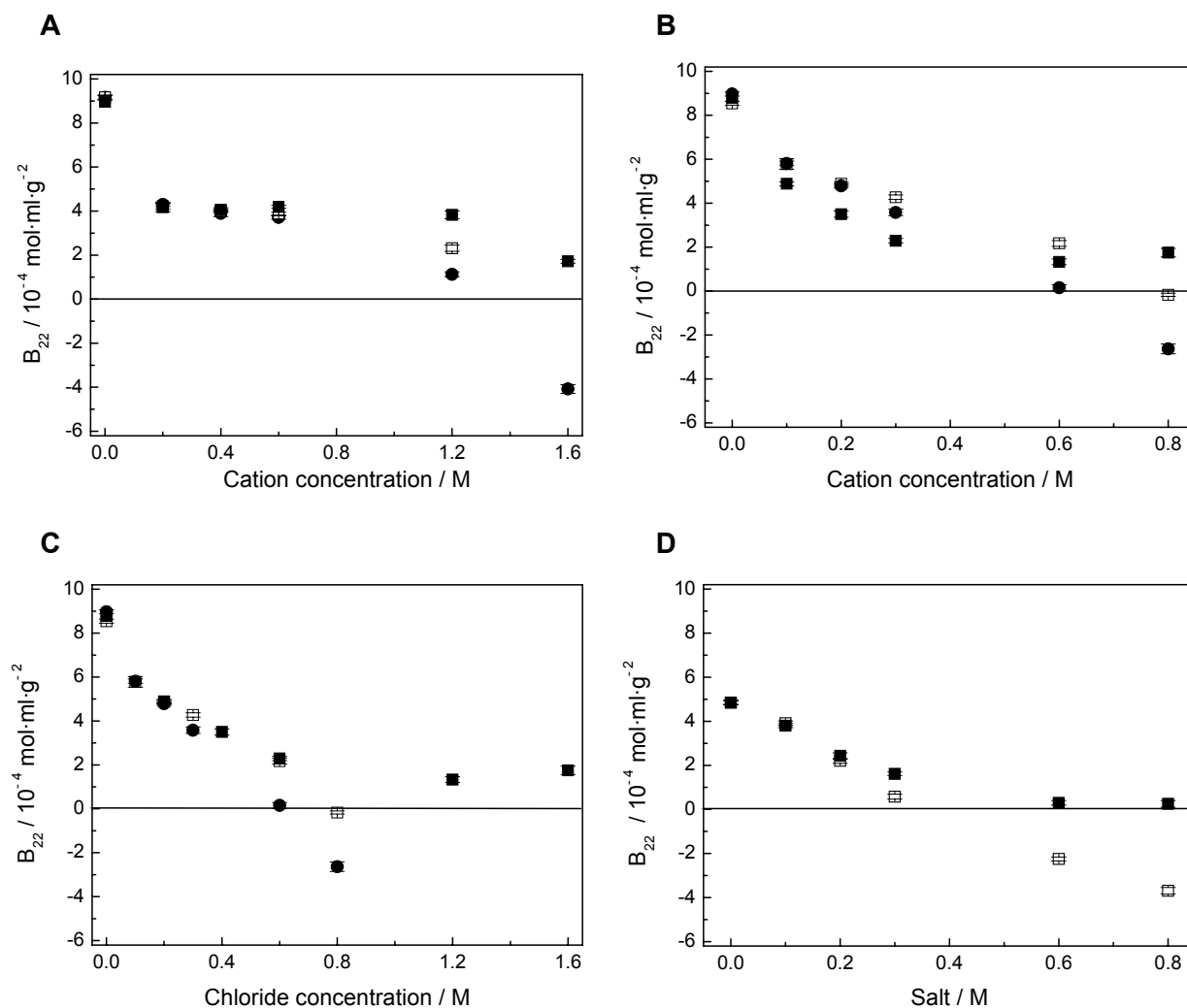


Fig. II-8: Effect of ionic strength on lysozyme  $B_{22}$  value at a loading of 18 mg/g in the presence of: (A) sulfate salts and 5 mM acetic acid at pH 4.5:  $(\text{NH}_4)_2\text{SO}_4$  (■),  $\text{K}_2\text{SO}_4$  (□),  $\text{Na}_2\text{SO}_4$  (●) (The sulfate concentration corresponds to the cation concentration),

(B) and (C) chloride salts cation and 5 mM acetic acid at pH 4.5:  $\text{MgCl}_2$  (■),  $\text{KCl}$  (□),  $\text{NaCl}$  (●) ((B) cation concentration, (C) chloride concentration),

(D) chloride salts and 5 mM sodium phosphate at pH 7.4:  $\text{NH}_4\text{Cl}$  (■),  $\text{NaCl}$  (□).

### 3.2.3. Effect of sucrose and glycerol

Sugars and polyols are commonly used in protein formulation as stabilizing excipients. In the presence of glycerol in the concentration range from 0 to 6 % and in the presence of sucrose up to a concentration of 20 % the  $B_{22}$  data were all strongly

positive and nearly independent of excipient concentration (Fig. II-9). The reported data were between 8 and  $10 \cdot 10^{-4} \text{ mol} \cdot \text{ml} \cdot \text{g}^{-2}$ . Thus, the presence of e.g. sucrose favored repulsive interactions between lysozyme molecules. Sugars and polyols are known to stabilize protein formulations according to the principle of excluded volume described by Timasheff (1993). They influence the conformational dynamics of proteins by favoring the most compact conformation in the native state ensemble, since these cosolvents preferably interact with water and thus migrate away from the protein surface.

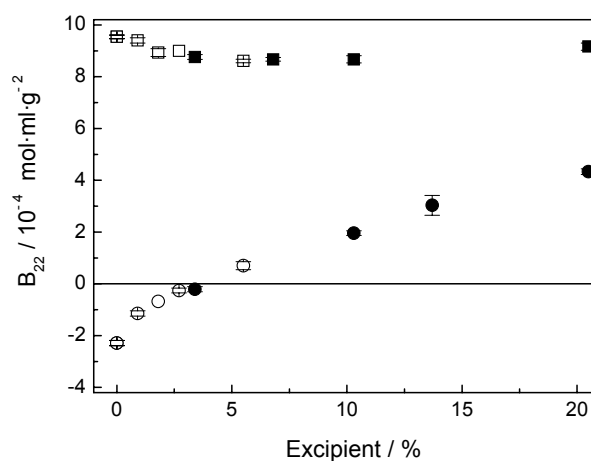


Fig. II-9: Effect of sucrose and glycerol in the presence of 5 mM acetic acid at pH 4.5 on lysozyme  $B_{22}$  value at a loading of 18 mg/g: glycerol (□), sucrose (■), glycerol + 800 mM NaCl (○), sucrose + 800 mM NaCl (●).

The additional presence of high concentrations of NaCl (0.8 M) induced a strong decrease of  $B_{22}$ . However, the presence of high sugar concentrations (up to 10 % of sucrose) overcompensated the charge screening effect of the salt, which led to a salting-out effect. Thus the overall solution condition properties became positive in the sense of favoring protein solubility at sucrose concentration larger than 10 %. The presence of glycerol also induced an increase of  $B_{22}$  in the presence of NaCl in protein solution (Fig. II-9). This phenomenon was comparable to the results of Valente and co-workers (2005b) with lysozyme in the presence of various disaccharides and polyols. The structure stabilizing effect of sucrose and glycerol was independent of the ionic strength. Nevertheless, the presence of cosolvent favored the protein compact form, reducing the protein volume but also the hydrophobicity of its surface. Attractive hydrophobic interactions are increased with addition of salt (Curtis *et al.*, 2002) and reducing the protein hydrophobicity by addition of sugars or polyols should decrease the negative effect of salt on attractive interactions.



### 3.2.4. Effect of PEG molecular weight

Polyethylene glycols (PEG) are known as protein precipitating agents. The influence of three different PEG qualities on  $B_{22}$  of lysozyme was tested at the acidic pH of 4.5. Under the tested solution conditions, the  $B_{22}$  values were all positive for the three tested PEG qualities with molecular weights of 6000, 4000 and 400 g/mol (Fig. II-10A). Under these conditions protein precipitation is unlikely. The trend for the high molecular weight PEG was very similar. Increasing the PEG concentration even led to a salting-in effect, indicative of an increased positive  $B_{22}$ . The presence of PEG 400 showed basically no effect on the  $B_{22}$  data, which lied between 7 and  $10 \cdot 10^{-4} \text{ mol} \cdot \text{ml} \cdot \text{g}^{-2}$  for the concentration range from 0 to 24 % PEG 400. Depending on the overall solution conditions, PEG can also act as a precipitation reagent as shown by Tessier and co-workers (2003). For Ribonuclease A (pH 8 and 50 mM NaCl) with increasing the concentration of PEG 3350 g/mol  $B_{22}$  decreased strongly and in the presence of 15 w% PEG values of  $-18 \cdot 10^{-4} \text{ mol} \cdot \text{ml} \cdot \text{g}^{-2}$  were determined (Tessier *et al.*, 2003).

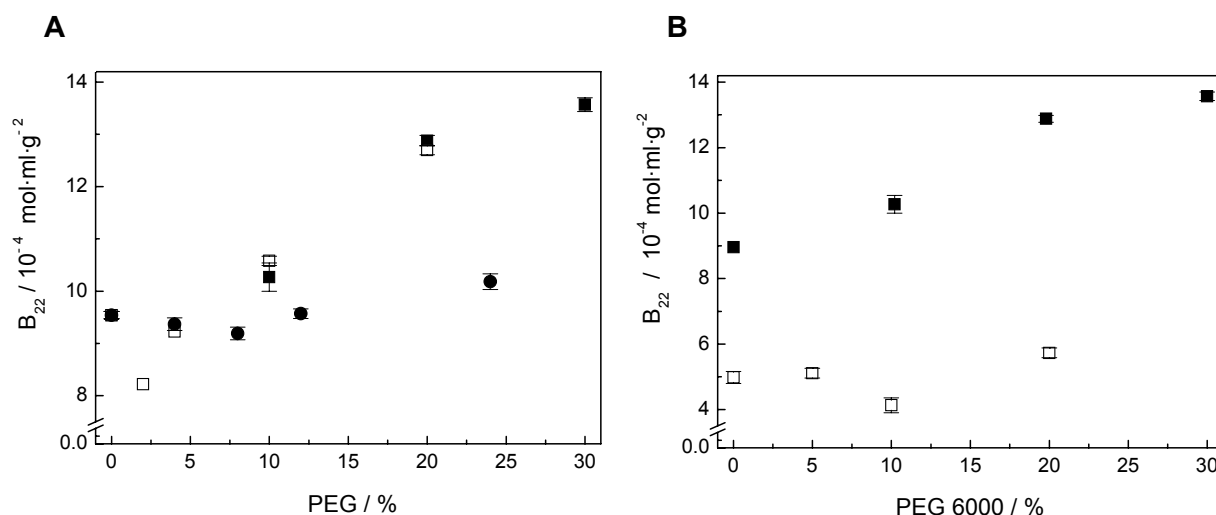


Fig. II-10: Effect of PEG on lysozyme  $B_{22}$  value at a loading of 18 mg/g:

(A) influence of PEG molecular weight in the presence of 5 mM acetic acid at pH 4.5: PEG 6000 (■), PEG 4000 (□), PEG 400 (●),

(B) influence of pH in the presence of PEG 6000: pH 4.5 (■) with 5 mM acetic acid, pH 7.4 (□) with 5 mM sodium phosphate.

However, changing the solution pH to 7.4 modulated the effect of PEG 6000 (Fig. II-10B). Raising the PEG concentration did not increase lysozyme repulsive interactions. The addition of PEG into protein solution caused a depletion reaction by inducing the steric exclusion of the polymer molecules from the zone between two protein molecules (Arakawa and Timasheff, 1985). The amount of PEG that was needed to induce protein aggregation depended on the net charge of the protein and on the degree of polymerization of the polymer. In addition, PEG lowered the dielectric constant of the

solution, which increased the effective distance over which protein electrostatic effects occurred (McPherson, 1990). Varying the pH solution from 4.5 to 7.4 decreased the number of positive net charges beard by lysozyme. The repulsive interactions between lysozyme molecules were consequently diminished and the effect of PEG was reduced. Thus, as the action of PEG depends on the overall solution conditions, conditions which favor lysozyme precipitation by addition of PEG were not found.

### 3.3. Correlation between $B_{22}$ and protein solubility

For protein formulation, solution conditions favoring protein solubility are of interest in order to stabilize the protein solution. Figure II-11A, represents the correlation between  $B_{22}$  and protein solubility. The lowest protein solubility was set to 1, thus relative solubilities were reported in order to directly compare the impact on the formulation change. Protein solubility was the lowest under alkaline conditions because of the strong alkaline pI of lysozyme. Under these conditions negative  $B_{22}$  were determined, which indicated a predominance of attractive protein-protein interactions and thus reduced solubility. Under acidic conditions,  $B_{22}$  became positive and corresponded to an increase in solubility by a factor of 7. Increasing the ionic strength (Fig. II-11B) reduced strongly the protein solubility;  $B_{22}$  was below  $-2 \cdot 10^{-4} \text{ mol} \cdot \text{ml} \cdot \text{g}^{-2}$ . A removal of NaCl from the formulation induced a protein solubility increase by a factor of 20.

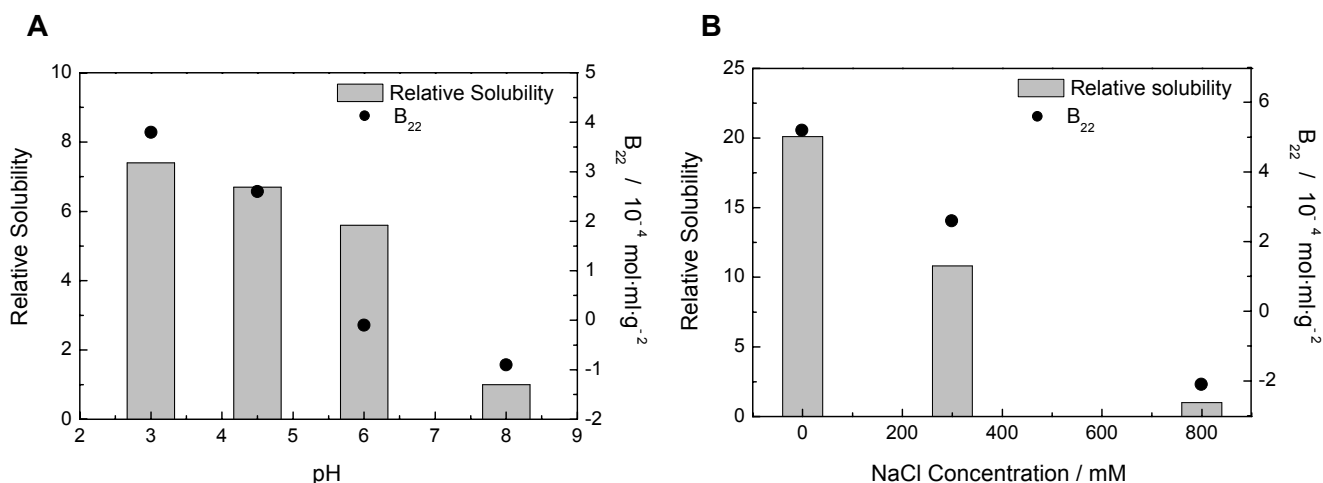


Fig. II-11: Correlation between  $B_{22}$  and lysozyme relative solubility under different conditions. (A) Influence of pH (3.0, 4.5, 6.0 and 8.0) at a constant NaCl concentration of 300 mM, (B) Influence the ionic strength (NaCl concentration of 300 and 800 mM) at a constant pH of 4.5. The buffer conditions for  $B_{22}$  determination and protein solubility were identical.

Within the framework of the sticky hard sphere model (Baxter, 1968), Rosenbaum and co-workers (1996) showed that the experimentally measured  $B_{22}$  can be correlated with solubility data (Haas *et al.*, 1999, Lima *et al.*, 2007, Ruppert *et al.*, 2001, Stigter and Hill, 1959, Wanka and Peukert, 2008). This signifies that short range attractive

interactions are the main interactions that describe the phase properties and behavior of a colloidal system (Polyakov *et al.*, 1991). Based on these considerations, the relation between  $B_{22}$  and the solubility  $S$  is given by:

$$B_{22} = (-\Delta\mu_2 / R \cdot T) \cdot (1 / 2 \cdot M_2 \cdot S) - (\ln S / 2 \cdot M_2 \cdot S) \quad (3)$$

where  $\Delta\mu_2 = \mu_2^0$  (solution) -  $\mu_2^0$  (solid),  $\mu_2^0$  (solution) is the chemical potential of the protein in solution,  $\mu_2^0$  (solid) is the chemical potential of the protein in a solid form (e.g. crystal),  $R$  is the gas constant,  $T$  is the absolute temperature,  $M_2$  is the molecular weight of the protein (denoted as 2) and  $S$  is the solubility expressed in  $\text{g} \cdot \text{ml}^{-1}$ . This approach clearly shows that the second virial coefficient and the solubility are correlated (Guo *et al.*, 1999, Haas *et al.*, 1999). The correlation between  $B_{22}$  and solubility as a function of pH was recently presented by Payne *et al.* for a 36 amino acid therapeutic peptide (Payne *et al.*, 2006). A good correlation between peptide solubility and  $B_{22}$  was found in the pH range of 6 to 10, emphasizing the validity of the method (see equation 2, which relates solubility to  $B_{22}$ ). Thus, the assay allows the identification of solution conditions leading to highest protein solubility.

## 4. CONCLUSIONS

The immobilization of lysozyme on chromatography particles did not modify the protein's secondary structure. SIC could then measure the interactions between two native protein molecules. Temperature was the chromatography parameter having the most influence on  $B_{22}$ . Its influence depended on the solvent conditions and the effect was enhanced by higher electrolyte concentrations. The overall protein solution conditions were dependent on a number of factors of the solution (e.g. pH, ionic strength, osmolarity) and the presence of excipients and cosolutes. The presence of various ions / excipients may have a more or less pronounced impact on the protein solution, depending on whether unspecific or specific interactions are involved. The interactions of ions with proteins are governed by electrostatic interactions, but the influence of solvation (and solvation forces) also has to be considered. The interactions of protein molecules in an aqueous environment are mediated by water molecules, and excipients and cosolutes can influence the protein surface characteristics, as well as the structure of the liquid water (kosmotropic and chaotropic agents). These effects on the water / protein interface influence directly the interfacial energies involved in the interaction and these interfacial energies can not be predicted so easily.

The presented study shows that self-interaction chromatography can be used as a rapid development tool for biopharmaceuticals. It has to be emphasized that the

method used is based on the characterization of protein-protein interactions in their native state. The osmotic second virial coefficient, which is derived from self-interaction chromatography, is a parameter of solution non-ideality that is useful for the prediction of solution conditions promoting protein solubility. SIC allows rapid determination of  $B_{22}$  under high throughput conditions using automated systems. The method can be used for screening evaluations, with column stability given for at least 3 months stored at 4 °C (for lysozyme). Thus, for formulation development, the determination of  $B_{22}$  allows the identification of solution conditions promoting protein solubility.

## 5. REFERENCES

Ahamed, T., Ottens, M., Van Dedem, G. W., and Van Der Wielen, L. A. Design of self-interaction chromatography as an analytical tool for predicting protein phase behavior. *Journal of Chromatography A*, 1089, 111-124 (2005).

Alderton, G., Ward, W. H., and Fevold, H. L. Isolation of lysozyme from egg white. *Journal of Biological Chemistry*, 157, 43-58 (1945).

Antipova, A. S., Semenova, M. G., and Belyakova, L. E. Effect of sucrose on the thermodynamic properties of ovalbumin and sodium caseinate in bulk solution and at air-water interface. *Colloids and Surfaces B-Biointerfaces*, 12, 261-270 (1999).

Arakawa, T., and Timasheff, S. N. Theory of protein solubility. *Methods in Enzymology*, 114, 49-77 (1985).

Bajaj, H., Sharma, V. K., and Kalonia, D. S. Determination of second virial coefficient of proteins using a dual-detector cell for simultaneous measurement of scattered light intensity and concentration in SEC-HPLC. *Biophysical Journal*, 87, 4048-4055 (2004).

Baxter, R. J. Percus-Yevick equation for hard spheres with surface adhesion. *Journal of Chemical Physics*, 49, 2770 (1968).

Beeckmans, S. Chromatographic methods to study protein-protein interactions. *Methods*, 19, 278-305 (1999).

Benas, P., Legrand, L., and Ries-Kautt, M. Strong and specific effects of cations on lysozyme chloride solubility. *Acta Crystallographica Section D-Biological Crystallography*, 58, 1582-1587 (2002).

Bonnete, F., Finet, S., and Tardieu, A. Second virial coefficient: variations with lysozyme crystallization conditions. *Journal of Crystal Growth*, 196, 403-414 (1999).

Byler, D. M., and Susi, H. Examination of the secondary structure of proteins by deconvolved FTIR spectra. *Biopolymers*, 25, 469-487 (1986).

Cacace, M. G., Landau, E. M., and Ramsden, J. J. The Hofmeister series: salt and solvent effects on interfacial phenomena. *Quarterly Reviews of Biophysics*, 30, 241-277 (1997).

Cheng, Y. C., Bianco, C. L., Sandler, S. I., and Lenhoff, A. M. Salting-out of lysozyme and ovalbumin from mixtures: Predicting precipitation performance from protein-protein interactions. *Industrial & Engineering Chemistry Research*, 47, 5203-5213 (2008).

Curtis, R. A., Ulrich, J., Montaser, A., Prausnitz, J. M., and Blanch, H. W. Protein-protein interactions in concentrated electrolyte solutions. *Biotechnology and Bioengineering*, 79, 367-380 (2002).

Dephillips, P., and Lenhoff, A. M. Pore size distributions of cation-exchange adsorbents determined by inverse size-exclusion chromatography. *Journal of Chromatography A*, 883, 39-54 (2000).

Dumetz, A. C., Chockla, A. M., Kaler, E. W., and Lenhoff, A. M. Effects of pH on protein-protein interactions and implications for protein phase behavior. *Biochimica et Biophysica Acta*, 1784, 600-610 (2008a).

Dumetz, A. C., Chockla, A. M., Kaler, E. W., and Lenhoff, A. M. Protein phase behavior in aqueous solutions: crystallization, liquid-liquid phase separation, gels, and aggregates. *Biophysical Journal*, 94, 570-583 (2008b).

Dumetz, A. C., Snellinger-O'Brien, A. M., Kaler, E. W., and Lenhoff, A. M. Patterns of protein protein interactions in salt solutions and implications for protein crystallization. *Protein Science*, 16, 1867-1877 (2007).

Garidel, P., and Schott, H. Fourier-transform midinfrared spectroscopy for analysis and screening of liquid protein formulations. Part 2: detailed analysis and applications. *BioProcess International*, 4, 48-50, 52, 54 (2006).

George, A., Chiang, Y., Guo, B., Arabshahi, A., Cai, Z., and Wilson, W. W. Second virial coefficient as predictor in protein crystal growth. *Macromolecular Crystallography, Pt A*, 276, 100-110 (1997).

Gripon, C., Legrand, L., Rosenman, I., Vidal, O., Robert, M. C., and Boue, F. Lysozyme-lysozyme interactions in under- and super-saturated solutions: a simple relation between the second virial coefficients in H<sub>2</sub>O and D<sub>2</sub>O. *Journal of Crystal Growth*, 178, 575-584 (1997a).

Gripon, C., Legrand, L., Rosenman, I., Vidal, O., Robert, M. C., and Boue, F. Lysozyme solubility in H<sub>2</sub>O and D<sub>2</sub>O solutions: A simple relationship. *Journal of Crystal Growth*, 177, 238-247 (1997b).

Guo, B., Kao, S., Mcdonald, H., Asanov, A., Combs, L. L., and Wilson, W. W. Correlation of second virial coefficients and solubilities useful in protein crystal growth. *Journal of Crystal Growth*, 196, 424-433 (1999).

Haas, C., Drenth, J., and Wilson, W. W. Relation between the solubility of proteins in aqueous solutions and the second virial coefficient of the solution. *Journal of Physical Chemistry B*, 103, 2808-2811 (1999).

Haynes, C. A., Tamura, K., Korfer, H. R., Blanch, H. W., and Prausnitz, J. M. Thermodynamic Properties of Aqueous Alpha-Chymotrypsin Solutions from Membrane Osmometry Measurements. *Journal of Physical Chemistry*, 96, 905-912 (1992).

Hofmeister, F. Zur Lehre von der Wirkung der Salze. *Archiv fur Experimentelle Pathologie und Pharmakologie*, 24, 247-260 (1888).

Lima, E. R. A., Biscaia, E. C., Bostrom, M., Tavares, F. W., and Prausnitz, J. M. Osmotic second virial coefficients and phase diagrams for aqueous proteins from a much-improved Poisson-Boltzmann equation. *Journal of Physical Chemistry C*, 111, 16055-16059 (2007).

Mcmillan, W. G., and Mayer, J. E. The Statistical Thermodynamics of Multicomponent Systems. *Journal of Chemical Physics*, 13, 276-305 (1945).

Mcperson, A. Current approaches to macromolecular crystallization. *European Journal of Biochemistry*, 189, 1-23 (1990).

Muschol, M., and Rosenberger, F. Interactions in undersaturated and supersaturated lysozyme solutions: static and dynamic light scattering results. *Journal of Chemical Physics*, pp. 10424-10432, (1995).

Muschol, M., and Rosenberger, F. Lack of evidence for prenucleation aggregate formation in lysozyme crystal growth solutions. *Journal of Crystal Growth*, 167, 738-747 (1996).

Muschol, M., and Rosenberger, F. Liquid-liquid phase separation in supersaturated lysozyme solutions and associated precipitate formation/crystallization. *Journal of Chemical Physics*, 107, 1953-1962 (1997).

Patro, S. Y., and Przybycien, T. M. Self-interaction chromatography: A tool for the study of protein-protein interactions in bioprocessing environments. *Biotechnology and Bioengineering*, 52, 193-203 (1996).

Payne, R. W., Nayar, R., Tarantino, R., Del Terzo, S., Moschera, J., Di, J., Heilman, D., Bray, B., Manning, M. C., and Henry, C. S. Second virial coefficient determination of a therapeutic peptide by self-interaction chromatography. *Biopolymers*, 84, 527-533 (2006).

Pelton, J. T., and Mclean, L. R. Spectroscopic methods for analysis of protein secondary structure. *Analytical Biochemistry*, 277, 167-176 (2000).

Piazza, R. Protein interactions and association: an open challenge for colloid science. *Current Opinion in Colloid & Interface Science*, 8, 515-522 (2004).

Polyakov, V. I., Dezhenkova, L. G., and Vainerman, E. S. An approach to determine the second virial-coefficient for calculation of phase-equilibria in water-protein-neutral polymer systems. *Polymer Bulletin*, 25, 709-716 (1991).

Rice, P., Longden, I., and Bleasby, A. EMBOSS: the European Molecular Biology Open Software Suite. *Trends in Genetics*, 16, 276-277 (2000).

Ries-Kautt, M., and Ducruix, A. F. Relative effectiveness of various ions on the solubility and crystal-growth of lysozyme. *Journal of Biological Chemistry*, 264, 745-748 (1989).

Robertson, A. D., and Murphy, K. P. Protein structure and the energetics of protein stability. *Chemical Reviews*, 97, 1251-1267 (1997).

Rosenbaum, D., Zamora, P. C., and Zukoski, C. F. Phase behavior of small attractive colloidal particles. *Physical Review Letters*, 76, 150-153 (1996).

Rosenbaum, D. F., Kulkarni, A., Ramakrishnan, S., and Zukoski, C. F. Protein interactions and phase behavior: Sensitivity to the form of the pair potential. *Journal of Chemical Physics*, 111, 9882-9890 (1999).

Rosenbaum, D. F., and Zukoski, C. F. Protein interactions and crystallization. *Journal of Crystal Growth*, pp. 752-758, (1996).

Rosenberger, F., Vekilov, P. G., Muschol, M., and Thomas, B. R. Nucleation and crystallization of globular proteins - What we know and what is missing. *Journal of Crystal Growth*, 168, 1-27 (1996).

Ruppert, S., Sandler, S. I., and Lenhoff, A. M. Correlation between the osmotic second virial coefficient and the solubility of proteins. *Biotechnology Progress*, 17, 182-187 (2001).

Shaw, K. L., Grimsley, G. R., Yakovlev, G. I., Makarov, A. A., and Pace, C. N. The effect of net charge on the solubility, activity and stability of ribonuclease Sa. *Protein Science*, 10 (2001).

Sorensen, S. P. L. Enzymstudien. II: Mitteilung. Über die Messung und die Bedeutung der Wasserstoffionenkonzentration bei enzymatischen Prozessen. *Biochemische Zeitschrift*, 21, 131-304 (1909).

Stigter, D., and Hill, T. L. Theory of the Donnan membrane equilibrium. 2. Calculation of the osmotic pressure and of the salt distribution in a Donnan system with highly charged colloid particles. *Journal of Physical Chemistry*, 63, 551-556 (1959).

Teske, C. A., Blanch, H. W., and Prausnitz, J. M. Measurement of lysozyme-lysozyme interactions with quantitative affinity chromatography. *Journal of Physical Chemistry B*, 108, 7437-7444 (2004).

Tessier, P. M., Johnson, H. R., Pazhianur, R., Berger, B. W., Prentice, J. L., Bahnsen, B. J., Sandler, S. I., and Lenhoff, A. M. Predictive crystallization of ribonuclease A via rapid screening of osmotic second virial coefficients. *Proteins: Structure, Function, and Genetics*, pp. 303-311, (2003).

Tessier, P. M., Lenhoff, A. M., and Sandler, S. I. Rapid measurement of protein osmotic second virial coefficients by self-interaction chromatography. *Biophysical Journal*, 82, 1620-1631 (2002).

Timasheff, S. N. The control of protein stability and association by weak interactions with water - How do solvents affect these processes. *Annual Review of Biophysics and Biomolecular Structure*, 22, 67-97 (1993).

Valente, J. J., Payne, R. W., Manning, M. C., Wilson, W. W., and Henry, C. S. Colloidal behavior of proteins: effects of the second virial coefficient on solubility, crystallization and aggregation of proteins in aqueous solution. *Current Pharmaceutical Biotechnology*, 6, 427-436 (2005a).

Valente, J. J., Verma, K. S., Manning, M. C., Wilson, W. W., and Henry, C. S. Second virial coefficient studies of cosolvent-induced protein self-interaction. *Biophysical Journal*, 89, 4211-4218 (2005b).

Van De Weert, M., Haris, P. I., Hennink, W. E., and Crommelin, D. J. A. Fourier transform infrared spectrometric analysis of protein conformation: Effect of sampling method and stress factors. *Analytical Biochemistry*, 297, 160-169 (2001).

Veronese, F. M., and Morpurgo, M. Bioconjugation in pharmaceutical chemistry. *Il Farmaco*, 54, 497-516 (1999).

Wanka, J., and Peukert, W. Die Bedeutung des zweiten osmotischen Virialkoeffizienten für die Proteinkristallization. *Chemie Ingenieur Technik*, 2996, 273-278 (2008).

Wetter, L. R., and Deutsch, H. F. Immunological studies on egg white proteins .4. Immunochemical and physical studies of lysozyme. *Journal of Biological Chemistry*, 192, 237-242 (1951).



Winzor, D. J., Scott, D. J., and Wills, P. R. A simpler analysis for the measurement of second virial coefficients by self-interaction chromatography. *Analytical Biochemistry*, 371, 21-25 (2007).

Yamasaki, M., Yano, H., and Aoki, K. Differential scanning calorimetric studies on bovine serum albumin: II. Effects of neutral salts and urea. *International Journal of Biological Macromolecules*, 13, 322-328 (1991).

Zhang, X., El-Bourawi, M. S., Wei, K., Tao, F., and Ma, R. Precipitants and additives for membrane crystallization of lysozyme. *Biotechnology Journal*, 1, 1302-1311 (2006).

Zimm, B. H. Application of the methods of molecular distribution to solutions of large molecules. *Journal of Chemical Physics*, 14, 164-179 (1946).

Zschornig, O., Paasche, G., Thieme, C., Korb, N., and Arnold, K. Modulation of lysozyme charge influences interaction with phospholipid vesicles. *Colloids and Surfaces B-Biointerfaces*, 42, 69-78 (2005).

---

## CHAPTER 3

### LYSOZYME INTERACTIONS IN THE DENATURED STATE DETERMINED BY SELF-INTERACTION CHROMATOGRAPHY

#### 1. INTRODUCTION

Protein aggregates denote high molecular weight species formed by several monomers. Different pathways lead to their formation and involve native-like as well as non native protein species. Even though the majority of published models on protein aggregation assume a single reactive monomer state, both native and non-native monomers can participate in aggregation (Roberts, 2007). The prevention of protein aggregation consists of the stabilization of the protein native state and of avoiding attractive intermolecular interactions between native as non-native species. Native protein molecules are usually investigated, even if the denatured states of proteins are equal in importance to the native states in determining the stability of a protein. Nevertheless, the characterization of the protein denatured state is difficult, since unfolded proteins could transform quickly into many different conformational states of similar energy (Dill and Shortle, 1991, Liu *et al.*, 2005). Thus the denatured state, which is reported to be structured and compact (Choy *et al.*, 2002), should be viewed as a distribution of many microstates that change with the solution conditions and with the protein sequence. Moreover, it depends on the nature of the stress applied (Cieplak and Sulkowska, 2005, Paci and Karplus, 2000). Indeed, for example, the unfolding pathway of ubiquitin was found random in thermal unfolding, whereas a statistically preferred unfolding order was identified upon mechanical stress (Irback and Mitternacht, 2006).

Because of structural modifications, denatured proteins are expected to interact with their environment differently than their corresponding native forms. The interactions can be studied via the virial coefficient. The virial coefficient of lysozyme has been measured by static light scattering in the presence of increasing or decreasing concentration of guanidinium chloride to characterize protein denaturation (Liu *et al.*, 2005) or protein renaturation (Ho *et al.*, 2003) respectively. However, the presence of denaturant limits the study of protein renaturation, as denaturants, e.g. guanidinium chloride, are chaotrope agents. Another method to understand protein interactions in

the denatured state lies in the comparison of interactions of lysozyme to a more hydrophobic mutant lysozyme (Curtis *et al.*, 2002), as denatured states of proteins are often described with persistent hydrophobic clusters (Dill and Shortle, 1991). Recently the virial coefficient of recombinant human interleukin-1 receptor has been characterized by SLS and membrane osmometry (Alford *et al.*, 2008) according to the protein species in solution, distinguishing the interactions of monomer-monomer from these of dimer-dimer and monomer-dimer. The irreversible dimer species was generated by incubation of the protein at 37 °C during 2 weeks and isolated by SE-HPLC. Only the interactions between dimer and monomer species were found attractive.

In order to better understand protein aggregation via unfolding in protein formulations, this study focused on the assessment of lysozyme interactions in the denatured state. To avoid the addition of chemical denaturant, thermal and mechanical stresses were preferred. The characterization of the denatured state of lysozyme was conducted by self-interaction chromatography (SIC) at high temperature. The influence of pH and salt was measured in the native and in the denatured state of lysozyme. Finally, the measured interactions were compared to the stability of lysozyme under both stirring and thermal stresses.

## 2. MATERIALS AND METHODS

### 2.1. Materials

Lysozyme from chicken egg white (135500 U/mg cryst.) was obtained from Serva (Heidelberg, Germany), Toyopearl AF Formyl 650M from Tosoh Bioscience (Stuttgart, Germany), potassium phosphate, sodium chloride, glacial acetic acid and sodium cyanoborohydride from Merck (Darmstadt, Germany), ethanolamine von VWR Prolabo (Fontenay sous bois, France) and BCA protein assay kit from Novagen (Madison, WI, USA).

All mobile phase solutions were buffered with 5 mM acetic acid at pH 3.0 and 4.5 or with 5 mM sodium phosphate at pH 6.0-8.0. Lysozyme was dissolved in the studied solutions at 20 mg/ml. The pH of the solutions was adjusted using hydrochloric acid or sodium hydroxide and measured with a pH meter Inolab level 1 from WTW (Weilheim, Germany). The protein concentrations were evaluated with an Agilent 8453 Instrument (Agilent technology, Waldbronn, Germany) at 280 nm using as extinction coefficient  $2.63 \text{ ml}\cdot\text{mg}^{-1}\cdot\text{cm}^{-1}$ .

## **2.2. Methods**

### **2.2.1. Self-interaction chromatography (SIC)**

The lysozyme immobilization and the measurement of lysozyme interactions by SIC were performed as described previously (see Chapter 2). The SIC column was tempered in a water bad at 25 °C and 80 °C for studies under native and denatured conditions respectively. The lysozyme samples were likewise tempered in the autosampler at 25 °C and 40 °C respectively.

### **2.2.2. Microcalorimetry**

The differential scanning calorimetry (DSC) thermograms of 2 mg/ml lysozyme solutions were determined in triplicate by using a Differential Scanning Calorimeter type VPDSC (Microcal, Northampton, USA) at a scan rate of 60 °C/h. Thermograms were obtained after subtraction of the corresponding buffer scan. The change in heat capacity ( $\Delta C_p$ ) corresponded to the shift of the baseline to a higher value upon completion of the transition, whereas the enthalpy change ( $\Delta H$ ) was determined by integration of the area under the peak.

### **2.2.3. Lysozyme stability**

#### **2.2.3.1 Stirring stress**

Stirring stress was performed using 10 R glass vials (Schott, Mainz, Germany) filled with 5 ml of 10 mg/ml lysozyme solution. A Teflon coated stirring bar (Carl Roth, Karlsruhe, Germany) of 12 mm length and 4.5 mm diameter was used and stirred on a R 10 power Ikamag multiple-stirrer (IKA<sup>®</sup> Werke, Staufen, Germany) at 1200 rpm (pounds per minute) at room temperature. At defined time points, a vial was removed and analyzed for protein aggregation by turbidity. As control experiments the pure buffer solutions were stirred. In addition, the protein formulations were stored at 25 °C non-stirred.

#### **2.2.3.2. Thermal stress**

Thermal stress was applied at 80 °C during 24 h in 6 R glass vials (Schott, Mainz, Germany) filled with 5 ml of 10 mg/ml lysozyme solution. The solution turbidity was checked visually at regular time intervals. As control, a pure buffer solution was heated at 80 °C.

## 3. RESULTS AND DISCUSSION

### 3.1. Protein interactions: native versus unfolded state

#### 3.1.1. Lysozyme unfolding conditions

High temperature induces protein unfolding that promotes in many cases aggregation. The melting temperature ( $T_m$ ) of lysozyme, which is defined as the midpoint of the unfolding transition, was measured by microcalorimetry as a function of the NaCl concentration. The DSC thermograms of lysozyme showed a single endothermic peak during the first scan and lysozyme unfolding started at about 65 °C for all the formulations (Fig. III-1). The  $T_m$  value of lysozyme at pH 4.5 was 77.0 °C (5 mM acetic acid) (Table III-1), corresponding to the data reported in the literature (Burova *et al.*; 2000; Elkordy *et al.*; 2008). The addition of 300 or 800 mM sodium chloride reduced the lysozyme  $T_m$  by 1.3 °C and slightly reduced  $\Delta C_p$  and  $\Delta H$ . The lysozyme thermodynamical parameters were modified in a similar manner at both salt concentrations tested. A Change in  $\Delta C_p$  is associated with protein unfolding and is a result of changes in hydration of protein side chains that are buried in the native state and that become solvent-exposed in the denatured state (Pace *et al.*, 1996). The higher  $\Delta C_p$  value of lysozyme in the absence of salt signified a higher thermal stability of this formulation as compared to the two other formulations containing sodium chloride. In addition, the higher  $\Delta H$  value of the lysozyme solution formulated without salt confirmed the higher structural stability of this solution as more thermal energy was required for unfolding. Thus, the three thermodynamic parameters  $T_m$ ,  $\Delta C_p$  and  $\Delta H$  led to the same conclusion. Lysozyme exhibited a poorer thermal stability in the presence of NaCl. Moreover, lysozyme refolded after cooling. The second scan lysozyme profiles differed slightly from the initial profiles. Unfolding began earlier at about 55 °C. The endothermic peak presented a shoulder at the beginning, which could result from a non total protein refolding.

Thus, lysozyme could be considered denatured above 80 °C at pH 4.5. Due to the molecules refolding after cooling, the measurements of interactions between denatured lysozyme molecules are to be conducted at temperature higher than its  $T_m$ . Like most proteins, denatured lysozyme may comprise a mixture of conformational isomers that exist in a state of thermodynamic equilibrium. Indeed, the structure of heat-denatured lysozyme was shown to be heterogeneous. Three main denatured lysozyme species account for about 40 % within denatured lysozyme (Chang and Li, 2002).

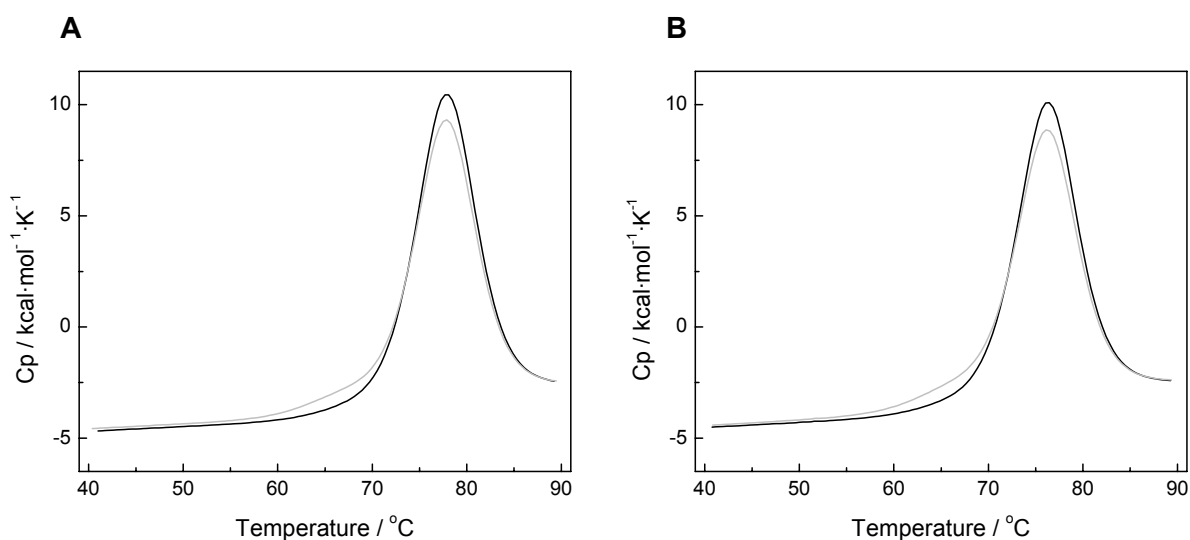


Fig. III-1: DSC thermograms of lysozyme at pH 4.5 (5 mM acetic acid) in the absence of salt (A) and in the presence of 800 mM NaCl (B): 1<sup>st</sup> scan (black) and 2<sup>nd</sup> scan (grey).

NaCl (mM)	T <sub>m</sub> (°C)	$\Delta C_p$ (kcal·mol <sup>-1</sup> ·K <sup>-1</sup> )	$\Delta H$ (kcal·mol <sup>-1</sup> )
0	77.0 ± 0.4	2.1 ± 0.2	131 ± 8
300	75.7 ± 0.3	1.8 ± 0.1	123 ± 2
800	75.7 ± 0.3	1.8 ± 0.2	122 ± 8

Table III-1: T<sub>m</sub> values,  $\Delta C_p$  and  $\Delta H$  of lysozyme solutions at different NaCl concentrations.

### 3.1.2. Characterization of the lysozyme interactions

Consequently, lysozyme interactions were measured at both 25 °C for the native form and 80 °C for the denatured form. The term second virial coefficient is not used in this context for the interactions since at high temperature the lysozyme population was heterogeneous. Only interactions between different denatured lysozyme species could be considered and an average virial coefficient was measured.

At first, the influence of pH on both native and denatured states was studied. Increasing the pH decreased the repulsive interactions between lysozyme molecules at both 25 and 80 °C (Fig. III-2). This loss of repulsive interactions was stronger at 80 °C when lysozyme was unfolded. At pH 3 and pH 4.5, when repulsive forces are predominant, the virial coefficient was only marginally reduced in the unfolded state compared to the native state. At pH 6 and 7, the attractive forces are drastically enhanced in the more hydrophobic unfolded state. In addition, the quantity of unfolded protein eluted diminished at higher pH values, reflecting the pronounced attractive interactions. The virial coefficient values measured after cooling of the column to 25 °C were close to the initial values measured at 25 °C, reflecting lysozyme renaturation. The non total refolding of the protein, as assessed by the DSC thermograms, was reflected by a slight diminution of the virial coefficients, an effect which was more pronounced with increasing pH.

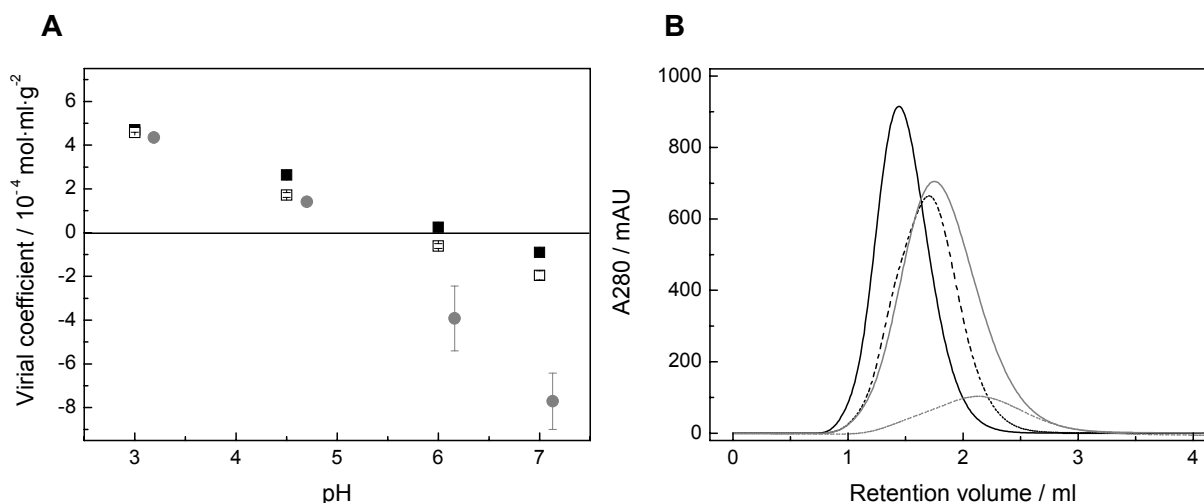


Fig. III-2: (A) Influence of pH on the virial coefficient of lysozyme at 25 °C (■), 80 °C (●) and 25 °C after renaturation (□). (B) Corresponding chromatograms of lysozyme at pH 3 at 25 °C (—) and 80 °C (- -), and pH 7 at 25 °C (—) and 80 °C (- -).

The influence of sodium chloride was studied under similar conditions. Increasing the salt concentration from 0 to 800 mM diminished the repulsive interactions at both temperatures (Fig. III-3). The attractive forces were much stronger at 80 °C and became predominant already above 300 mM NaCl as compared to 600 mM NaCl at 25 °C. In the presence of 800 mM NaCl, the lysozyme interactions were highly attractive at 80 °C with a value of  $-20 \cdot 10^{-4} \text{ mol} \cdot \text{ml} \cdot \text{g}^{-2}$ . As described previously, the quantity of protein eluted was limited as attractive interactions were predominant, most significantly at the NaCl concentration of 800 mM. In addition, the lysozyme unfolding was reversible in the presence of salt as well and interactions measured after renaturation by cooling to 25 °C were only slightly shifted towards stronger attraction as compared to the initial lysozyme  $B_{22}$  values.

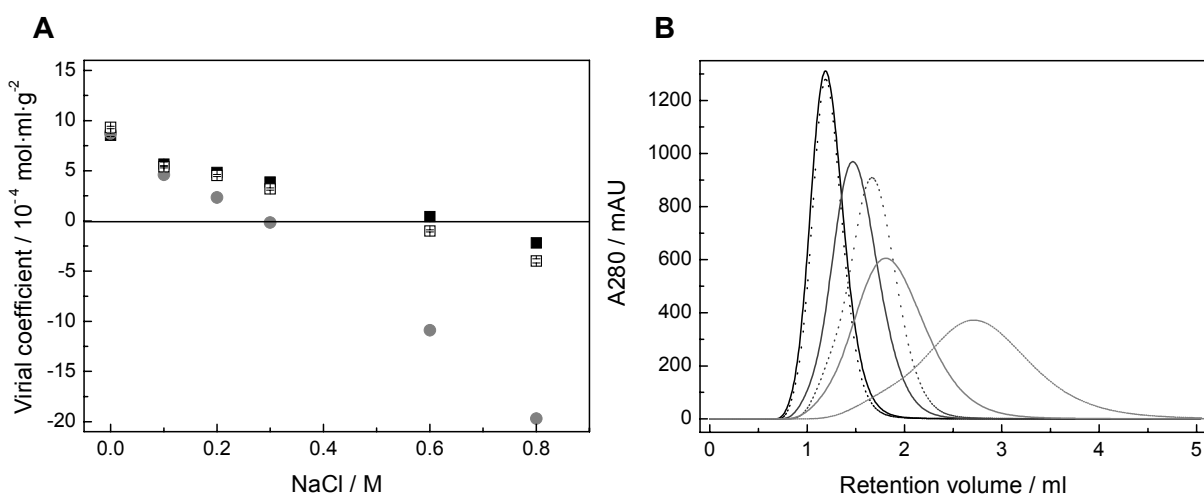


Fig. III-3: (A) Influence of NaCl on the virial coefficient of lysozyme at 25 °C (■), 80 °C (●) and 25 °C after renaturation (□). (B) Corresponding chromatograms of lysozyme for 0 mM NaCl at 25 °C (—) and 80 °C (- -), in the presence of 300 mM NaCl at 25 °C (—) and 80 °C (- -) and 800 mM NaCl at 25 °C (—) and 80 °C (- -).

Different possible mechanisms were reported for the origin of the strong attractive interactions in the denatured state. Unfolded proteins have been mainly characterized by the formation of hydrophobic clusters and small units of hydrogen bonded secondary structural elements (particularly helices or turns) (Cho *et al.*, 2008, Choy *et al.*, 2002, Dill and Shortle, 1991, Whitten and Garcia-Moreno, 2000). The hydrophobic interactions, which occur between non-polar protein surfaces, are attractive and should play a major role. The role of hydrophobic clusters in the denatured state has been emphasized by NMR studies (Klein-Seetharaman *et al.*, 2002, Neri *et al.*, 1992). Recently, electrostatic interactions have been demonstrated to be also significant in the denatured state ensemble (Bowler, 2007, Cho *et al.*, 2008), since protein molecules in the denatured state owned a high charge density and a compact form (Whitten and Garcia-Moreno, 2000). The pKa value of an ionizable group differs in the native state from the denatured state (Bowler, 2007), causing differences in the net charges and thus in the protein electrostatic repulsions. The strong dependence of lysozyme on the salt concentration may point out the probable role of hydrophobic interactions in the denatured state, since hydrophobic interactions have been already reported to increase with addition of salt (Curtis *et al.*, 2002) but also electrostatic shielding could provide a major contribution. Thus, the formation of hydrophobic clusters and electrostatic repulsions could both contribute to the observed increase in attraction of lysozyme molecules after denaturation.

## **3.2. Lysozyme stability studies**

As native and denatured protein molecules coexist in solution and can be both involved in protein aggregation, knowing the strength of the protein interactions under the two states could help in the prediction of protein stability. Furthermore, since the protein denatured state is dependent on the nature of the stress, two different kinds of stress were applied: stirring stress and thermal stress. In both studies the stability of the different formulations was assessed by turbidity measurements as indicator of insoluble protein particle formation. The influence of pH and NaCl on lysozyme stability was assessed under both stresses.

### **3.2.1. Stirring stress**

Lysozyme stability was first investigated by fast stirring (1200 rpm) of 10 mg/ml lysozyme formulations at 25 °C. All buffers showed a turbidity of 0.4-1 FNU, which did not increase during the experiment. The freshly prepared lysozyme formulations showed a turbidity at 1-1.3 FNU. For the stressed lysozyme formulations a strong



increase in turbidity was observed that intensified with increasing solution pH (Fig. III-4A) and NaCl concentration (Fig. III-4B). After stirring of the formulation at pH 8 for 24 h, its turbidity reached approx. 24 FNU, whereas the turbidity of the formulation containing 800 mM NaCl increased to 85 FNU. Furthermore, visible, insoluble particles were observed. As further reference samples, all lysozyme formulations were stored at room temperature for 24 h (no stirring). The turbidity was unaffected. Thus, stirring induced the formation of insoluble protein aggregates, which was more pronounced with increasing pH and salt concentration. Under acidic conditions, positive virial coefficient data were measured in the native and denatured states, indicating solution conditions that favored protein-protein repulsion, whereas at higher pH virial coefficient became negative for both states. Besides, in the absence of NaCl at pH 4.5, virial coefficient was positive in the native state as well as in the denatured state, revealing favorable repulsive interactions, whereas the addition of 800 mM NaCl induced strongly negative virial coefficient values in both cases, corresponding to strong attractive interactions. The addition of 300 mM NaCl gave intermediate virial coefficient numbers near zero. As stronger protein-protein repulsive interactions would be expected at high pH and low salt concentration, the stability of lysozyme stressed by stirring correlated to the virial coefficient data.

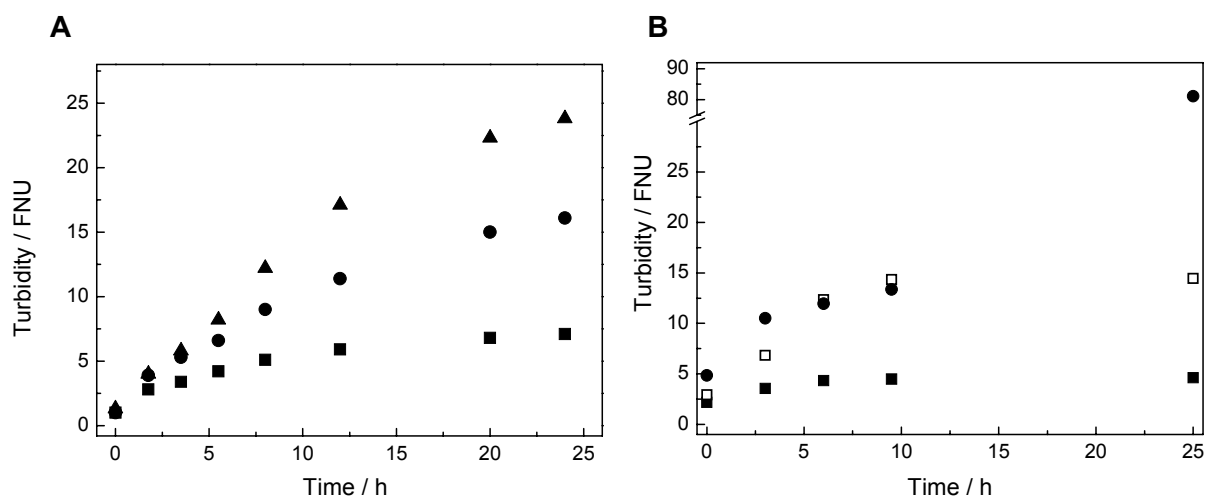


Fig. III-4: (A) Turbidity of 10 mg/ml lysozyme solutions during stirring at 1200 rpm as a function of: (A) pH in the presence of 300 mM NaCl: pH 3 (■), pH 6 (●) and pH 8 (▲), (B) NaCl concentration at pH 4.5: 0 mM NaCl (■), 300 mM NaCl (□) and 800 mM NaCl (●).

### 3.2.2. Thermal stress

For the thermal stress study, lysozyme solutions were kept at 80 °C for 24 h. Since lysozyme renatures upon cooling, the solution turbidity was assessed visually to maintain the solution temperature at 80 °C. In buffer solutions no turbidity was observed after 24 h at 80 °C. The first visual control was operated after 30 min of stress. Already at this time point the lysozyme formulations with 300 mM NaCl at pH 8

(Fig. III-5A) and with 800 mM NaCl at pH 4.5 (Fig. III-6A) showed strong precipitation. Lowering the pH of the lysozyme solutions and reducing the salt concentration delayed the haze formation. The lysozyme solution formulated with 300 mM NaCl at pH 6 became turbid after 3 h at 80 °C and the 300 mM NaCl containing formulations at pH 4.5 and 3 after 10 h and 24 h respectively. Only one solution, the formulation without NaCl in 5 mM acetic acid at pH 4.5, did not show visible aggregate formation after 24 h of stress. Its turbidity was assessed by nephelometry at the end of the thermal stress and was unchanged, whereas the turbidity of all other formulations could not be quantified since the detection limit of 1300 FNU was exceeded.

Thus, no evidence of insoluble protein aggregate formation at 80 °C was found for the formulation presenting the highest positive virial coefficients under the native and denatured states (no salt, pH 4.5), whereas the less stable formulations (300 mM NaCl at pH 8 and 800 mM NaCl at pH 4.5) exhibited the lowest virial coefficient values.

Solutions presenting unfavorable repulsive interactions measured by SIC in both native and denatured states aggregated faster and stronger under thermal stress as well as under stirring stress. The initial microcalorimetry study pointed at a higher stability of lysozyme in the absence of salt, but did not differentiate the two formulations containing NaCl. Even though changes in  $\Delta H$  reflect changes in protein hydrophobic interactions and hydrogen bonding (Pace *et al.*, 1996), the strength of protein interactions could be better evaluated with SIC. The virial coefficient measurement appears to be an alternative method to simulate the formation of protein associates and aggregates. Compared to stability studies, SIC requires lower protein quantity and reduces the time of experimentation.

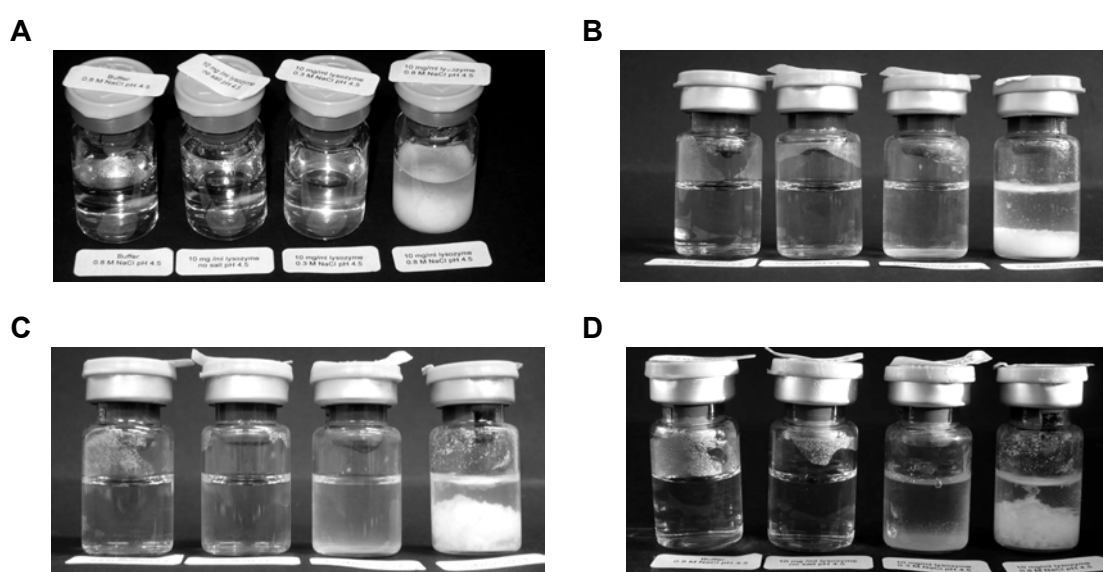


Fig. III-5: Stability of 10 mg/ml lysozyme solutions as a function of the NaCl concentration (pH 4.5) at 80 °C NaCl (samples from left to right): reference (800 mM NaCl buffer), 0 mM NaCl, 300 mM NaCl and 800 mM after 30 min (A), 3 h (B), 10 h (C) and 24 h (D).

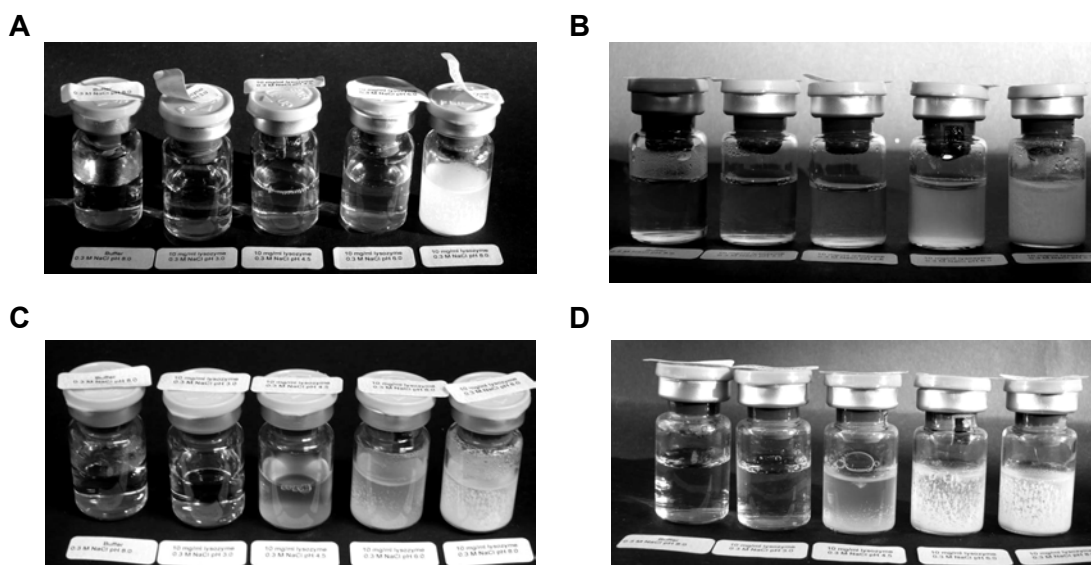


Fig. III-6: Stability of 10 mg/ml lysozyme solutions as a function of pH (300 mM NaCl) at 80 °C (samples from left to right): reference (300 mM NaCl buffer pH 8.0), pH 3.0, pH 4.5, pH 6.0 and pH 8.0 after 30 min (A), 3 h (B), 10 h (C) and 24 h (D).

## 4. CONCLUSIONS

Since lysozyme unfolds reversibly and formation of large aggregates takes time, measurement of the lysozyme interactions in the denatured state could be assessed via the virial coefficient by self-interaction chromatography at 80 °C. The lysozyme interactions in the denatured state were characterized by an average virial coefficient that represented the interactions within the heterogeneously denatured lysozyme population. The denatured state showed decreasing repulsive interactions by increasing pH and salt concentration as did the native state. The repulsive interaction decrease was almost linear for both states. However, this decrease was more pronounced in the denatured state, most likely caused by changes in electrostatic interactions and the formation of hydrophobic clusters. Moreover, in formulations stressed either by stirring or by 80 °C treatment, the lysozyme stability matched with the measured protein-protein interactions in the denatured and native states, as the conditions with less attractive interactions in both states showed better lysozyme stability.

## 5. REFERENCES

Alford, J. R., Kwok, S. C., Roberts, J. N., Wuttke, D. S., Kendrick, B. S., Carpenter, J. F., and Randolph, T. W. High concentration formulations of recombinant human interleukin-1 receptor antagonist: I. Physical characterization. *Journal of Pharmaceutical Sciences*, 97, 3035-3050 (2008).

Bowler, B. E. Thermodynamics of protein denatured states. *Molecular Biosystems*, 3, 88-99 (2007).

Chang, J. Y., and Li, L. The unfolding mechanism and the disulfide structures of denatured lysozyme. *FEBS Letters*, 511, 73-78 (2002).

Cho, J. H., Sato, S., Horng, J. C., Anil, B., and Raleigh, D. P. Electrostatic interactions in the denatured state ensemble: Their effect upon protein folding and protein stability. *Archives of Biochemistry and Biophysics*, 469, 20-28 (2008).

Choy, W. Y., Mulder, F. A. A., Crowhurst, K. A., Muhandiram, D. R., Millett, I. S., Doniach, S., Forman-Kay, J. D., and Kay, L. E. Distribution of molecular size within an unfolded state ensemble using small-angle X-ray scattering and pulse field gradient NMR techniques. *Journal of Molecular Biology*, 316, 101-112 (2002).

Curtis, R. A., Steinbrecher, C., Heinemann, A., Blanch, H. W., and Prausnitz, J. M. Hydrophobic forces between protein molecules in aqueous solutions of concentrated electrolyte. *Biophysical Chemistry*, 98, 249-265 (2002).

Dill, K. A., and Shortle, D. Denatured states of proteins. *Annual Review of Biochemistry*, 60, 795-825 (1991).

Ho, J. G. S., Middelberg, A. P. J., Ramage, P., and Kocher, H. P. The likelihood of aggregation during protein renaturation can be assessed using the second virial coefficient. *Protein Science*, 12, 708-716 (2003).

Irbach, A., and Mitternacht, S. Thermal versus mechanical unfolding of ubiquitin. *Proteins-Structure Function and Bioinformatics*, 65, 759-766 (2006).

Klein-Seetharaman, J., Oikawa, M., Grimshaw, S. B., Wirmer, J., Duchardt, E., Ueda, T., Imoto, T., Smith, L. J., Dobson, C. M., and Schwalbe, H. Long-range interactions within a nonnative protein. *Science*, 295, 1719-1722 (2002).

Liu, W., Cellmer, T., Keerl, D., Prausnitz, J. M., and Blanch, H. W. Interactions of lysozyme in guanidinium chloride solutions from static and dynamic light-scattering measurements. *Biotechnology and Bioengineering*, 90, 482-490 (2005).

Neri, D., Billeter, M., Wider, G., and Wuthrich, K. NMR determination of residual structure in a urea-denatured protein, the 434-repressor. *Science*, 257, 1559-1563 (1992).

Pace, C. N., Shirley, B. A., McNutt, M., and Gajiwala, K. Forces contributing to the conformational stability of proteins. *The FASEB Journal*, 10, 75-83 (1996).

Roberts, C. J. Non-native protein aggregation kinetics. *Biotechnology and Bioengineering*, 98, 927-938 (2007).

Whitten, S. T., and Garcia-Moreno, B. pH dependence of stability of staphylococcal nuclease: Evidence of substantial electrostatic interactions in the denatured state. *Biochemistry*, 39, 14292-14304 (2000).

---

## CHAPTER 4

# EVALUATION OF THE OSMOTIC SECOND VIRIAL COEFFICIENT IN PROTEIN FORMULATION: A CASE STUDY OF A MONOCLONAL ANTIBODY

## 1. INTRODUCTION

As proteins have poor bioavailability by most routes, protein drugs are usually administered intravenously that favors a good control during clinical administration (Shire *et al.*, 2004). Nowadays protein therapies go by increasing use of antibody pharmaceuticals because of their more specific action and their potential conjugated action to another therapeutic drug, enhancing its delivery and its efficacy (Wang *et al.*, 2007). Antibodies play a major role in the treatment of many diseases such as cancer, infections diseases, allergy, autoimmune diseases and inflammation. In numerous cases monoclonal antibodies have to be administered frequently and at high doses. To improve patient compliance, subcutaneous dosage forms are favored leading to a small injection volume with a high protein dose. Consequently, high concentrated protein formulations (up to 150 mg/ml) with good protein stability are required, which also raises challenges in manufacturing.

Reaching high concentrated protein formulations needs the control of both chemical and physical stability. The main physical instability lies in protein aggregation that can be prevented by two main mechanisms: the first one consists of increasing the thermodynamic stability of the protein native state, shifting the equilibrium away from unfolded protein, the latter being also more prone for aggregation. The second route is based on improving the protein's colloidal stability by reducing attractive protein-protein interactions (Chi *et al.*, 2003b). Beyond this, it is also possible to design the protein framework such to avoid hot spots prone for the formation of protein aggregates (Baynes and Trout, 2004, Broglia *et al.*, 1998, Dudgeon *et al.*, 2009, Trovato *et al.*, 2007).

The screening of formulation parameters that are suitable for high concentrated protein formulation requires adapted analytical methods that notably minimize the protein quantity. Furthermore, analytical methods avoiding sample dilution before acquiring

data should be preferred, as the study of the diluted protein solution may not be representative of the high concentration solution. Protein structural changes of high concentration protein solutions were directly characterized by differential scanning calorimetry (DSC), front surface fluorescence spectroscopy, circular dichroism (CD) and Fourier transform infrared spectroscopy (FTIR) (Harn *et al.*, 2007), whereas protein interactions were studied by static light scattering (SLS), isothermal titration calorimetry (ITC) (Alford *et al.*, 2008a, 2008b), ultrasonic storage modulus (Saluja *et al.*, 2007) or sedimentation equilibrium and osmotic pressure (Jimenez *et al.*, 2007). Besides, the strength and the range of protein colloidal interactions can be evaluated by the osmotic second virial coefficient ( $B_{22}$ ), which measures the non-ideal solution behavior arising from two body interactions. As  $B_{22}$  of diluted protein solutions has been shown to correlate with  $B_{22}$  of concentrated protein solutions (Haynes *et al.*, 1992),  $B_{22}$  measurements may be realized under diluted conditions and be representative of concentrated protein solutions.

Determining the strength of protein-protein interactions via  $B_{22}$  could be used for formulation screening even if it was mostly studied with model proteins such as lysozyme mainly with SLS methods (Bonnete *et al.*, 1999, Liu *et al.*, 2004) and self-interaction chromatography (SIC) (Johnson *et al.*, 2009, Tessier *et al.*, 2002). Only few data of therapeutic relevant proteins are available. SIC was recently used to establish the crystallization conditions of a MAb (Ahamed *et al.*, 2007). By correlating phase diagrams with  $B_{22}$  data, Ahamed and co-workers provided useful information not only for a fundamental understanding of the phase behaviour of monoclonal antibodies, but also for understanding the reason why certain proteins are extremely difficult to crystallize.

$B_{22}$  of different MAbs was also studied by sedimentation equilibrium to determine reversible self-association mediated by electrostatic interactions (Liu *et al.*, 2005). The effect of buffer on the stability of interferon-tau (IFN-tau) was compared to  $B_{22}$  determined by SIC (Katayama *et al.*, 2006) indicating that histidine buffer, which gave the better stabilization of IFN-tau during the thermal stress, had a minor effect on the colloidal stabilization of IFN-tau, as the buffer species had little effect on  $B_{22}$ . The study of an IgG2 showed that the  $B_{22}$  analysis based on light scattering was consistent with rheology studies (Bajaj *et al.*, 2006, Saluja *et al.*, 2007), but no correlation was found between  $B_{22}$  and long-term aggregation as the transition to the IgG2 unfolded state was first responsible for protein aggregation. Similarly, the stability of recombinant human granulocyte colony-stimulating factor (rh-GCSF) was compared to the free energy of protein unfolding and  $B_{22}$  measured by SLS. No correlation between  $B_{22}$  and protein stability was evident given that the rh-GCSF aggregation first involved perturbation of

its native structure (Chi *et al.*, 2003a). Lastly, Alford and co-workers (2008a, 2008b) measured the attraction forces between monomer-monomer ( $B_{22}$ ), monomer-dimer ( $B_{23}$ ) and dimer-dimer ( $B_{33}$ ) of recombinant human interleukin-1 receptor antagonist (rhIL-1ra) by membrane osmometry and SLS to differentiate the contribution of the different protein species and showed that only the interactions between monomer-dimer were attractive. By incubation of 100 mg/ml rhIL-1ra solutions at 37 °C, the attractive monomer-dimer interactions conducted to the formation of a trimer form, which was the rate-limiting step in rhIL-1ra aggregation.

Overall,  $B_{22}$  was a poor predictive tool of protein stability in those previous examples, since the colloidal stability was not the rate-limiting step of protein aggregation. Even if the correlation of  $B_{22}$  to protein solubility has been already demonstrated with lysozyme, ovalbumin or equine serum albumin (Demoruelle *et al.*, 2002, Guo *et al.*, 1999), little interest was shown in the prediction of the solubility of therapeutic proteins with  $B_{22}$ . Only  $B_{22}$  of *Pseudomonas* amylase determined by SIC was compared and correlated to its solubility and its enzymatic activity (Valente *et al.*, 2006).

This work was focused on the application of SIC for a monoclonal antibody type IgG1. At first, the SIC parameters were established. Subsequently, the influence of the following solution conditions was tested with regard to interactions between the IgG1 molecules: (a) protonation degree of IgG1 (pH); (b) buffer species and their concentration; (c) NaCl concentration; (d) presence of amino acids; and (e) presence of mannitol or sucrose. Finally,  $B_{22}$  was compared to IgG1 solubility and IgG1 stability to evaluate its impact as a screening tool for protein formulation.

## 2. MATERIALS AND METHODS

### 2.1. Materials

A humanized monoclonal IgG1 antibody, which was formulated as a 5 mg/ml solution in phosphate buffered saline (PBS) at pH 6.2, was provided by Boehringer Ingelheim. Toyoperal AF Formyl 650M was obtained from Tosoh Bioscience (Stuttgart, Germany), sodium acetate, sodium chloride, sodium citrate, sodium cyanoborohydride, L-arginine monohydrochloride, L-histidine and L-methionine from Merck (Darmstadt, Germany), ethanolamine form Prolabo (Fontenay sous bois, France), sodium phosphate and mannitol from Riedel-de Haën (Seelze, Germany), sodium succinate from Alfa Aesar (Karlsruhe, Germany), glycine, 4,4'-dianilino-1,1'-binaphthyl-5,5' disulfonic acid (Bis-ANS) and ethylenediaminetetraacetic acid (EDTA) from Sigma Aldrich (Steinheim, Germany), sucrose from Suedzucker (Mannheim, Germany) and BCA protein assay kit from Novagen (Madison, WI, USA).



The pH of the solutions was adjusted using hydrochloric acid or sodium hydroxide and measured with a pH meter Inolab level 1 from WTW (Weilheim, Germany). The protein concentrations were evaluated with an Agilent 8453 instrument (Agilent technology, Waldbronn, Germany) at 280 nm using as extinction coefficient  $1.44 \text{ ml}\cdot\text{mg}^{-1}\cdot\text{cm}^{-1}$ .

## 2.2. Methods

### 2.2.1 IgG1 immobilization

3 ml Toyopearl AF Formyl 650M particles were washed on a glass frit with  $0.2 \mu\text{m}$  hydrophilic polyethersulfone membrane filter with first 250 ml de-ionized water and secondly 50 ml of 0.1 M potassium phosphate buffer pH 7.5. The washed particles were recovered and mixed with 10 ml IgG1 solution (5.0 mg/ml in 0.1 M potassium phosphate buffer pH 7.5) and 90 mg sodium cyanoborohydride was added as activator of protein binding. The suspension was mixed over night on a rotary mixer. At the end of the coupling reaction the particles were first washed with 200 ml of 0.1 M potassium phosphate buffer to remove unbound protein and then added to 15 ml of 1 M ethanolamine pH 8.0 and 20 mg sodium cyanoborohydride to cap the remaining active groups of the matrix. The suspension was incubated on a rotary mixer for 4 h. At the end of the reaction the particles were washed with 200 ml of 1M sodium chloride solution pH 7.0. The amount of bound IgG1 was determined both by analyzing the difference between the absorbance of the initial protein solution and the wash solutions (A280) and in addition by determining the immobilized protein quantity directly by BCA protein assay.

The chromatography particles were suspended as a 50 % slurry in 1 M NaCl and 50 mM sodium phosphate solution pH 6.0. Approximately 2.5 ml slurry was packed in a Tricorn<sup>®</sup> 5/50 column (GE Healthcare, Uppsala, Sweden) with the same buffer at 3 ml/min flow rate during 15 min using a FPLC system (Äkta Purifier, GE Healthcare, Uppsala, Sweden). At the end of the packing procedure the flow rate was maintained to 0.75 ml/min for at least 1 h. Columns were stored at 4 °C in a 5 mM sodium phosphate solution pH 7.0 containing 0.05 % sodium azide.

### 2.2.2. ATR-FTIR adsorption spectra and second derivatives

FTIR spectroscopy measurements were conducted with a Tensor 37 spectrometer (Bruker Optics, Ettlingen, Germany). Filtered samples were dried overnight at room temperature and measured by the attenuated total reflection (ATR) technique with the MVP unit at 20 °C. Each sample measurement was the average of 120 scans and was measured 3 times. The spectra were collected from  $4000$  to  $1000 \text{ cm}^{-1}$  with a  $4 \text{ cm}^{-1}$

resolution. The particle spectrum was manually subtracted from the bound protein particle spectrum and the protein spectra were further processed by vector normalization on the amide I band.

### 2.2.3. Fluorescence spectroscopy

Fluorescence spectroscopy measurements were conducted with a Cary Eclipse spectrophotometer (Varian, Darmstadt, Germany) with a solid sampler holder. 4 nmol of Bis-ANS were added to the chromatographic particle suspensions. Samples were homogenized and then centrifuged to separate particles from solution. Particle fractions were placed in the solid sample holder, excited at 385 nm and the emission measured from 400 to 600 nm.

### 2.2.4. Determination of the osmotic second virial coefficient

$B_{22}$  measurements were realized with a FPLC Äkta Purifier system equipped with an UV detector (A280) and an auto-sampler. Before each run the column was equilibrated with 10 ml of the protein free mobile phase. The column dead volume was estimated by injection of a 1 % acetone solution. All experiments were carried at 25 °C and at a flow rate of 0.3 ml/min. 0.1 mg of IgG1 was injected. Each sample was measured 3 times. Chromatogram peaks were analyzed with the UNICORN® software (GE Healthcare, Uppsala, Sweden). The retention volume was determined at the peak maximum. The retention measurements were used to calculate the retention factor  $k'$  (equation 1):

$$k' = \frac{V_o - V_r}{V_o} \quad (1)$$

where  $V_r$  is the volume required to elute the protein in the mobile phase and  $V_o$  is the retention volume of non-interacting species (e.g. acetone).  $B_{22}$  is related to the retention factor as follow (Tessier *et al.*, 2002):

$$B_{22} = B_{HS} - \frac{k'}{\rho_s \Phi_2} \quad (2)$$

$$B_{HS} = \frac{16}{3} \pi r^3 \frac{N_A}{M_2^2} \quad (3)$$

where  $\rho_s$  is the number of immobilized molecules per unit area,  $\Phi$  is the phase ratio, which is the total surface available to the mobile phase protein,  $r$  is the protein radius,  $N_A$  is the Avogadro's number and  $M_2$  is the protein (index 2) molecular weight.  $\rho_s$  was calculated by dividing the immobilized concentration by the porosity (0.811 for Toyopearl AF Formyl 650M) and the phase ratio of one IgG1 molecule. As the IgG1 had a radius of 5.8 nm, which was calculated from the molecular volume of the protein, and a molecular weight of 146 kDa, the following phase ratios of IgG1 were taken:

15.4 m<sup>2</sup>/ml for  $\Phi_1$  (5.8 nm) and 6.3 m<sup>2</sup>/ml for  $\Phi_2$  (17.5 nm) (DePhillips and Lenhoff, 2000). The first value corresponds to the phase ratio of one IgG1 molecule that was used to determine  $\rho_s$ , whereas the second one value represents the phase ratio of three molecules, which represents two molecules immobilized and one free molecule and corresponds to the  $\Phi_2$  value in the equation 2.

### **2.2.5. Determination of the IgG1 net charge**

The IgG1 molecule net charge was calculated with the EMBOSS software (Rice *et al.*, 2000).

### **2.2.6. Turbidity**

Turbidity was measured as photometric absorbance at 350 nm against WFI as blank value in triplicate with a Fluostar Omega microplate reader (BMG Labtech, Offenburg, Germany). The reference suspensions described in the European Pharmacopeia present the following absorbance at 350 nm (Mahler *et al.*, 2005): Ref. I  $<17 \pm 2$  mAbs, Ref. II  $<32 \pm 3$  mAbs, Ref. III  $<85 \pm 1$  mAbs and Ref. IV  $<144 \pm 5$  mAbs.

### **2.2.7. Size exclusion high performance liquid chromatography (SE-HPLC)**

SE-HPLC was used to determine the amount of soluble protein aggregates in the IgG1 solutions. The measurements were performed on a HP 1100 instrument (Agilent Technology, Waldbronn, Germany) in connection with a SWXL guardcolumn and a TSK3000SWXL column (Tosoh Bioscience, Stuttgart, Germany). The mobile phase consisted of 0.05 M sodium-dihydrogen phosphate dihydrate and 0.6 M sodium chloride and was adjusted to pH 7.0 with NaOH 2 N. The flow rate was 0.5 ml/min, the injection volume 10  $\mu$ l and the UV signal was detected at 280 nm. For the specific detection of unfolded protein species 10  $\mu$ M Bis-ANS were added to the sample solutions. The fluorescence detection was performed with a Spectra system FL3000 fluorescence detector (Thermo, Dreieich, Germany) at the excitation wavelength of 385 nm and the emission was recorded at 485 nm.

### **2.2.8. Microcalorimetry**

The DSC thermograms of 2 mg/ml IgG1 solutions were determined in triplicate by using a Differential Scanning Calorimeter of type VPDSC (Microcal, Northampton, USA) at a scan rate of 60 °C/h. Thermograms were obtained after subtraction of the corresponding buffer scan.

### **2.2.9. Lyophilization**

IgG1 was diafiltrated into water and concentrated to 48.0 mg/ml by tangential flow filtration using a 30 kDa MWCO polyethersulfone membrane (Pall Filtron Ultracel Lab, Schleicher & Schuell, Dassel, Germany). 3.8 ml of the IgG1 solution were dried in 10R vials from Schott (Mainz, Germany) in the Epsilon 2-12D freeze-drier (Christ, Osterrode, Germany). The samples were frozen first to -40 °C with a cooling rate of 1 °C/min and finally to -45 °C with a cooling rate of 0.17 °C/min. Primary drying was conducted at a shelf-temperature of -30 °C and a pressure of 0.05 mbar. For secondary drying the shelf-temperature was increased to -15 °C while the pressure was kept constant at 0.05 mbar.

### **2.2.10. Viscosity**

The sample viscosity was measured with a MCR100 rheometer (Anton Paar, Ostfildern, Germany) using a CP50-1 cone and plate measuring system. Approximately 600 µl sample were loaded onto the plate measuring system and were allowed to come to thermal equilibrium at 20 °C. The sample viscosity was measured by applying a shear rate over a range of 10-3000 s<sup>-1</sup>.

## **3. RESULTS AND DISCUSSION**

### **3.1. Establishment of B<sub>22</sub> measurement via SIC for the IgG1**

#### **3.1.1. Protein characterization after binding on chromatography particles**

The SIC method consists of the immobilization of the studied protein on chromatography particles and of the injection of the same initial protein, in various solution conditions, to measure free protein - immobilized protein interactions. IgG1 primary amines can be coupled to the aldehyde-bearing Toyopearl AF Formyl 650 chromatography particles under mild conditions, resulting in the formation of stable secondary amine linkage between IgG1 and the resin. Protein binding to chromatography resins can be characterized by electro-acoustic measurements that reflect small changes in resins according to their environment (Muller and Mann, 2007). Structural modifications of the protein can be determined with spectroscopic methods such as FTIR spectroscopy, CD or fluorescence spectroscopy. Specifically FTIR spectroscopy allows analysis of the protein's secondary structure. The protein structure can be studied focusing on the amide I band located near 1650 cm<sup>-1</sup>, reflecting C=O stretching vibrations, the amide II and the amide III bands located near 1550 cm<sup>-1</sup> and

1300  $\text{cm}^{-1}$  respectively, reflecting both N-H and C-N bending vibrations. Especially the amide I band, which is the sum of sub-bands, is used to assign protein secondary structural elements, as a significant shift towards higher wavenumbers, broadening and loss in intensity are signs of structural difference (Pelton and Mclean, 2000).

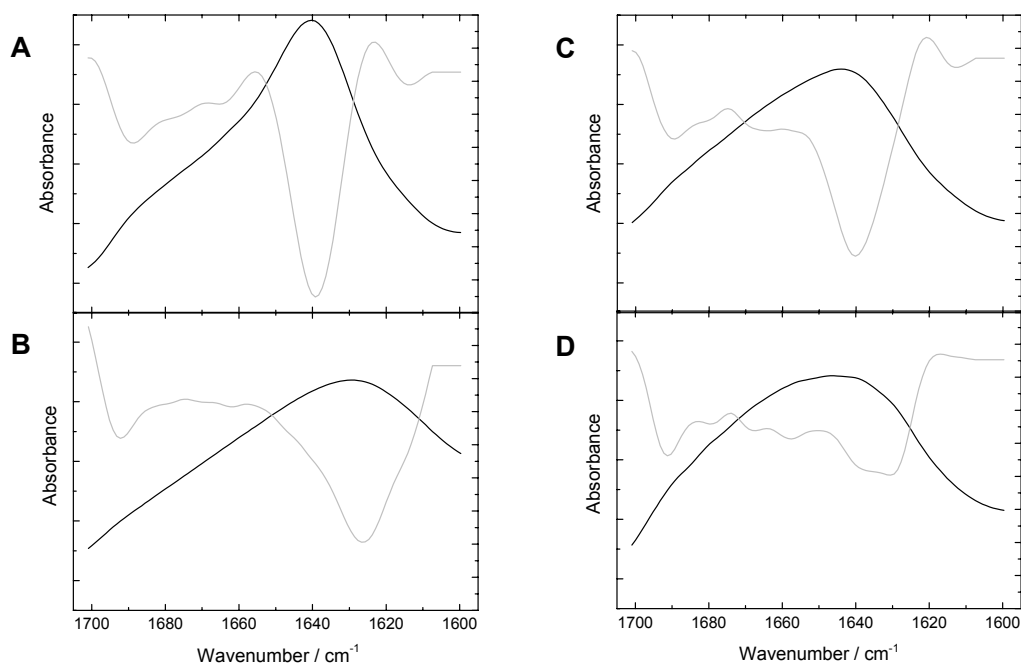


Fig. VI-1: ATR-FTIR adsorption spectra (black) and second derivatives (light gray) of IgG1 (A), IgG1 after thermal stress (95°C, 1h) (B), immobilized IgG1 (C), immobilized IgG1 after thermal stress (95 °C, 1h) (D) measured at 20°C.

The second derivative spectrum of the amide I band of the native IgG1 measured in transmission (Fig. IV-1) was characterized by three sub-bands at 1614, 1639 and 1690  $\text{cm}^{-1}$  that are typical for IgGs having a predominant  $\beta$ -sheet secondary structure (Bandeekar, 1992, Byler and Susi, 1986, Dong *et al.*, 1997). IgG1 bound to Toyopearl particles was characterized by a main band at 1640  $\text{cm}^{-1}$  and two small bands at 1687 and 1611  $\text{cm}^{-1}$ . Although the overall band shape is slightly altered, no major structural change could be detected due to the protein binding process. Thus the protein secondary structure is mainly retained after coupling of the antibody to the chromatography particles.

This trend could be confirmed by comparison with thermally stressed sample spectra (95 °C for 1h). Both IgG1 in solution and immobilized IgG1 samples showed a decrease in intensity and a shift in wavelength for the main band compared to the initial samples. In the spectra of thermally treated protein, the band detected around 1620-1630  $\text{cm}^{-1}$  originates from intermolecular antiparallel  $\beta$ -sheet formation (van de Weert *et al.*, 2001), which are often observed during protein denaturation and aggregation.

The similar behavior with temperature treatment of the bound and the unbound IgG1 points to a similar nature after binding and mainly structural integrity.

### 3.1.2. Chromatogram analysis: retention volume determination

Usual chromatogram analysis to determine the retention volume is based on the peak maximum assuming that peak is symmetric. However chromatograms deriving from self-interaction chromatography do not necessarily present this alleged symmetry. Moreover a shoulder or a second peak could appear. Thus, other modes of retention volume determination could be more appropriate such as the use of the point at 50 % of the total area under the curve (AUC) or at 50 % AUC of the 1<sup>st</sup> peak, if a 2<sup>nd</sup> peak appears, or based on the centre of gravity.

The influence of chromatogram analysis on the obtained  $B_{22}$  values of IgG1 was tested for samples with varying pH and mannitol concentration. Because of the peak asymmetry (symmetry coefficient >1), considering the peak maximum resulted in higher  $B_{22}$  values compared to determining it at 50 % of the total AUC (Fig. IV-2). Even though the resulting  $B_{22}$  values differed slightly, both procedures gave the same trend for the pH influence, as in both cases the  $B_{22}$  decrease was steadily. In the case of the mannitol study, because of the appearance of a second peak probably reflecting the presence of a second protein species, focusing on the 1<sup>st</sup> peak to determine the retention volume overestimated  $B_{22}$  compared to its calculation at 50 % of the total AUC. As the easiest method of calculation was the evaluation of the peak maximum,  $B_{22}$  was determined using with this parameter, if the chromatograms showed only one peak.

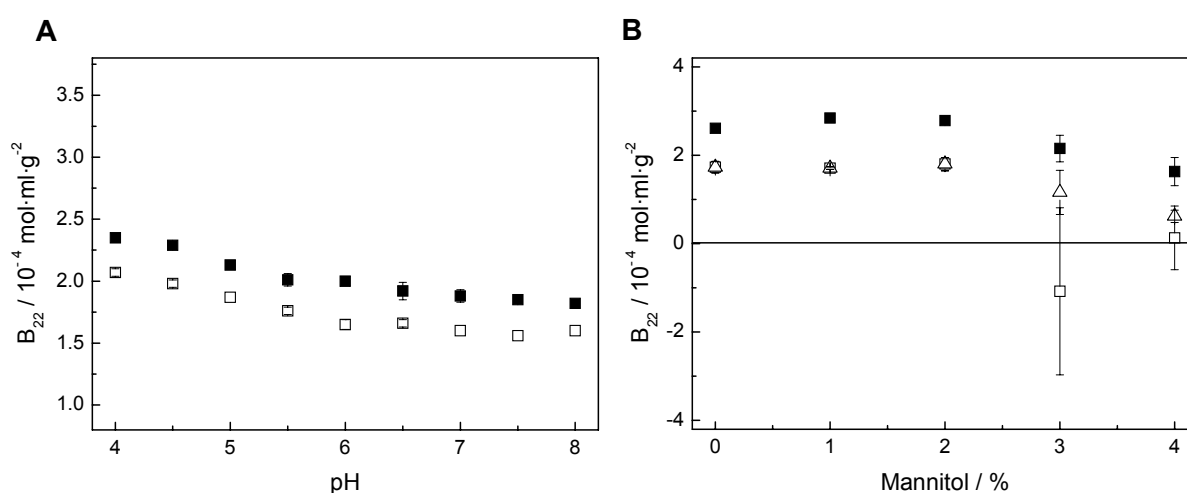


Fig. IV-2: Effect of retention volume determination on  $B_{22}$  value of IgG1 with regard to (A) pH solution, (B) mannitol concentration; retention volume at the peak maximum (■), retention volume at 50 % of the total AUC (□), retention volume at 50 % of the AUC of the 1<sup>st</sup> peak (△).

### 3.1.3. Influence of chromatography parameters on $B_{22}$ of IgG1

#### 3.1.3.1. Flow rate

Since equilibrium should be reached in the chromatography system in order to measure  $B_{22}$ , the retention volume of free protein could be influenced by the flow rate, which also determines the time of analysis and thus throughput of the screening method. The flow rate influence was tested from 0.10 ml/min to 0.75 ml/min (Fig. IV-3).

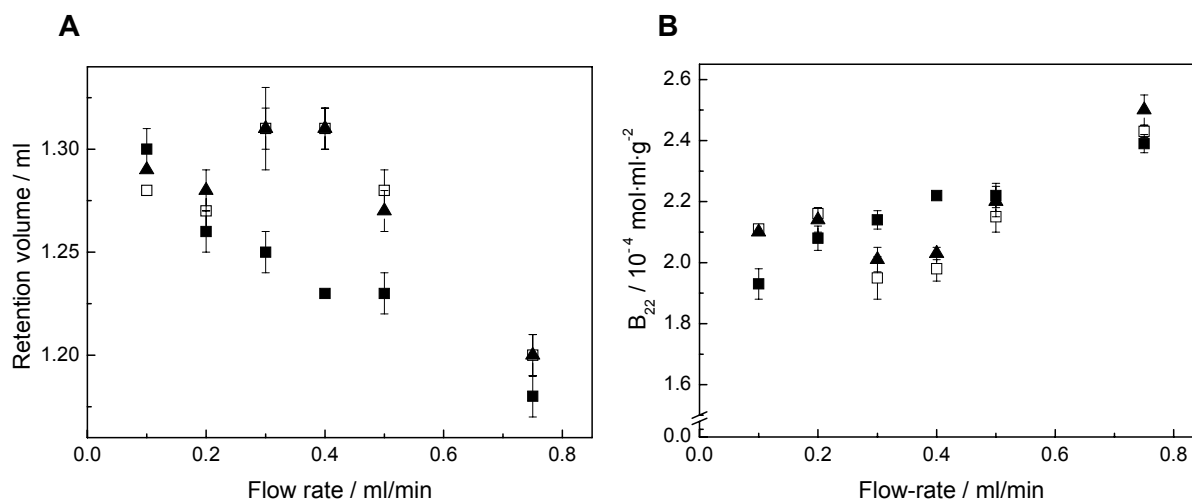


Fig. IV-3: Effect of flow rate on retention volume (A) and  $B_{22}$  value (B) of IgG1 as a function of NaCl concentration in the presence of 50 mM sodium phosphate buffer pH 6.0 at a loading of 16 mg/g: no salt (■), 300 mM NaCl (□) and 800 mM NaCl (▲).

An increase in flow rate led a gradual but not linear decrease in retention volume. The flow rate had however no influence on the scatter of the results and the standard deviations. In the absence of salt the retention volume decreased gradually with increasing flow rate whereas in the presence of salt buffers retention volume remained constant until 0.4 ml/min subsequently followed by a decrease. Increasing the flow rate minimized differences in the  $B_{22}$  values, decreasing the sensitivity of the system to changing effects on  $B_{22}$ . A too high flow rate diminished the interaction time between free IgG1 molecules and immobilized IgG1 molecules by forcing protein motion. A plateau in  $B_{22}$  values resulted at flow rates of 0.3 and 0.5 ml/min. Two different trends were observed at flow rates slower than 0.3 ml/min: In the presence of 50 mM phosphate buffer only,  $B_{22}$  decreased whereas  $B_{22}$  was became higher in presence of 300 or 800 mM sodium chloride. However it was expected that increasing sodium chloride concentration screened protein-protein interactions and thus should decrease  $B_{22}$ . This salt effect was only observed for the flow rate comprised between 0.3 and 0.5 ml/min that promoted equilibrium and interactions between IgG1 molecules. Slower flow rate could perturb  $B_{22}$  values seem to result in holding excessively free protein molecules at the surface of immobilized protein molecules leading to distorting

protein elution. Contrary to Garcia and co-workers (2003), decreasing the flow rate did not infinitely improve resolution and sensitivity. In the studies the favorable flow rate was between 0.3 and 0.5 ml/min due to robust results and short analysis.

### 3.1.3.2. Protein concentration

The  $B_{22}$  coefficient describes the interactions between two bodies of the same species by the mean force, which depends on the separation of the two bodies and is a function of all orientations.  $B_{22}$  measurement via SIC is based on the assumption that the interactions between one immobilized protein molecule and one free protein molecule are the same as between two free protein molecules. The outcome of SIC analysis should depend on interaction between immobilized neighboring molecules and the ability of the coupled protein to interact with different orientation. Consequently, the SIC results could be affected by the protein surface coverage of the chromatography resin and the free protein concentration in the mobile phase.

#### 3.1.3.2.1. Injection quantity

The influence of the IgG1 quantity injected was tested in the presence of 300 mM NaCl in 50 mM sodium phosphate buffer at pH 6.0 under constant surface coverage (16 mg/ml), flow rate (0.5 ml/min) and temperature (25 °C) conditions. Increasing the protein quantity from 0.1 to 0.3 mg did not have an influence on the retention volume (Fig. IV-4); AUC and peak height increased proportionally. No significant difference in  $B_{22}$  values was observed ( $2.31 \cdot 10^{-4}$  mol·ml·g<sup>-2</sup>). Given that  $B_{22}$  values were constant and that chromatogram responses were linear, an average protein quantity of 0.1 mg was chosen for the next experiments. The lower level was selected in order to avoid any potential overloading.

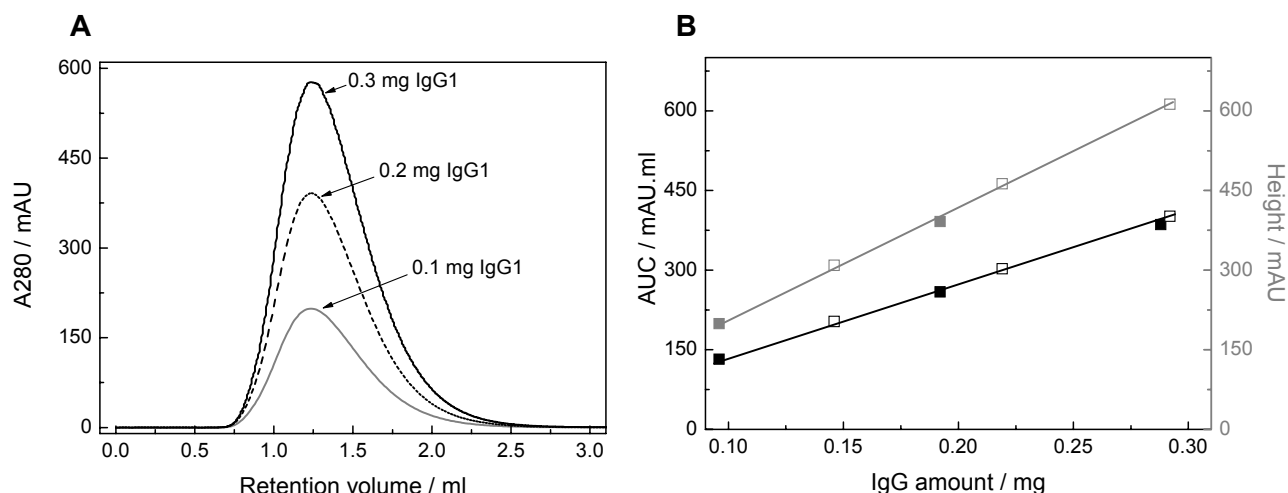


Fig. IV-4: Effect of IgG1 quantity injected on (A) peak shape and peak position and (B) area under the curve (black) and peak height (gray), with 10 mg/ml IgG1 solution (■) and 15 mg/ml IgG1 solution (□) in the presence of 300 mM NaCl and 50 mM sodium phosphate buffer pH 6.0 (flow rate 0.5 ml/min and column loading of 16 mg/g).



### 3.1.3.2.2. Surface coverage

The influence of salt on the  $B_{22}$  of IgG1 was tested at two different protein surface coverages: 11 mg/g and 17 mg/g (Fig. IV-5A). At low surface coverage (11 mg/g) sodium chloride affected  $B_{22}$  only at high concentration. Increasing sodium chloride concentration above 100 mM decreased  $B_{22}$  values and NaCl screened electrostatic repulsions. However at higher surface coverage (17 mg/g) increasing the NaCl concentration until 150 mM had only marginal influence on  $B_{22}$  ( $B_{22}$  values about  $1.60 \cdot 10^{-4} \text{ mol} \cdot \text{ml} \cdot \text{g}^{-2}$ ) and  $B_{22}$  values were smaller than those obtained with the lower surface coverage. According to Liu et al., the addition of 150 mM NaCl had a negative effect on  $B_{22}$  of two different monoclonal antibodies (Liu *et al.*, 2005) and was responsible for a  $B_{22}$  decrease by one unit. This salt influence matched with the results obtained with the low surface coverage column.

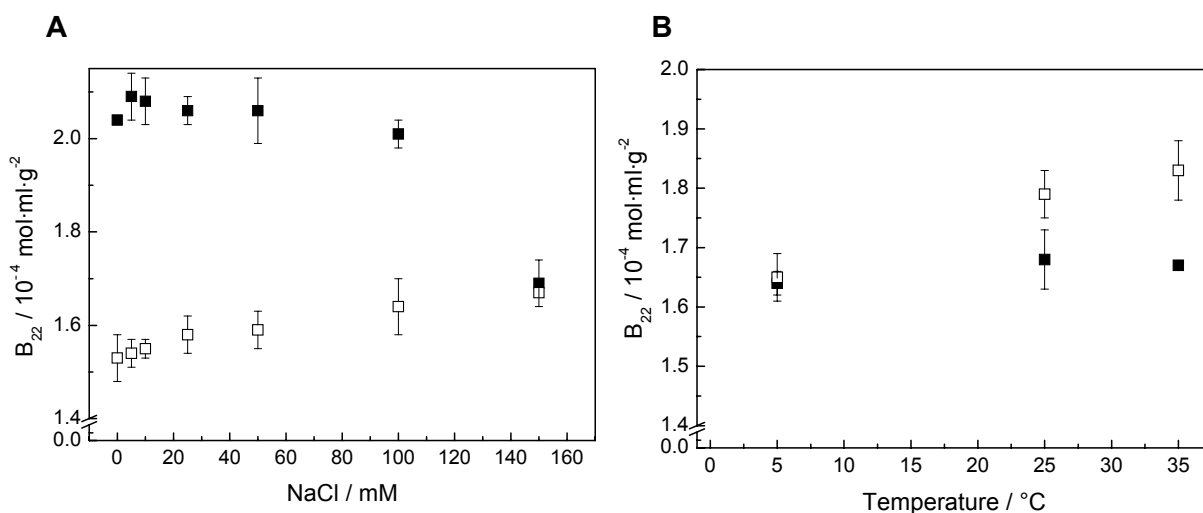


Fig. IV-5: (A) Effect of surface coverage on  $B_{22}$  value of IgG1 at varying NaCl concentration in the presence of 5 mM sodium succinate pH 6.2: 11 mg/g (■) and 17 mg/g (□).

(B) Effect of temperature from 5 °C to 35 °C on  $B_{22}$  value of IgG1 in the presence of 5 mM sodium succinate pH 6.2 at a loading of 17 mg/g: 10 mM NaCl (■) and 150 mM NaCl (□).

Raising the immobilized protein quantity increased protein density and thus protein molecule proximity, reducing the interaction volume between adjacent protein molecules at higher surface coverage. If protein molecules were close enough, they could interact cooperatively with free molecules causing strongly absorbing sites (Tessier *et al.*, 2002). Moreover protein-protein interaction forces are influenced by the protein concentration in solution (Saluja and Kalonia, 2008). In dilute protein solutions, electrostatic and hydrophobic interactions are the predominant forces, whereas hydrogen bonding, van der Waals forces and excluded volume constitute minor forces. Increasing the protein concentration reduces the importance of electrostatic interactions and increases the effect of excluded volume and van der Waals forces. Given that salts screen protein electrostatic repulsions,  $B_{22}$  measurements were more

sensitive to protein concentration in the presence of higher sodium chloride concentration. Thus higher IgG1 immobilization minimized the effect of electrostatic repulsion induced by salt and no changes in  $B_{22}$  were measured. Consequently, a lower surface coverage should be preferred for  $B_{22}$  studies.

### 3.1.3.3. Temperature

The influence of temperature on  $B_{22}$  of IgG1 was tested in the range of 5 °C to 35 °C at two sodium chloride concentrations (10 and 150 mM) at pH 6.2 (Fig. IV-5B). The investigated temperatures were kept well below the  $T_m$  of the IgG1 to measure only  $B_{22}$  of native IgG1.  $B_{22}$  was not significantly modified by temperature at low salt concentration, whereas it depended on temperature at a 150 mM salt concentration. Increasing the temperature increased the repulsive force effect. A similar trend has been described for lysozyme (Valente *et al.*, 2005) corresponding to lysozyme solubility enhancement by increasing temperature. This is the case for temperatures well below the denaturation temperature of the protein. This strong temperature dependence was reported not to derive from electrostatic repulsions but more from hydrophobic interactions, which are known to depend strongly on temperature and mediate very short-ranged interparticle forces (Piazza, 2004). The effect was enhanced in the presence of salt, which shields electrostatic interactions.

### 3.1.3.4. Column stability

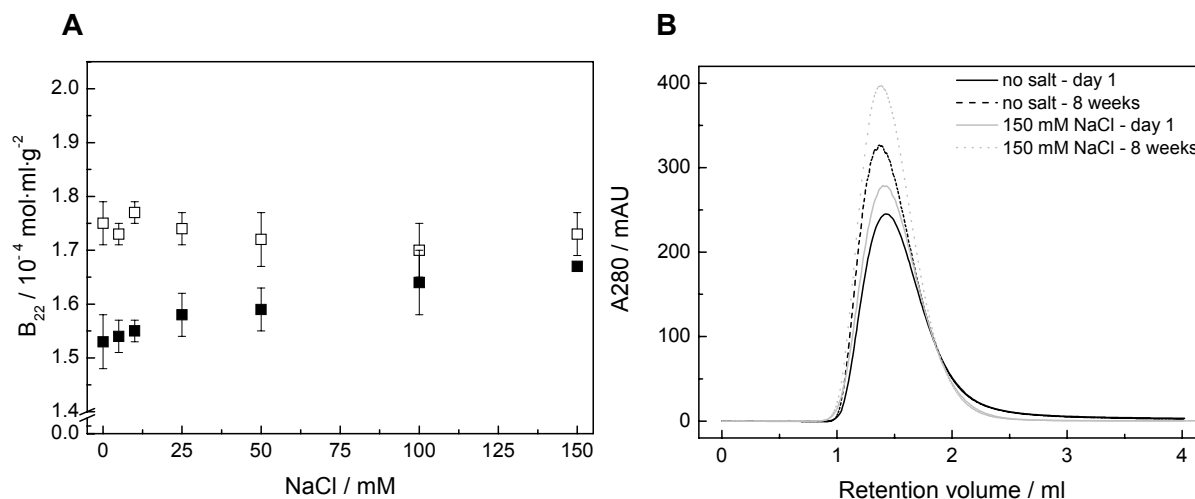


Fig. IV-6: Column stability at a loading of 17 mg/g: (A)  $B_{22}$  value of IgG1 as a function of NaCl concentration in the presence of 5 mM sodium succinate at pH 6.2 after 1 day (■) and 8 weeks (□) and (B) corresponding elution profiles.

Column stability is important to allow for reproducible measurements over months without the need to establish new columns. The stability of an IgG1 column having a protein loading of 17 mg/g was tested as a function of NaCl concentration (Fig. IV-6).

$B_{22}$  was not influenced by changes in NaCl concentration in the studied range at day 1 and after 8 weeks of storage at 4 °C. In addition, the elution profiles remained similar after the 8 week storage, since neither shift of the elution peak nor shoulder appeared on the chromatograms after 8 weeks of storage. Given that the  $B_{22}$  discrepancies were minimal, the IgG1 column remained stable at least 8 weeks when it was conserved at 4 °C in 5 mM sodium phosphate buffer pH 7.0 containing 0.05 % sodium azide.

## 3.2. Influence of formulation parameters on $B_{22}$ of IgG1

### 3.2.1. IgG1 protonation degree

Depending on the solution pH, protein molecules bear a net charge resulting from the sum of all charged ionized groups of the amino acids making up the protein. As the pH value approaches the protein's pI, the protein net charge diminishes. The protein net charge determines the electrostatic repulsions within its structure but also between different protein molecules in solution. On the one hand, a protein that is highly charged is affected by strong non specific repulsions within its structure, which can destabilize its folded conformation (Dill, 1990). On the other hand, charges on protein molecules enhance the intermolecular electrostatic repulsions and thus stabilize protein solution from a colloidal point of view (Chi *et al.*, 2003b). In addition, protein solubility is known to be pH dependent, as it varies with the square of the protein net charge (Shaw *et al.*, 2001).

Based on the protein sequence, the protein net charge was calculated as a function of the environmental pH with the EMBOSS software. The pH influence on  $B_{22}$  was measured using a mixed buffer system containing sodium acetate, sodium phosphate and sodium succinate to maintain a consistent buffer composition over the pH range tested (Fig. IV-7). Increasing the pH value from 4 to 8 near the IgG1 isoelectric point (about 8.3) decreased the IgG1 net charges and so did the  $B_{22}$  value. As the protein net charge decreased, the repulsive interactions between protein molecules bearing the same charge weakened. Thus, under alkaline pH conditions the formation of attractive protein-protein interactions are more likely as compared to the repulsive interactions encountered under acidic pH conditions. The  $B_{22}$  value changed by only  $0.6 \cdot 10^{-4} \text{ mol} \cdot \text{ml} \cdot \text{g}^{-2}$  between pH 4 and 8, which is rather small compared to the values of lysozyme (Tessier *et al.*, 2002) where a change in  $B_{22}$  of approximately  $4.5 \cdot 10^{-4} \text{ mol} \cdot \text{ml} \cdot \text{g}^{-2}$  was detected. Additionally, the ionic strength of the buffer system limits the pH dependent change in  $B_{22}$ . Indeed, the buffer ionic strength increased progressively by increasing pH and the ionic strength was 3 times higher at pH 8 than at pH 4. Electrolytes modulate the strength of electrostatic interactions between the charged groups both within the protein and between protein molecules (Chi *et al.*,

2003b). At low concentrations, salt ions shield protein charges, which reduces protein electrostatic repulsions. Indeed, the influence of the pH on the  $B_{22}$  of an IgG2 was considerably reduced by increasing the buffer ionic strength from 4 to 40 mM (Saluja *et al.*, 2007). Increasing the buffer ionic strength could screen the repulsive interactions between protein charges and leveled  $B_{22}$  values. Consequently, at a constant weak ionic strength,  $B_{22}$  of IgG1 would decrease in a more pronounced manner by increasing pH. Increasing the pH value to IgG1's pI decreased intermolecular repulsive forces, even though the pH effect was modulated by the presence of buffer electrolytes, which screened protein charges.

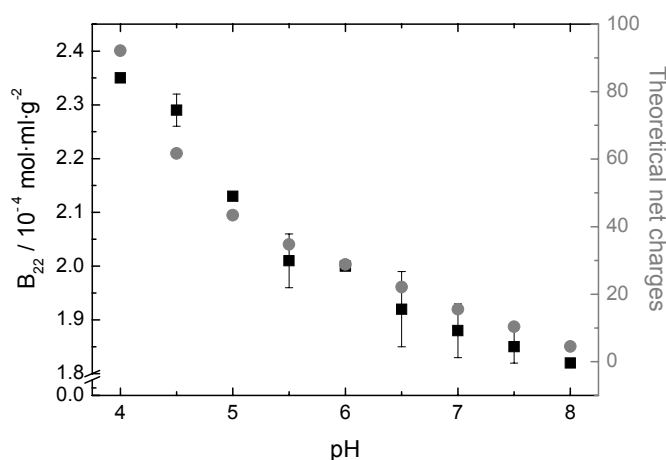


Fig. IV-7: Influence of pH on IgG1 theoretical net charges (●) and  $B_{22}$  (■) of IgG1 in the presence of mixed buffer (10 mM sodium acetate, 10 mM sodium phosphate, 10 mM sodium succinate) at a loading of 16 mg/g.

### 3.2.2. Buffer composition

The influence of the buffer species was studied with four different buffers (histidine, citrate, phosphate and succinate) in the concentration range of 5 to 50 mM at a fixed pH value of 6.2 (Fig. IV-8). The addition of buffer can be essential to stabilize protein formulations, since buffer inhibits a change of pH in solution, which is a crucial factor for protein stability. Furthermore, buffer ions may directly interact with the protein.  $B_{22}$  was sensitive to the buffer species at low buffer concentration. At 5 mM concentration, histidine showed the highest  $B_{22}$  value ( $2.32 \pm 0.07 \cdot 10^{-4} \text{ mol}\cdot\text{ml}\cdot\text{g}^{-2}$ ) whereas citrate and phosphate buffer had the lowest value ( $1.56 \pm 0.05$  and  $1.68 \pm 0.05 \cdot 10^{-4} \text{ mol}\cdot\text{ml}\cdot\text{g}^{-2}$  respectively). Increasing the buffer concentration diminished the difference between the buffer species until a similar  $B_{22}$  value of approx.  $1.86 \cdot 10^{-4} \text{ mol}\cdot\text{ml}\cdot\text{g}^{-2}$  was reached for all the tested buffers at 50 mM concentration. With increasing histidine concentration  $B_{22}$  decreased while increasing the other buffer concentration resulted in a slight increase or did not have an influence.

The three anionic buffers presented a higher ionic strength than histidine at equivalent concentration and this could induce observed differences in  $B_{22}$ . Another aspect to consider is the binding of the excipient to the protein molecule. Katayama and co-workers (2006) observed slight differences in  $B_{22}$  values of IFN-tau in the presence of histidine, Tris or phosphate buffers at 20 mM. These authors determined a very weak binding constant by isothermal titrating calorimetry and fluorescence titration between histidine and IFN-tau of  $K_b \approx 1 \cdot 10^2$  to  $4 \cdot 10^2 \text{ M}^{-1}$  and discussed that probably this very weak binding may stabilize IFN-tau against thermally induced aggregation by increasing the difference between the changes of the free Gibbs energy of native and unfolded state ( $\Delta G_{n-unf}$ ). A colloidal stabilization mechanism is of minor importance to understand the IFN-tau stabilization effect in the presence of histidine. Based on the obtained  $B_{22}$  data, the buffer species had a higher impact on antibody-antibody interactions compared to the interactions observed for IFN-tau. Overall, the buffer concentration should be high enough to control the formulation pH, but as low as possible to favor strong positive  $B_{22}$  values.

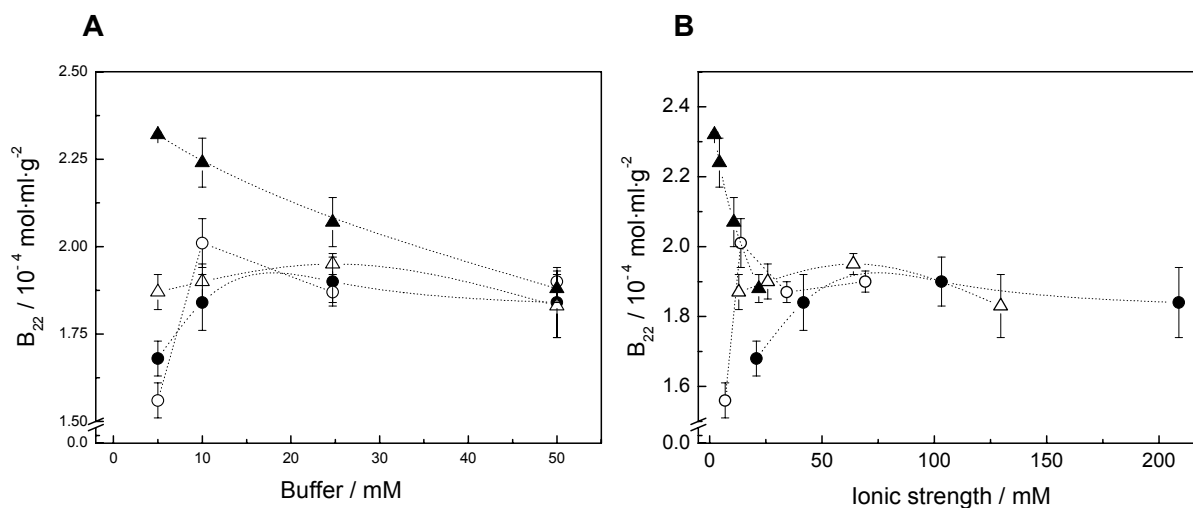


Fig. IV-8: Effect of buffer species at pH 6.2 on  $B_{22}$  value of IgG1 at a loading of 11mg/g: histidine (▲), succinate (△), citrate (●) and phosphate (○) as a function (A) buffer concentration and (B) ionic strength.

### 3.2.3. Salt concentration

The influence of sodium chloride was tested in the concentration range of 0 to 150 mM in the presence of 5 mM sodium succinate pH 6.2, since salt is commonly added to obtain isotonic drug solutions and to adjust the ionic strength. Up to a concentration of 100 mM, NaCl had little influence on  $B_{22}$  values (Fig. IV-9). Further increasing the NaCl concentration to 150 mM decreased the  $B_{22}$  value reflecting the fact that ionic screening reduced the repulsive charge effect or any repulsive charge interactions between protein molecules. Indeed, electrostatic repulsive forces usually decrease with addition of salt ions due to their inverse dependence on ionic strength (Saluja and Kalonia,

2008). It corresponded to a similar effect reported on two humanized monoclonal antibodies constructed from the same IgG1 (Liu *et al.*, 2005). In both cases, the decrease in  $B_{22}$  value was not strong enough to reach negative  $B_{22}$  values, revealing less favorable repulsive particle conditions but no majority of attractive protein-protein interactions. Consequently, the addition of up to 100 mM NaCl barely perturbed the IgG1 intermolecular interactions and could be used as isotonic agent.

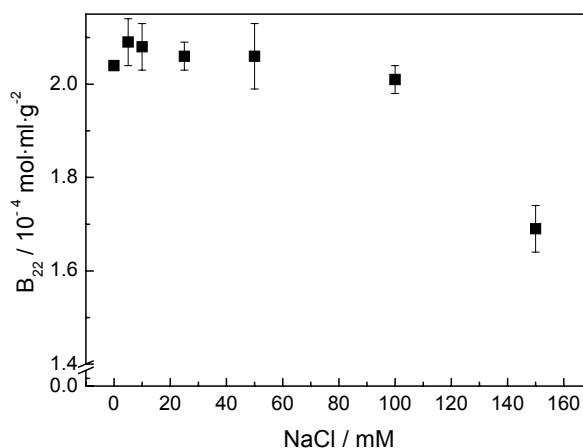


Fig. IV-9: Effect of NaCl on  $B_{22}$  value of IgG1 in the presence of 5 mM sodium succinate pH 6.2 at a loading of 11 mg/g.

### 3.2.4. Influence of amino acids

Amino acids are commonly used as solvent additives in protein purification and as excipients for protein formulations. Arginine, glycine and histidine are the most frequently utilized to stabilize protein formulation, to improve protein solubility and to avoid protein aggregation (Arakawa *et al.*, 2007b). The influence of arginine, glycine, histidine and methionine was tested in the concentration range of 0 to 100 mM in the presence of 5 mM sodium succinate at pH 6.2. The addition of glycine or methionine did not perturb  $B_{22}$  whereas histidine and arginine modified it (Fig. IV-10). Both arginine and histidine acted differently on  $B_{22}$  depending on their concentrations in solution. Adding both amino acids at 5 or 10 mM decreased  $B_{22}$ , which is more pronounced for arginine. However, buffer concentrations equal or higher than 20 mM led to a slight  $B_{22}$  increase. Most amino acids are known to stabilize protein by preferential exclusion from the protein surface (Arakawa *et al.*, 2007b). Stabilization via preferential exclusion was reflected by constant  $B_{22}$  values by addition of the methionine or glycine. Histidine and arginine presented a different  $B_{22}$  profile. Both amino acids are reported to weakly bind to protein (Arakawa *et al.*, 2007a, Katayama *et al.*, 2006).

The influence of the amino acid side chain structure has been studied by Shiraki and co-workers (2002) with lysozyme as model protein at pH 6.5 in 50 mM sodium phosphate buffer. Positively charged amino acids were more effective than

hydrophobic and negatively charged amino acids to prevent protein heat induced and dilution induced aggregation. Arginine presented the most pronounced effect. Increasing the arginine concentration increased its preventive action (Shiraki *et al.*, 2002); a maximal effect was obtained at 300 mM. Furthermore, the most substantial preventive effect of arginine against aggregation was confirmed with various proteins of different pI and molecular weights (Shiraki *et al.*, 2002). According to Arakawa and co-workers (2007a), the protective effect of arginine against heat induced aggregation results from its interaction with the peptide bonds and most amino acid side chains (both hydrophobic and hydrophilic) especially tyrosine and tryptophan, leading to a reduction of both electrostatic (hydrogen bonding and ionic interactions) and hydrophobic interactions. Histidine also presented the property to bind to protein, but its binding was reported weak ( $K_b \approx 1 \cdot 10^2$  to  $4 \cdot 10^2 \text{M}^{-1}$ ) (Katayama *et al.*, 2006). Its effect on thermodynamic stabilization of IFN-tau (Katayama *et al.*, 2006) and EPO (Arakawa *et al.*, 2001) was preponderant. Thus at low amino acid concentrations (up to 10 mM) the  $B_{22}$  decrease might reflect arginine or histidine binding to the IgG1 molecule or changes of the hydration property of the IgG1 molecules. The  $B_{22}$  decrease was stronger in the presence of arginine as compared to histidine, which could reflect the stronger binding of arginine to protein surface. At higher concentration all amino acids act similarly, corresponding to the protective and solubilization effect due to preferential exclusion.

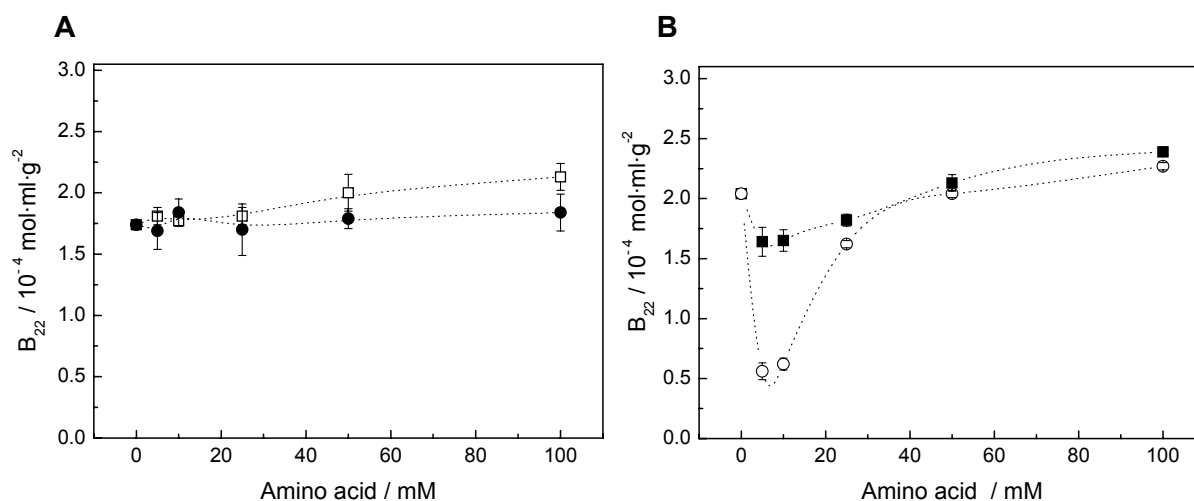


Fig. IV-10: Effect of amino acids on  $B_{22}$  of IgG1 in the presence of 5 mM sodium succinate pH 6.2: (A) methionine (●) and glycine (□) at a loading of 12 mg/ml, (B) arginine (○) and histidine (■) at a loading of 11 mg/ml.

### 3.2.5. Mannitol and sucrose addition

Mannitol and sucrose are preferred excipients in protein formulation, as they can stabilize proteins by preferential exclusion from the protein domain and consequently preferential hydration of the protein (Timasheff, 1993). The influence of mannitol and

sucrose was tested in the presence of glycine and histidine buffer at pH 6.2. Adding mannitol up to 2 % slightly increased  $B_{22}$  and the free IgG fraction was quickly eluted from the column (Fig. IV-11A), but the chromatograms presented a shoulder that became more pronounced with higher mannitol concentration (Fig. IV-11B). More mannitol perturbed the protein behavior:  $B_{22}$  decreased and fluctuated strongly above 2 % mannitol. In the presence of 3 % mannitol a second distinct peak appeared in the chromatogram but all injected protein was eluted. At 4 % mannitol  $B_{22}$  was reduced considerably. Moreover, only one peak with a strongly reduced AUC was detectable meaning that only a fraction of the protein could be eluted. Thus, a protein fraction could be quickly eluted, corresponding to significant repulsive interactions. Another fraction was more strongly retained on the column, revealing substantial protein attraction in the presence of mannitol and corresponding probably to protein association or aggregation. Furthermore the column could not give reliable results for standard samples without mannitol after those runs in the presence of high amounts of mannitol indicating severe modification of the immobilized IgG1 molecules.

Addition of sucrose affected the  $B_{22}$  of IgG1 in a clearly different way than mannitol.  $B_{22}$  values took little change by sucrose addition but the IgG1 elution profiles were modified in a sucrose concentration range (Fig. IV-11A) between 2 % and 4 % (Fig. IV-12). A shoulder appeared at 2 % sucrose whereas a second elution peak was present at 3 % and 4 % concentration formulations indicating two different fractions of protein. The column was also disturbed after the sucrose study as no reliable results could be obtained afterwards. As studies of lysozyme in the presence up to 20 % polyol or sugar did not show this dramatic effect and different protein fractions, incompatibility between the excipients and the chromatography particles does not explain the effect with IgG1 found in this study.

Even though mannitol is commonly used as stabilizing agent in protein formulation, it could cause reversible protein associations in IgG solutions, when formulated at higher concentration (Schüle *et al.*, 2007). In order to compare the results obtained with the studies by Schüle and co-workers, the IgG1 was formulated at 50 mg/ml in the same buffer composed of histidine and glycine at pH 6.2 with increasing content of mannitol up to 6 % to illustrate the previous SIC results. Samples were incubated 24 h at room temperature, before turbidity and SE-HPLC analysis were carried out to measure the level of protein aggregation and self-association. By addition of Bis-ANS to SE-HPLC samples, structural changes of monomeric and oligomeric IgG1 can be detected and thus folded monomers could be discriminated from partially unfolded and folded dimers from unfolded dimers. Indeed, the Bis-ANS fluorescence properties depend on its interaction with protein molecules, which results in changes of polarity



and viscosity of the environment, and is dominated by hydrophobic interactions (Hawe *et al.*, 2008). Therefore an increase in Bis-ANS emission intensity can reveal an increase in protein unfolding as unfolded protein exposes more hydrophobic regions. Two different batches of IgG1 containing a different initial aggregate content were prepared in glycine histidine buffer: Batch I contained 4.5 % dimers and batch II 0.6 % both detected by UV. By addition of mannitol up to 6 %, no difference in turbidity and in dimer content could be measured in both batches. Differences could only be measured by addition of Bis-ANS to SE-HPLC samples (Fig. IV-13). In batch II which presented a low initial aggregate content (0.6 %), the addition of mannitol did not influence the content of partially unfolded monomers and unfolded dimers. Batch I showed a different profile. With increasing concentration of mannitol, the quantity of partial unfolded monomers remained constant, while the quantity of unfolded dimers increased linearly (Fig. IV-13). Thus, mannitol had an influence on unfolded dimer formation only when the initial IgG1 solution contained a higher initial amount of dimers, but no evidence for reversible association was found which could correlate to  $B_{22}$  results.

Consequently, further analysis of the immobilized protein was performed. In FTIR spectra, the IgG1 amide I band (Fig. IV-11C) at  $1640\text{ cm}^{-1}$  presented no shift in wavenumber and no diminution in intensity compared to the initial sample. Fluorescence spectroscopy can be employed for protein tertiary structure analysis. The Bis-ANS extrinsic fluorescent dye was added to the chromatography particles to detect unfolded protein structures by fluorescence spectroscopy (Fig. IV-11D). The maximum emission wavelength in all samples was at 485 nm. No increase in intensity could be notified for the immobilized protein comparing the sample before and after elution in the presence of 6 % mannitol. Only immobilized IgG1 heat stressed at  $95^{\circ}\text{C}$  for 1 h showed an intensity increase. Thus, no significant increase in hydrophobic protein region and consequently no increase in IgG1 unfolding could be shown after elution with high mannitol concentrations.

To sum up, the passage of both excipients mannitol and sucrose disturbed the chromatography column probably due to strong protein-protein interactions. No excipient incompatibility with the chromatographic resin could be held responsible as sucrose has already been studied at higher concentration in the presence of the same chromatographic resin and lysozyme. The strong protein-protein interactions on the SIC column remain unexplained, as no hint for protein unfolding on the column, protein aggregation or self-association could be found.

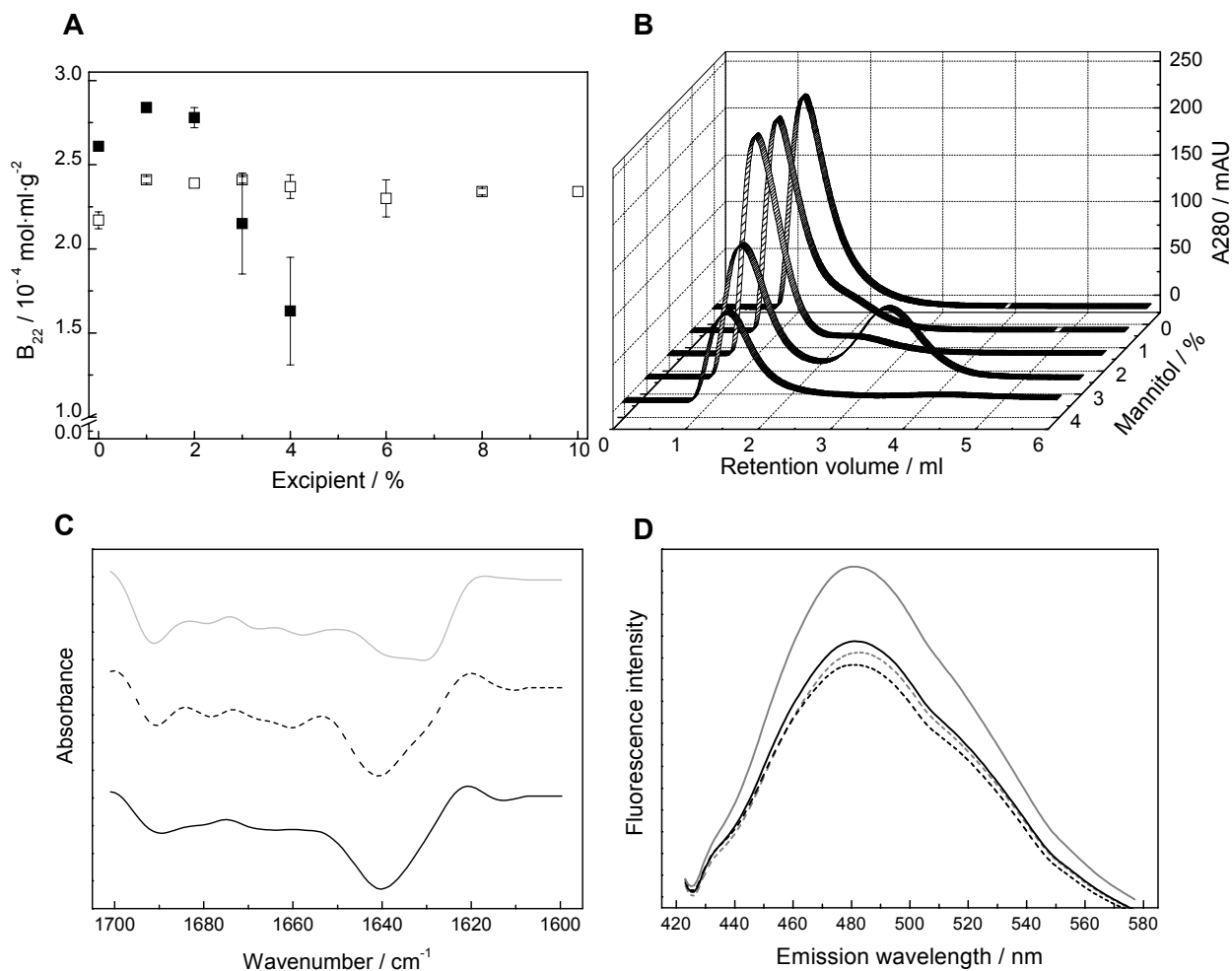


Fig. IV-11: (A) Effect of mannitol (■) and sucrose (□) on  $B_{22}$  of IgG1 in the presence of glycine histidine buffer pH 6.2 at a loading of 11 mg/g, (B) Elution profiles of IgG1 in the presence of mannitol, (C) ATR-FTIR spectra and (D) fluorescence emission spectra in the presence of 4 nmol Bis-ANS of Toyopearl (- -), immobilized IgG1 before mannitol elution (-), immobilized IgG1 after 6% mannitol elution (- -) and immobilized IgG1 after thermal stress (95 °C, 1h) (-).

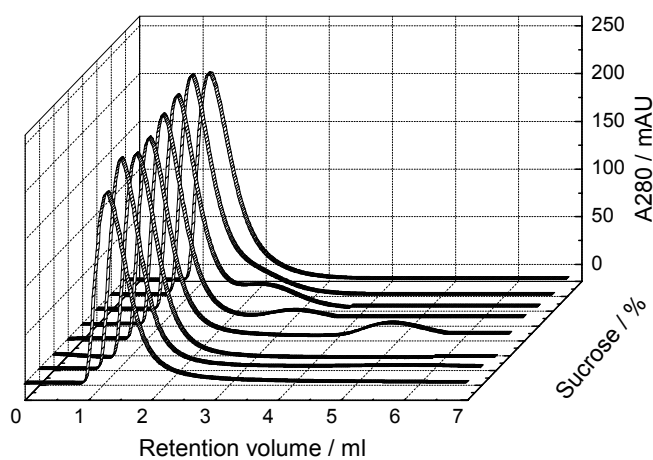


Fig. IV-12: Elution profiles of IgG1 in the presence of sucrose and glycine histidine buffer pH 6.2.

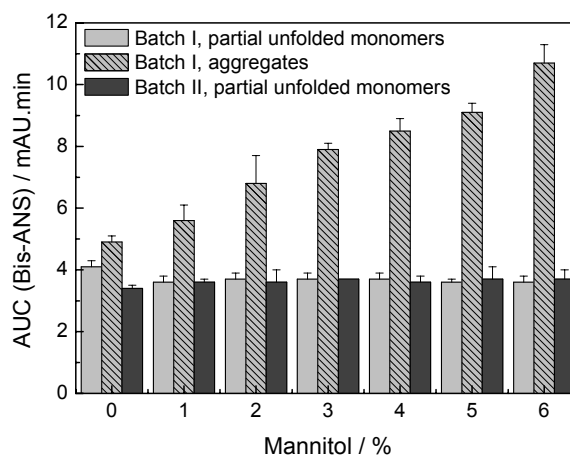


Fig. IV-13: Influence of mannitol content on fluorescence signal in SE-HPLC in the presence of 10  $\mu$ M Bis-ANS in 50 mg/ml IgG1 solution in glycine histidine buffer pH 6.2.

### 3.3. Is $B_{22}$ a relevant predictive tool in protein formulation?

#### 3.3.1. Comparison of $B_{22}$ to protein solubility

Because of the lack of adapted methods to determine protein solubility, one common approach for its evaluation consists of concentrating a protein solution by ultrafiltration until its concentration remains constant.

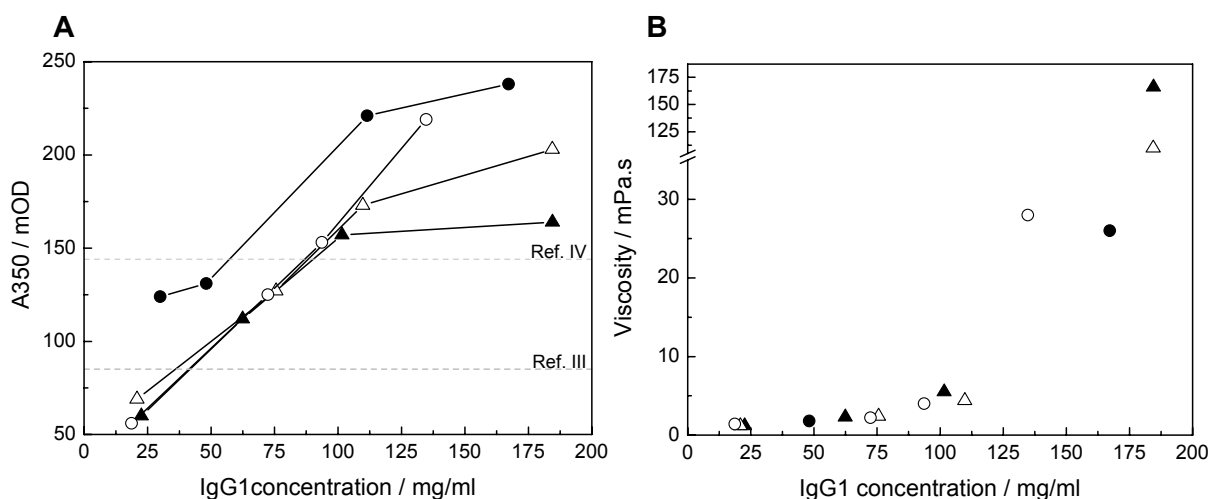


Fig. IV-14: Concentration process of IgG1 solution according to buffer species (5 mM concentration, pH 6.2): histidine (▲), succinate (△), citrate (●) and phosphate (○). Influence of IgG1 concentration on (A) solution turbidity and (B) solution viscosity.

Four different buffer species were compared at pH 6.2 at 5 mM: histidine, sodium citrate, sodium phosphate and sodium succinate. IgG1 solutions having an initial concentration of 20 mg/ml were concentrated with ultrafiltration spin columns (MWCO of 30 kDa). During the process, the IgG1 concentration in supernatant and the corresponding solution turbidity and viscosity were measured. IgG1 turbidity increased linearly with IgG1 concentration for the four tested formulations until a 100 mg/ml

concentration was reached (Fig. IV-14). The approximately linear turbidity increase with protein concentration suggested the absence of significant concentration dependent association. The highest final IgG1 concentrations could be achieved for 5 mM histidine and 5 mM sodium succinate formulations, both at approximately 185 mg/ml. Moreover both protein solutions presented a reduced turbidity (164 mOD for histidine and 203 mOD for succinate) in comparison to the 5 mM sodium citrate and 5 mM sodium phosphate formulations. The IgG1 solution viscosity remained reduced (below 5 mPa.s) up to a concentration of 100 mg/ml for the four tested formulations and the buffer species did not have a significant impact. Above 100 mg/ml viscosity increased strongly for all formulations. The concentration process was more effective with histidine and succinate than with citrate or phosphate. This ranking could be compared to the same obtained with  $B_{22}$ : histidine ( $2.32 \cdot 10^{-4} \text{ mol} \cdot \text{ml} \cdot \text{g}^{-2}$ ) > succinate ( $1.87 \cdot 10^{-4} \text{ mol} \cdot \text{ml} \cdot \text{g}^{-2}$ ) > citrate ( $1.68 \cdot 10^{-4} \text{ mol} \cdot \text{ml} \cdot \text{g}^{-2}$ ) > phosphate ( $1.56 \cdot 10^{-4} \text{ mol} \cdot \text{ml} \cdot \text{g}^{-2}$ ). Thus the experiment points to usefulness of  $B_{22}$  in predicting formulations facilitating a protein concentration process to achieve high protein concentration. The results also emphasized the described correlation between  $B_{22}$  and solubility (Guo *et al.*, 1999, Haas *et al.*, 1999, Payne *et al.*, 2006).

### 3.3.2. Comparison of $B_{22}$ to thermal stability

#### 3.3.2.1. Stability of 20 mg/ml IgG1 solutions

A stability study for 20 mg/ml IgG solutions was conducted for 12 weeks at 40 °C as a function of buffer species and concentration at pH 6.2 comparing sodium citrate, histidine, sodium phosphate and sodium succinate at both 5 and 50 mM. From the tested formulations only the two histidine containing systems showed a major increase in turbidity (Fig. IV-15A and IV-15B). The 5 mM histidine formulation presented a significant turbidity increase after 12 weeks whereas the turbidity of the 50 mM histidine formulation had already increased significantly after 4 weeks. This increase in turbidity went along with a yellow discoloration reflecting of chemical instability. As this solution discoloration appeared also in histidine buffer solutions stored under the same conditions, a chemical instability was imputed to the presence of histidine. Histidine is susceptible to oxidation either by photocatalyzed or by metal-ion catalyzed mechanisms. It is beside some intermediates mainly oxidized to 2-oxo-histidine, aspartic acid and asparagine (Bummer, 2008, Reubsæet *et al.*, 1998). A study with an IgG2 antibody (Chen *et al.*, 2003) also reported aggregation increase and solution discoloration during freeze-thaw studies in stainless steel containers and this instability was attributed to an effect caused by traces of iron leached from corrosion of steel containers in combination with histidine. The chemical instability

could be reduced by the addition of 20  $\mu\text{M}$  EDTA to the protein solution that contained 4 to 6 mM histidine (Chen *et al.*, 2003). Therefore to avoid the chemical instability 20  $\mu\text{M}$  EDTA were added to the 20 mg/ml IgG1 histidine solution, even though no metal ions could be detected by atomic absorption spectroscopy ( $< 0.02$  mg/g).

The addition of 20  $\mu\text{M}$  EDTA to the histidine containing samples inhibited the solution discoloration during the 12 week storage and the increase in turbidity was better controlled. The 5 mM histidine solution presented a similar increase in turbidity as the other buffers tested whereas the turbidity increase remained higher for the 50 mM histidine / EDTA solution.

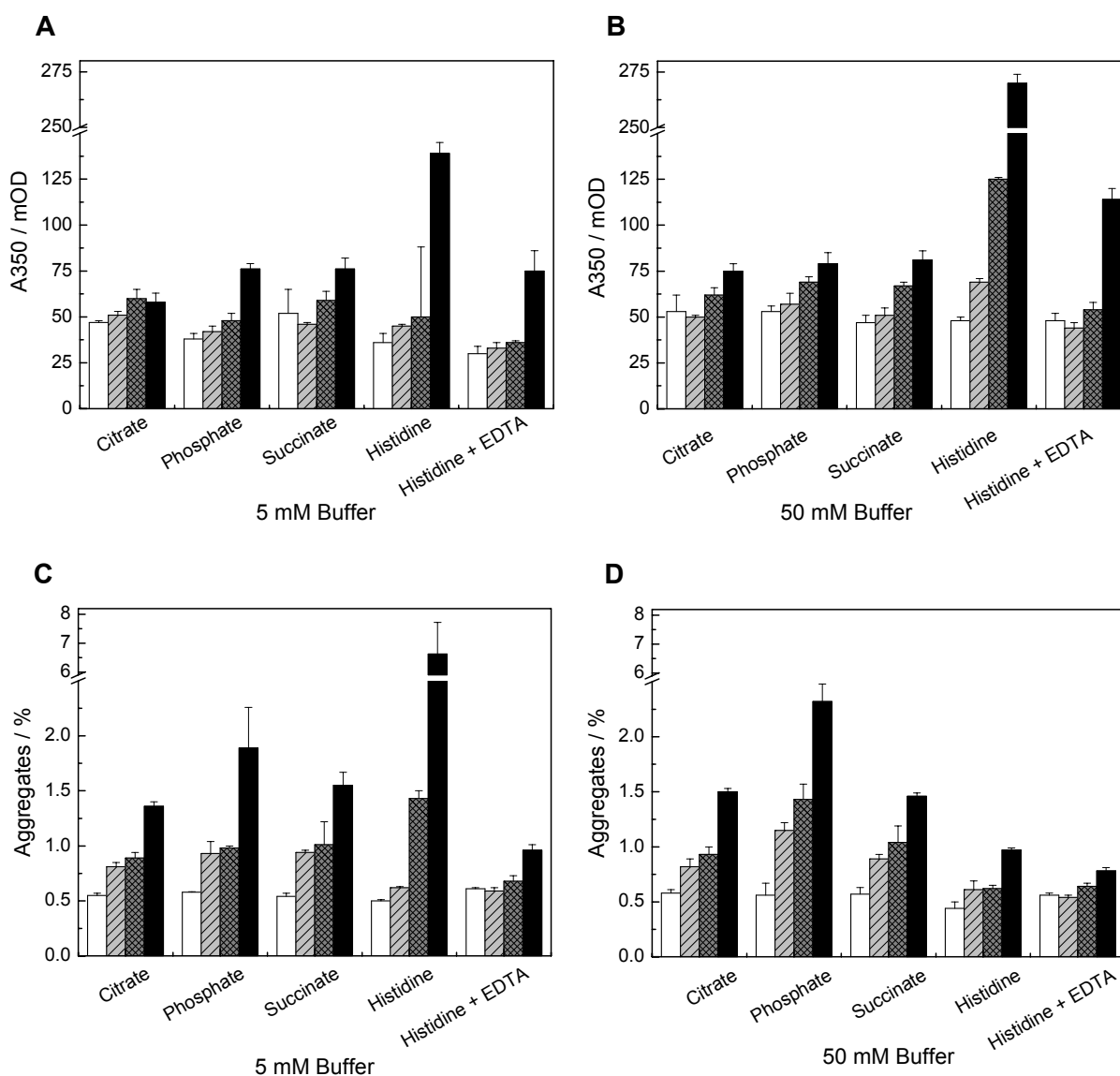


Fig. IV-15: Turbidity (A, B) and soluble aggregates (C, D) of 5 mM and 50 mM buffer pH 6.2 containing IgG1 solutions before (blank columns) and after 1 week (light gray columns), 4 weeks (grey columns) and 12 weeks (black columns) storage at 40 °C.

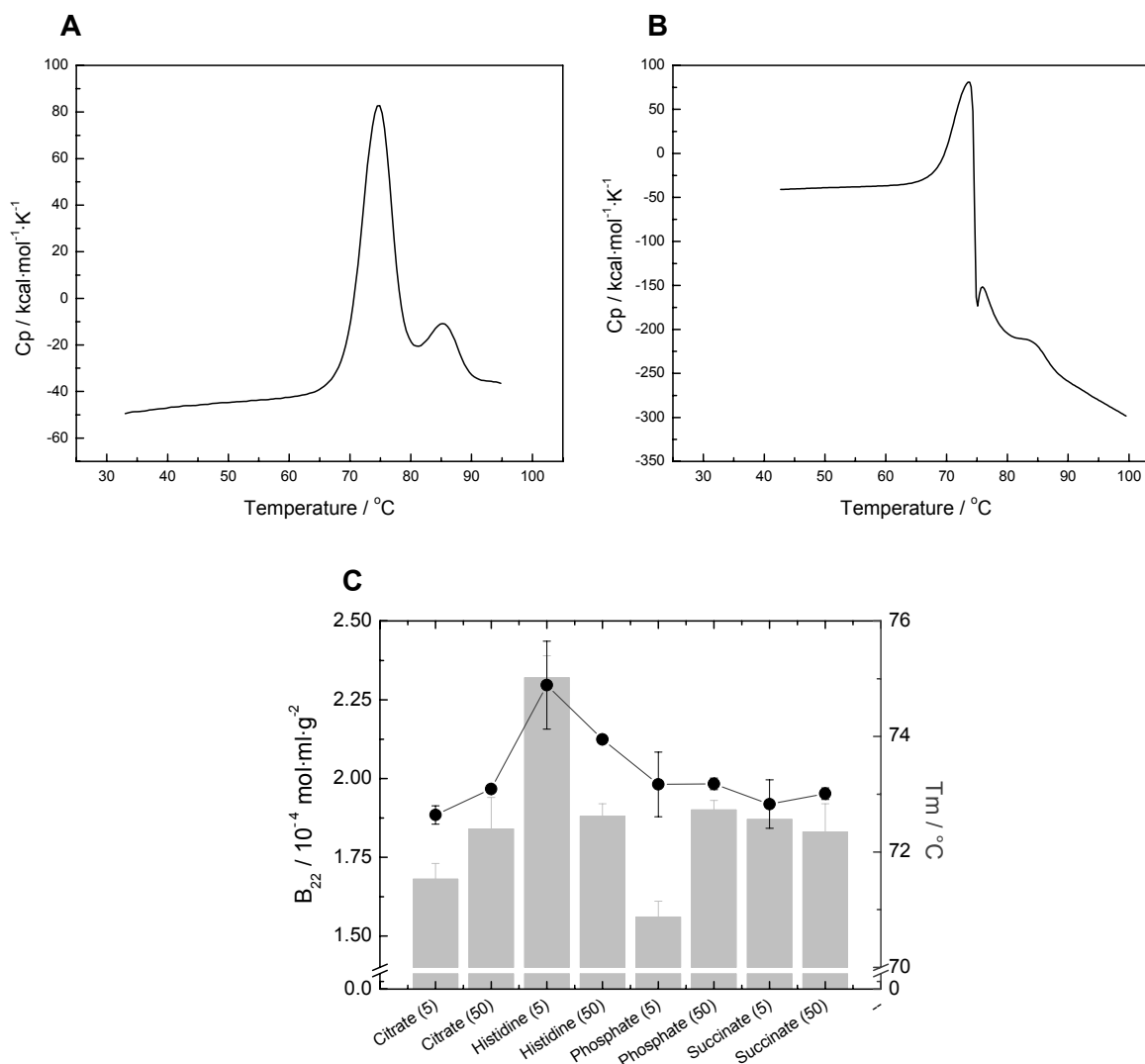


Fig. IV-16: DSC thermograms of IgG1 in 5 mM histidine buffer (A) and in 5 mM sodium phosphate buffer (B) at pH 6.2 and comparison of  $B_{22}$  value (gray column) to  $T_m$  value (black point) (C).

The soluble aggregate content was kept below 2 % for the majority of the tested formulations (Fig. IV-15C and IV-15D). The 5 mM histidine containing formulation showed the highest amount in soluble aggregates (6.6 %), but it could be stabilized by addition of EDTA. Indeed this latter solution presented the lowest increase in soluble aggregates (1 %) after 12 weeks at 40  $^{\circ}\text{C}$  within the 5 mM buffers. The two 50 mM histidine containing formulations did not present a substantially increased level of soluble aggregates after 12 weeks at 40  $^{\circ}\text{C}$ , but they presented higher turbidities compared to other buffer formulations indicating a higher propensity to form insoluble aggregates. Higher histidine buffer concentrations (10 and 50 mM at pH 6.0) were similarly reported to favor formation of medium to large size aggregates of cetuximab under elevated thermal storage conditions that were responsible for higher solution

turbidity but histidine did not influence the soluble aggregate content (Matheus *et al.*, 2006).

When its chemical instability was controlled 5 mM histidine was a well stabilizing protein formulation buffer. It has been already reported to stabilize IFN-tau better than phosphate or Tris buffer (Katayama *et al.*, 2006). Its mechanism of stabilization was attributed both to colloidal stabilization but also to conformational stabilization by weak binding to the native protein state. The  $B_{22}$  coefficient of IgG1 was slightly increased in the presence of histidine at low concentration in comparison to the other buffer systems. This was confirmed also by the study of Katayama and co-workers (2006). However the ability of histidine to increase the repulsive interactions in solution may not be the only mechanism leading to the best IgG1 stabilization. The conformational stability of the protein seemed to be improved as well. The DSC thermograms of the histidine containing formulations (Fig. IV-16A) presented two peaks representing the Fab and the Fc fragment, the Fab fragment having the larger experimental enthalpy (Ionescu *et al.*, 2008). The DSC thermograms of the other buffers (exemplarily shown for 5 mM sodium phosphate buffer in Fig. IV-16B) presented only the first peak followed by a sudden decrease of the signal and a shift of the baseline corresponding to IgG1 aggregation and precipitation at its thermal unfolding. Correspondingly, in 5 mM histidine buffer the IgG1 exhibited the highest  $T_m$ , whereas the  $T_m$  values for the other buffers were in a comparable range (Fig. IV-16C). The negligible impact of buffer composition at pH 6.2 on  $T_m$  was comparable to the results reported with cetuximab (Matheus *et al.*, 2006) and a recombinant human megakaryocyte growth factor (Narhi *et al.*, 1999). High buffer concentration did not improve IgG1 stability. This could reflect the self-buffering action of monoclonal antibodies in the pH range of 4-6 provided by the proteins' charged amino acids including aspartic acid, glutamic acid and histidine (Gokarn *et al.*, 2008). Thus the presented data show a correlation between protein colloidal stability and  $B_{22}$ .

### 3.3.2.2. Stability of 170 mg/ml IgG1 solutions

In addition, to reflect high protein concentration formulations, IgG1 behavior was studied at a concentration of about 170 mg/ml. For this purpose, 180 mg IgG1, which were first dialyzed into water and concentrated to 50 mg/ml solution (99.3 % monomers), were lyophilized. After the freeze-drying process, IgG1 lyophilisates reconstituted into water at 50 mg/ml contained 90.2 % monomers. The protein lyophilisates were further reconstituted with the buffer solutions studied in  $B_{22}$  experiments to reach a final protein concentration of about 170 mg/ml. IgG1 was dissolved during 24 h at room temperature before insoluble protein was removed by

centrifugation (14000g, 15 min) and IgG1 concentration and aggregate content were checked by SE-HPLC, as well as turbidity (A350) and viscosity. The different protein solutions were then stored at 40 °C during 4 weeks. The influence of pH (4, 6 and 8), buffer species (5 mM, pH 6.2), salt (25 and 150 mM) and arginine (10 and 100 mM) was tested.

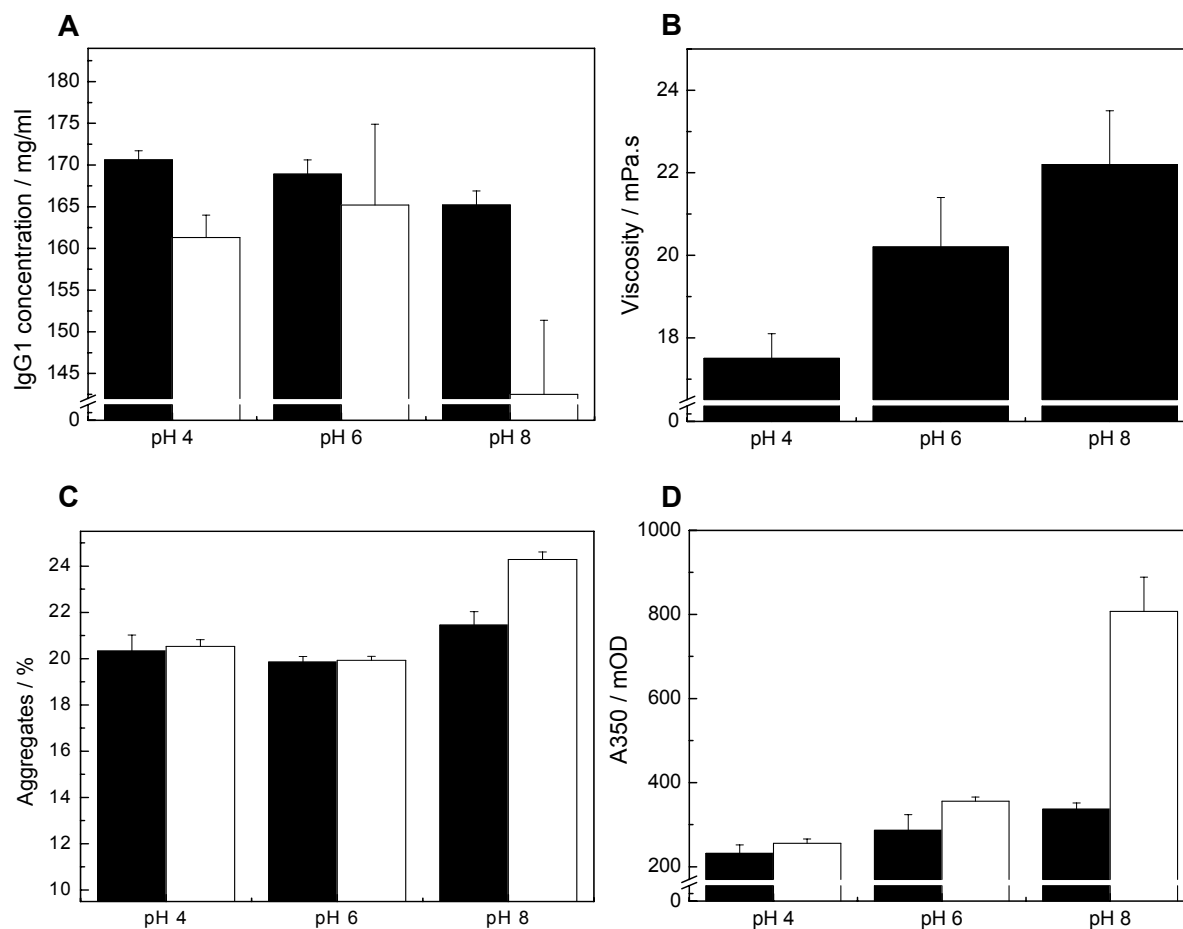


Fig. IV-17: Influence of pH on IgG1 concentration (A), viscosity (B), aggregate content (dimers and oligomers) (C) and turbidity (D) in the presence of mixed buffer before (black columns) and after 4 weeks of storage at 40 °C (blank columns) (10 mM sodium acetate, 10 mM sodium phosphate, 10 mM sodium succinate).

With increasing the pH towards the IgG1 isoelectric point of 8.3, the total IgG1 concentration in solution slightly decreased and the aggregate content as well as, solution turbidity and viscosity increased (Fig. IV-17). Protein solubility was higher under acidic conditions when the protein molecules net charge is higher favoring repulsive protein-protein interactions. After 4 weeks of storage, the IgG1 concentration was reduced in all three solutions. This decrease, which was particularly pronounced at pH 8, went along with an increase of the solution turbidity and thus with an increase in insoluble aggregate formation. Marginal differences in soluble aggregate content between the pH 4 and 6 formulations resulted but aggregation was highly pronounced



at pH 8. Formulating the protein solution at pH 8 enhanced not only insoluble aggregate but also soluble aggregate formation. Thus, increasing pH decreased IgG1 stability as well as B<sub>22</sub>; especially with the pH approaching the protein pI. Near its pI the protein electrostatic repulsions are reduced and protein molecules can come in closer contact as the energy barrier to come into physical contact decreases (Chi *et al.*, 2003b).

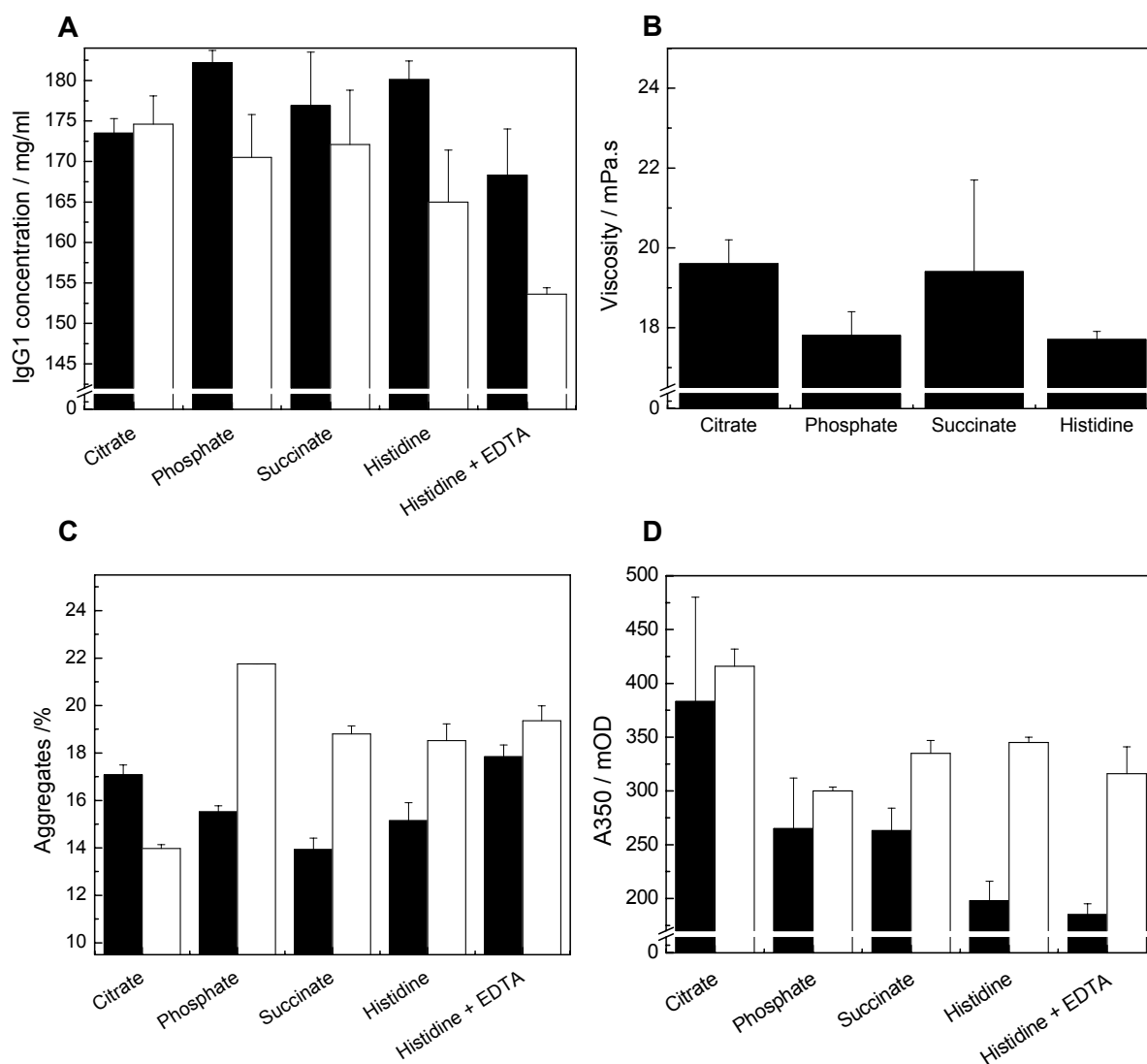


Fig. IV-18: Influence of buffer species on IgG1 concentration (A), viscosity (B), aggregate content (dimers and oligomers) (C) and turbidity (D) before (black columns) and after 4 weeks of storage at 40 °C (blank columns) (5 mM concentration, pH 6.2).

After reconstitution, IgG1 solutions (pH 6.2 in 5 mM histidine, sodium citrate, sodium phosphate or sodium succinate) showed protein concentrations varying between 170 and 180 mg/ml with an aggregate content between 14 % and 18 % (Fig. IV-18). The 5 mM histidine formulation presented the lowest initial turbidity in comparison to the three other formulations and the lowest viscosity together with phosphate buffer. To overcome potential chemical instability of histidine, 20  $\mu$ M EDTA were added to one

batch of histidine containing samples. After 4 weeks of storage at 40 °C, all solutions presented a comparable level of turbidity, except for the citrate buffered formulation. The increase in turbidity of histidine formulations was consequently more pronounced. The increase of solution turbidity went again parallel with a reduction in protein concentration during the storage. The addition of EDTA did not affect the stability of histidine containing IgG1 solution. The final soluble aggregate content remained low in the presence of citrate buffer (about 14 %), increased from a similar manner to about 19 % in the presence of succinate, histidine and histidine / EDTA buffers, and more strongly with phosphate buffer. On the other hand, the citrate buffer formulation showed the highest turbidity and the tendency to form larger aggregates. Even though histidine presented the higher  $B_{22}$  value and enhanced stability of IgG1 at a concentration of 20 mg/ml, histidine buffer did not better stabilize IgG1 at high concentration than the other buffer species tested. Thus, all buffer formulations at 5 mM resulted in similar IgG1 stability at pH 6.2, as the antibody contained enough charged amino acids that were able to provide buffering action in the pH range of 4-6 and the self-buffering capacity of antibody increased with increasing protein concentration in solution becoming an important factor for stability (Gokarn *et al.*, 2008).

The stabilization capacity of arginine was tested at two concentration levels (10 and 100 mM) in the presence of 5 mM sodium succinate buffer at pH 6.2. The addition of arginine did not influence the initial IgG1 concentration and turbidity level but increased the aggregate content as compared to the succinate buffer formulation (Fig. IV-19). Moreover, the addition of 100 mM arginine significantly decreased the solution viscosity. After 4 weeks of storage at 40 °C, the presence of arginine led to a more pronounced increase in solution turbidity but did not change the absolute soluble aggregate content. Both soluble and insoluble aggregate species were increased only in the presence of succinate buffer. Thus, the addition of arginine did not improve the protein stability after 4 weeks of stress but favored the formation of insoluble aggregates.

Similarly, the influence of sodium chloride on IgG1 stability was tested in the presence of sodium succinate at pH 6.2 (Fig. IV-19). The addition of sodium chloride had a different effect depending on its concentration. In the presence of 25 mM NaCl, the initial solution parameters were close to those of the succinate buffer. Only the soluble aggregate content was increased. The addition of 150 mM NaCl influenced in a more pronounced manner the protein behavior. The initial IgG1 concentration was reduced, whereas the soluble aggregate content as well as the solution viscosity were increased. After 4 weeks of storage, the IgG1 concentration decreased significantly in the presence of 25 mM NaCl as aggregation occurred. Obviously, the IgG1 aggregation

involved the formation of insoluble aggregates since the solution turbidity increased but the absolute aggregate content remained constant. On the other hand, in the presence of the higher amount of NaCl (150 mM), the IgG1 concentration remained constant while the formation of insoluble aggregate was favored. Thus,  $B_{22}$  could well predict the influence of NaCl on IgG1 solution parameters after reconstitution but did not correlate to the stability results. Those discrepancies could result from the high protein concentration, since protein-protein interactions differ with the protein concentration. Increasing the protein concentration diminishes the importance of electrostatic repulsions and consequently could explain the similar stability result.

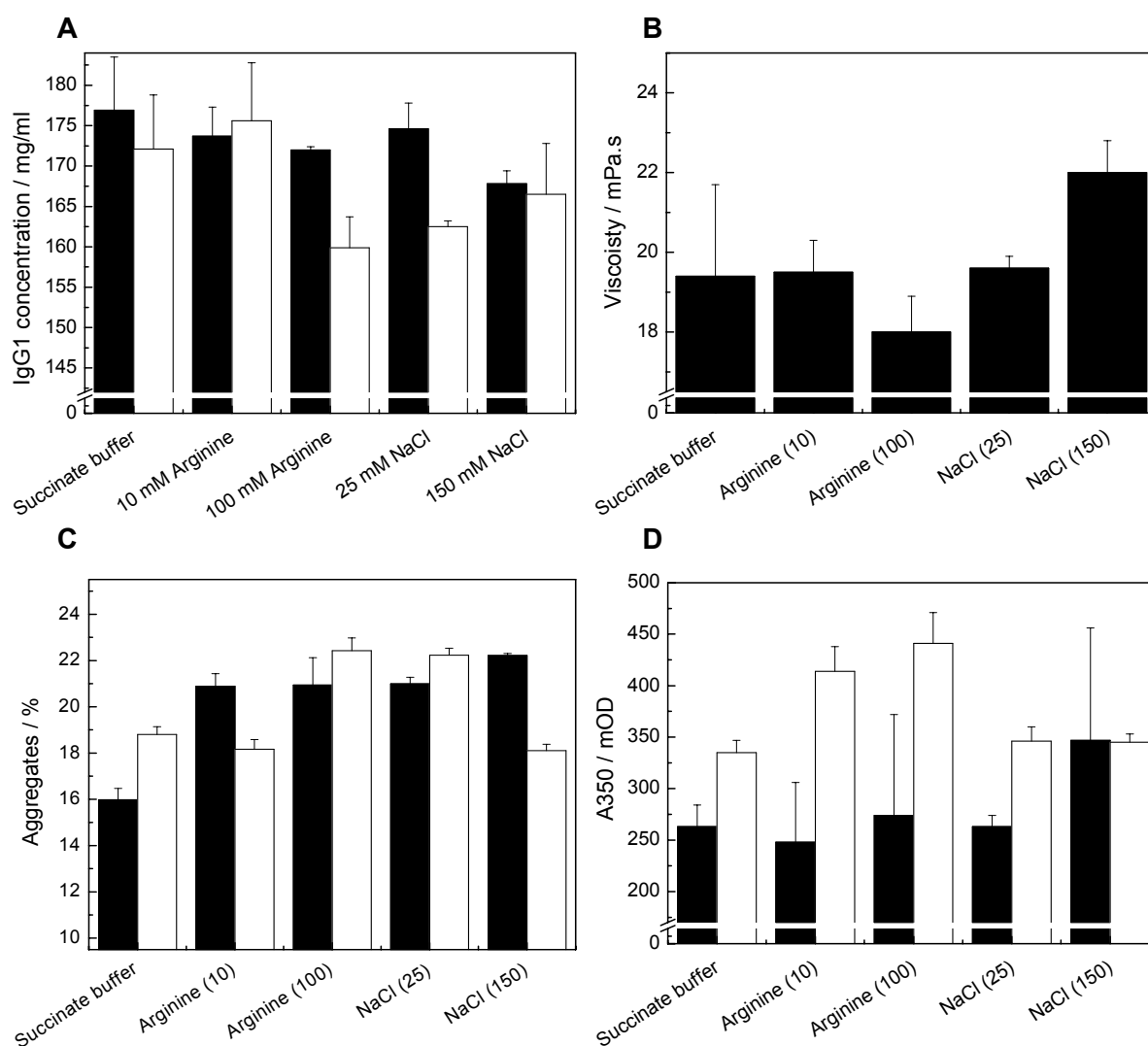


Fig. IV-19: Influence of salt and arginine on IgG1 concentration (A), viscosity (B), aggregate content (dimers and oligomers) (C) and turbidity (D) before (black columns) and after 4 weeks of storage at 40 °C (blank columns) (5 mM sodium succinate buffer, pH 6.2).

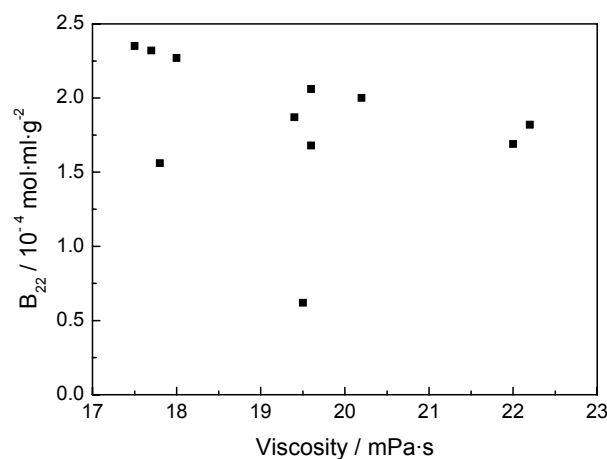


Fig. IV-20: Viscosity of 170 mg/ml IgG1 solutions as a function of  $B_{22}$  value.

Overall, there is a trend to higher viscosity for solutions presenting small  $B_{22}$  values (Fig. IV-20). Generally, the viscosity of a macromolecule in solution can be expressed as a virial expansion, where the viscosity  $\eta$  can be related to the solvent viscosity  $\eta_0$  and protein concentration  $C$  (g/ml) (Liu *et al.*, 2005, Shire *et al.*, 2004). As protein molecules interact in solution, most protein solutions exhibit non Newtonian behavior and viscosity depends also on the shape, molecular weight and molecular interaction of the solute and is influenced by the contribution from individual protein molecules as the effects from interactions between two protein molecules (Saluja and Kalonia, 2008). The viscosity could be related as follow:

$$\eta = \eta_0 \cdot (1 + k_1 \cdot C + k_2 \cdot C^2 + \dots) \quad (4)$$

Where in equation 4,  $k_1$  is related to the contribution from individual solute molecules,  $k_2$  and higher order are related to effects from interactions of two or more protein molecules and  $(k_1 \cdot C)$  is related to the intrinsic viscosity whereas  $(k_2 \cdot C^2 + k_3 \cdot C^3 + \dots)$  reflects the pairwise interactions or protein-protein interactions meaning charge-charge electrostatics, hydrophobic interactions and other weaker interactions including van der Waals and dipole-dipole interactions. Thus  $B_{22}$  would reflect the influence of  $k_2$  on viscosity and there is a correlation between  $B_{22}$  and protein solution viscosity.

At high protein concentration, the differences in IgG1 stability could not be correlated to  $B_{22}$ . The only parameter that had a clear influence on protein stability and that correlated to  $B_{22}$  was pH. Studying protein at high concentration, two parameters have to be considered: (i) protein-protein interactions differ with the protein concentration; and (ii) increasing protein concentration induces a macromolecular crowding that corresponds to the effect of high total volume occupancy by macromolecular solutes upon the behavior of each macromolecular species in solution (Minton, 2005).

Whereas electrostatic and hydrophobic forces are predominant in dilute protein solution, excluded volume and van der Waals forces prevail in concentrated protein solution (Saluja and Kalonia, 2008). Harn et al. observed that stabilization at higher protein concentration was consistent with excluded volume theory (Harn *et al.*, 2007) which argues that the unfolding of protein proteins at high concentrations should be reduced in crowded solutions, as the secondary structure stability of MAbs was probably increased by the decrease in solvent exposed surface area that occurs during protein self-association.

## 4. CONCLUSIONS

FTIR spectra did not reveal any relevant structural changes of immobilized IgG1 compared to the initial antibody solution. Based on this statement, SIC could measure the interactions between native IgG1 in solution and native like immobilized IgG1, and thus allowed  $B_{22}$  determination. The SIC method needed to be optimized to obtain  $B_{22}$  of IgG1 as some chromatographic parameters influenced IgG1 interaction measurements. Flow rate, protein concentration together with surface coverage of the chromatographic particles and temperature were parameters affecting  $B_{22}$  values of IgG1 and that needed to be adjusted before formulation parameter screening.

For the investigated monoclonal antibody, small variations in  $B_{22}$  values were measurable by varying physiologically relevant formulation parameters. Under all the tested conditions  $B_{22}$  remained positive indicating all the tested formulations favored repulsive interactions. Formulation parameters having the most impact on  $B_{22}$  were pH and ionic strength. Buffer species influenced only at low ionic strength whereas salt and amino acid played a role at high concentration. High NaCl concentration screened the repulsive interactions, when high amino acid concentrations maintained or increased repulsive interactions. The study of sugar and polyol turn out to be more difficult, even though its feasibility had been demonstrated for the model protein lysozyme. Columns were disturbed by mannitol and sucrose and no self-association / aggregation or precipitation mechanism could explain this phenomenon.

Increasing  $B_{22}$  values corresponded to an easier IgG1 concentration process for the different tested buffer formulations. Moreover increasing  $B_{22}$  values reflected a decrease of solution viscosity for high concentrated IgG1 formulations. According to  $B_{22}$ , the 5 mM histidine containing buffer formulation showed a higher potential to favor repulsive protein-protein interactions. This was also confirmed by a stability study conducted 12 weeks long at 40 °C with 20 mg/ml IgG1 solutions, when the chemical instability of histidine was eliminated by EDTA addition. However the colloidal

stabilization did not seem to be the only factor influencing the protein stability and the conformational stability also had to be considered.

Comparing the stability of IgG1 formulated at high concentration to  $B_{22}$  was more difficult. All tested protein formulations showed similar stability after 4 weeks of storage at 40 °C. Only pH had a significant influence on protein stability. The other parameters (buffer species, salt and arginine) had a negligible influence on protein stability at pH 6.2 probably due to the self-buffering action of monoclonal antibodies and due to the macromolecular crowding effect.

Thus, SIC gave reliable results of IgG1-IgG1 interactions depending on solution parameters predicting formulation parameters to increase IgG1 solubility, decrease IgG1 viscosity at high concentration, but also to increase IgG1 colloidal stability at low or intermediate protein concentration.  $B_{22}$  seems to correlate to protein solubility, protein viscosity and protein colloidal stability.

## 5. REFERENCES

Ahamed, T., Esteban, B. N. A., Ottens, M., Van Dedem, G. W. K., Van Der Wielen, L. A. M., Bisschops, M. A. T., Lee, A., Pham, C., and Thommes, J. Phase behavior of an intact monoclonal antibody. *Biophysical Journal*, 93, 610-619 (2007).

Alford, J. R., Kendrick, B. S., Carpenter, J. F., and Randolph, T. W. Measurement of the second osmotic virial coefficient for protein solutions exhibiting monomer-dimer equilibrium. *Analytical Biochemistry*, 377, 128-133 (2008a).

Alford, J. R., Kwok, S. C., Roberts, J. N., Wuttke, D. S., Kendrick, B. S., Carpenter, J. F., and Randolph, T. W. High concentration formulations of recombinant human interleukin-1 receptor antagonist: I. Physical characterization. *Journal of Pharmaceutical Sciences*, 97, 3035-3050 (2008b).

Arakawa, T., Ejima, D., Tsumoto, K., Obeyama, N., Tanaka, Y., Kita, Y., and Timasheff, S. N. Suppression of protein interactions by arginine: a proposed mechanism of the arginine effects. *Biophysical Chemistry*, 127, 1-8 (2007a).

Arakawa, T., Philo, J. S., and Kita, Y. Kinetic and thermodynamic analysis of thermal unfolding of recombinant erythropoietin. *Bioscience Biotechnology and Biochemistry*, 65, 1321-1327 (2001).

Arakawa, T., Tsumoto, K., Kita, Y., Chang, B., and Ejima, D. Biotechnology applications of amino acids in protein purification and formulations. *Amino Acids*, 33, 587-605 (2007b).

Bajaj, H., Sharma, V. K., Badkar, A., Zeng, D., Nema, S., and Kalonia, D. S. Protein structural conformation and not second virial coefficient relates to long-term irreversible aggregation of a monoclonal antibody and ovalbumin in solution. *Pharmaceutical Research*, 23, 1382-1394 (2006).

Bandekar, J. Amide modes and protein conformation. *Biochimica et Biophysica Acta*, 1120, 123-143 (1992).

Baynes, B. M., and Trout, B. L. Rational design of solution additives for the prevention of protein aggregation. *Biophysical Journal*, 87, 1631-1639 (2004).

Bonnete, F., Finet, S., and Tardieu, A. Second virial coefficient: variations with lysozyme crystallization conditions. *Journal of Crystal Growth*, 196, 403-414 (1999).

Brogli, R. A., Tiana, G., Pasquali, S., Roman, H. E., and Vigezzi, E. Folding and aggregation of designed proteins. *Proceedings of the National Academy of Sciences*, 95, 12930-12933 (1998).

Bummer, P. M. Chemical considerations in protein and peptide stability. *Drugs and the Pharmaceutical Sciences*, pp. 7-42, (2008).

Byler, D. M., and Susi, H. Examination of the secondary structure of proteins by deconvolved FTIR spectra. *Biopolymers*, 25, 469-487 (1986).

Chen, B., Bautista, R., Yu, K., Zapata, G. A., Mulkerrin, M. G., and Chamow, S. M. Influence of histidine on the stability and physical properties of a fully human antibody in aqueous and solid forms. *Pharmaceutical Research*, 20, 1952-1960 (2003).

Chi, E. Y., Krishnan, S., Kendrick, B. S., Chang, B. S., Carpenter, J. F., and Randolph, T. W. Roles of conformational stability and colloidal stability in the aggregation of recombinant human granulocyte colony-stimulating factor. *Protein Science*, 12, 903-913 (2003a).

Chi, E. Y., Krishnan, S., Randolph, T. W., and Carpenter, J. F. Physical stability of proteins in aqueous solution: Mechanism and driving forces in nonnative protein aggregation. *Pharmaceutical Research*, 20, 1325-1336 (2003b).

Demoruelle, K., Guo, B., Kao, S. M., Mcdonald, H. M., Nikic, D. B., Holman, S. C., and Wilson, W. W. Correlation between the osmotic second virial coefficient and solubility for equine serum albumin and ovalbumin. *Acta Crystallographica Section D-Biological Crystallography*, 58, 1544-1548 (2002).

Dephillips, P., and Lenhoff, A. M. Pore size distributions of cation-exchange adsorbents determined by inverse size-exclusion chromatography. *Journal of Chromatography A*, 883, 39-54 (2000).

Dill, K. A. Dominant forces in protein folding. *Biochemistry*, 29, 7133-7155 (1990).

Dong, A. C., Kendrick, B., Kreilgard, L., Matsuura, J., Manning, M. C., and Carpenter, J. F. Spectroscopic study of secondary structure and thermal denaturation of recombinant human factor XIII in aqueous solution. *Archives of Biochemistry and Biophysics*, 347, 213-220 (1997).

Dudgeon, K., Famm, K., and Christ, D. Sequence determinants of protein aggregation in human VH domains. *Protein Engineering*, 22, 217-220 (2009).

Garcia, C. D., Holman, S. C., Henry, C. S., and Wilson, W. W. Screening of protein-ligand interactions by affinity chromatography. *Biotechnology Progress*, 19, 575-579 (2003).

Gokarn, Y. R., Kras, E., Nodgaard, C., Dharmavaram, V., Fesinmeyer, R. M., Hultgen, H., Brych, S., Remmele, R. L., Brems, D. N., and Hershenson, S. Self-buffering antibody formulations. *Journal of Pharmaceutical Sciences*, 97, 3051-3066 (2008).

Guo, B., Kao, S., Mcdonald, H., Asanov, A., Combs, L. L., and Wilson, W. W. Correlation of second virial coefficients and solubilities useful in protein crystal growth. *Journal of Crystal Growth*, 196, 424-433 (1999).

Haas, C., Drenth, J., and Wilson, W. W. Relation between the solubility of proteins in aqueous solutions and the second virial coefficient of the solution. *Journal of Physical Chemistry B*, 103, 2808-2811 (1999).



Harn, N., Allan, C., Oliver, C., and Middaugh, C. R. Highly concentrated monoclonal antibody solutions: Direct analysis of physical structure and thermal stability. *Journal of Pharmaceutical Sciences*, 96, 532-546 (2007).

Hawe, A., Sutter, M., and Jiskoot, W. Extrinsic fluorescent dyes as tools for protein characterization. *Pharmaceutical Research*, 25, 1487-1499 (2008).

Haynes, C. A., Tamura, K., Korfer, H. R., Blanch, H. W., and Prausnitz, J. M. Thermodynamic properties of aqueous alpha-chymotrypsin solutions from membrane osmometry measurements. *Journal of Physical Chemistry*, 96, 905-912 (1992).

Ionescu, R. M., Vlasak, J., Price, C., and Kirchmeier, M. Contribution of variable domains to the stability of humanized IgG1 monoclonal antibodies. *Journal of Pharmaceutical Sciences*, 97, 1414-1426 (2008).

Jimenez, M., Rivas, G., and Minton, A. P. Quantitative characterization of weak self-association in concentrated solutions of immunoglobulin G via the measurement of sedimentation equilibrium and osmotic pressure. *Biochemistry*, 46, 8373-8378 (2007).

Katayama, D. S., Nayar, R., Chou, D. K., Valente, J. J., Cooper, J., Henry, C. S., Vander Velde, D. G., Villarete, L., Liu, C. P., and Manning, M. C. Effect of buffer species on the thermally induced aggregation of interferon-tau. *Journal of Pharmaceutical Sciences*, 95, 1212-1226 (2006).

Liu, J., Nguyen, M. D., Andya, J. D., and Shire, S. J. Reversible self-association increases the viscosity of a concentrated monoclonal antibody in aqueous solution. *Journal of Pharmaceutical Sciences*, 94, 1928-1940 (2005).

Liu, W., Bratko, D., Prausnitz, J. M., and Blanch, H. W. Effect of alcohols on aqueous lysozyme-lysozyme interactions from static light-scattering measurements. *Biophysical Chemistry*, 107, 289-298 (2004).

Mahler, H. C., Muller, R., Friess, W., Delille, A., and Matheus, S. Induction and analysis of aggregates in a liquid IgG1-antibody formulation. *European Journal of Pharmaceutics and Biopharmaceutics*, 59, 407-417 (2005).

Matheus, S., Mahler, H. C., and Friess, W. A critical evaluation of T<sub>m</sub> (FTIR) measurements of high-concentration IgG(1) antibody formulations as a formulation development tool. *Pharmaceutical Research*, 23, 1617-1627 (2006).

Minton, A. P. Influence of macromolecular crowding upon the stability and state of association of proteins: Predictions and observations. *Journal of Pharmaceutical Sciences*, 94, 1668-1675 (2005).

Muller, E., and Mann, C. Resin characterization by electro-acoustic measurements. *Journal of Chromatography A*, 1144, 30-39 (2007).

Narhi, L. O., Philo, J. S., Sun, B., Chang, B. S., and Arakawa, T. Reversibility of heat-induced denaturation of the recombinant human megakaryocyte growth and development factor. *Pharmaceutical Research*, 16, 799-807 (1999).

Payne, R. W., Nayar, R., Tarantino, R., Del Terzo, S., Moschera, J., Di, J., Heilman, D., Bray, B., Manning, M. C., and Henry, C. S. Second virial coefficient determination of a therapeutic peptide by self-interaction chromatography. *Biopolymers*, 84, 527-533 (2006).

Pelton, J. T., and Mclean, L. R. Spectroscopic methods for analysis of protein secondary structure. *Analytical Biochemistry*, 277, 167-176 (2000).

Piazza, R. Protein interactions and association: an open challenge for colloid science. *Current Opinion in Colloid & Interface Science*, 8, 515-522 (2004).

Reubsaet, J. L., Beijnen, J. H., Bult, A., Van Maanen, R. J., Marchal, J. A., and Underberg, W. J. Analytical techniques used to study the degradation of proteins and peptides: chemical instability. *Journal of Pharmaceutical and Biomedical Analysis*, 17, 955-978 (1998).

Rice, P., Longden, I., and Bleasby, A. EMBOSS: The European molecular biology open software suite. *Trends in Genetics*, 16, 276-277 (2000).

Saluja, A., Badkar, A. V., Zeng, D. L., Nema, S., and Kalonia, D. S. Ultrasonic storage modulus as a novel parameter for analyzing protein-protein interactions in high protein concentration solutions: Correlation with static and dynamic light scattering measurements. *Biophysical Journal*, 92, 234-244 (2007).

Saluja, A., and Kalonia, D. S. Nature and consequences of protein-protein interactions in high protein concentration solutions. *International Journal of Pharmaceutics*, 358, 1-15 (2008).

Schule, S., Friess, W., Bechtold-Peters, K., and Garidel, P. Conformational analysis of protein secondary structure during spray-drying of antibody/mannitol formulations. *European Journal of Pharmaceutics and Biopharmaceutics*, 65, 1-9 (2007).

Shaw, K. L., Grimsley, G. R., Yakovlev, G. I., Makarov, A. A., and Pace, C. N. The effect of net charge on the solubility, activity, and stability of ribonuclease Sa. *Protein Science*, 10, 1206-1215 (2001).

Shiraki, K., Kudou, M., Fujiwara, S., Imanaka, T., and Takagi, M. Biophysical effect of amino acids on the prevention of protein aggregation. *J.Biochem.*, 132, 591-595 (2002).

Shire, S. J., Shahrokh, Z., and Liu, J. Challenges in the development of high protein concentration formulations. *Journal of Pharmaceutical Sciences*, 93, 1390-1402 (2004).

Tessier, P. M., Lenhoff, A. M., and Sandler, S. I. Rapid measurement of protein osmotic second virial coefficients by self-interaction chromatography. *Biophysical Journal*, 82, 1620-1631 (2002).

Timasheff, S. N. The control of protein stability and association by weak-interactions with water - How do solvents affect these processes. *Annual Review of Biophysics and Biomolecular Structure*, 22, 67-97 (1993).

Trovato, A., Senol, F., and Tosatto, S. C. E. The PASTA server for protein aggregation prediction. *Protein Engineering*, 20, 521-523 (2007).

Valente, J. J., Fryksdale, B. G., Dale, D. A., Gaertner, A. L., and Henry, C. S. Screening for physical stability of a *Pseudomonas* amylase using self-interaction chromatography. *Analytical Biochemistry*, 357, 35-42 (2006).

Valente, J. J., Payne, R. W., Manning, M. C., Wilson, W. W., and Henry, C. S. Colloidal behavior of proteins: effects of the second virial coefficient on solubility, crystallization and aggregation of proteins in aqueous solution. *Current Pharmaceutical Biotechnology*, 6, 427-436 (2005).

Van De Weert, M., Haris, P. I., Hennink, W. E., and Crommelin, D. J. A. Fourier transform infrared spectrometric analysis of protein conformation: Effect of sampling method and stress factors. *Analytical Biochemistry*, 297, 160-169 (2001).

Wang, W., Singh, S., Zeng, D. L., King, K., and Nema, S. Antibody structure, instability, and formulation. *Journal of Pharmaceutical Sciences*, 96, 1-26 (2007).

## CHAPTER 5

### LIMITS OF THE PROTEIN SOLUBILITY DETERMINATION BY PRECIPITATION WITH POLYETHYLENE GLYCOL

#### 1. INTRODUCTION

One of the most common approaches that is used to quantify protein solubility derives from chemistry and consists in adding an excess of solid into solution until the solution is saturated (Trevino *et al.*, 2008). The insoluble part of the drug is removed by centrifugation and the remaining concentration in supernatant, corresponding to drug solubility, is determined. Thus, protein solubility has been defined as the maximum amount of protein in the presence of specified co-solutes that is not sedimented by 30,000 g centrifugation for 30 min (Schein, 1990). This method assumes that the initial protein drug is solid, and not in solution, and that huge protein quantities are available when the studied protein is highly soluble.

Another approach consists of reducing protein solubility in some regular and quantitatively definable manner and extrapolating to true solubility (Middaugh *et al.*, 1979). For this purpose an inert macromolecule such as polyethylene glycol (PEG) is added to the protein solution which induces attraction between protein molecules. This attraction phenomenon, which is called depletion interaction, results from the exclusion of the polymer molecules from the zone between two proteins named depletion zone (Asakura and Oosawa, 1958). Adding PEG molecules to protein solution decreases the surface tension (Bhat and Timasheff, 1992) and induces the steric exclusion of the polymer from the protein surface, as protein molecules are preferentially hydrated. If the depletion zones overlap, the volume accessible to the polymers increases resulting in an increase of the entropy of the system (Boncina *et al.*, 2008, Finet *et al.*, 2003). Because of the steric exclusion from regions of the solvent occupied by PEG, protein molecules concentrate in the aqueous phase until their solubility is exceeded and their precipitation occurs. Thermodynamically, PEG increases the chemical potential of the protein until it exceeds that of the pure solid state resulting in the precipitation of the protein molecules (Kumar *et al.*, 2009). The increase in the protein chemical potential by PEG and its precipitation depend on

the area of the protein molecules exposed to the solvent and thus on the protein size. The depletion reaction also depends on the polymer size and its concentration. There is a considerable ordering of water around the PEG chain since two or three water molecules are closely associated with each ethylene oxide unit (Cocke *et al.*, 1997). Protein interaction releases some of this water of solvation and produces a positive entropy change. The excess number of water molecules around a protein increases with the presence of increasing PEG molecular weight and is almost proportional to the exclusion volume (Shulgin and Ruckenstein, 2006).

Even though no change in protein circular dichroism spectrum was first observed (Atha and Ingham, 1981), PEG can interact with protein molecules and destabilize proteins, as a reduction of the melting temperature has been reported in the presence of the polymer (Arakawa and Timasheff, 1985). Indeed, Kumar and co-workers (2009) have shown that small PEG molecules are not appropriate for estimating the activity of proteins as they can induce subtle changes in protein conformation and can significantly affect protein precipitation. In some cases, there is significant evidence that PEG specifically interacts with protein and mechanisms other than depletion forces are also likely to be involved (Dumetz *et al.*, 2008). Because of its hydrophobic nature, PEG can interact with the non polar region of the protein molecules. Nevertheless PEG causes only little protein denaturation, as it can probably not reach the interior of the protein molecules because of its size (McPherson, 1990). On the other hand, contrary to the common depletion theory, PEG has been described to induce repulsion between protein molecules (Bloustine *et al.*, 2006, Kozer *et al.*, 2007), which would preclude its use in protein solubility determination.

According to Ogston (Hasko *et al.*, 1982), protein solubility could be described by the following empirical equation 1:

$$\mu = \mu_s^0 + R \cdot T (\ln S + d \cdot S + a \cdot C) \quad (1)$$

where  $\mu$  is the chemical potential of the protein,  $\mu_s^0$  is the standard chemical potential,  $S$  and  $C$  are respectively the protein concentration and the polymer concentration,  $a$  and  $d$  are constants that are characteristic for the protein-polymer ( $a$ ) and protein-protein interactions ( $d$ ),  $R$  is the gas constant and  $T$  is the absolute temperature. The equation 1 can be reduced as follow, providing  $d$  is negligible at low protein concentration (Ingham, 1990):

$$\log S = \log S_0 - a \cdot C \quad (2)$$

where  $S$  is the protein solubility in the presence of PEG at concentration  $C$  and  $S_0$  is the apparent intrinsic protein solubility in the absence of PEG. Thus the logarithm of the protein concentration in solution can be plotted as a function of the PEG concentration and the protein solubility in the absence of PEG can be obtained by extrapolation to

zero PEG concentration. As this quantification method has been reported to be independent of initial protein concentration (Hasko *et al.*, 1982, Ingham, 1978) and as protein solubility limit has not been reached, protein quantity could be minimized.

Originally the precipitation of protein by PEG has been described to analyze the solubility of plasma proteins (Hasko *et al.*, 1982) and to develop a plasma protein fractionation system (Polson *et al.*, 1964). The method has been well described with  $\alpha$ -,  $\beta$ - and  $\gamma$ -globulins, albumin, transferrin but also with deoxyhemoglobin S, insulin, IgM, IgG,  $\beta$ -lactoglobulin (Middaugh *et al.*, 1979) or more recently with recombinant bovine somatotropin (Stevenson and Hageman, 1995) or lysozyme (Boncina *et al.*, 2008). Lately a patent (Li *et al.*, 2007) described the use of PEG precipitation method to quantify the solubility of polypeptides comprising monoclonal antibodies such as IgG.

This work focused on the feasibility of the protein precipitation method by PEG with an IgG1 to determine protein solubility and to optimize formulation conditions. At first, the method parameters had to be optimized for the IgG1, before the influence of different formulation parameters were tested and the capability of the PEG method in solubility prediction by this precipitation method could be judged.

## **2. MATERIALS AND METHODS**

### **2.1. Materials**

A humanized monoclonal IgG1 antibody, which was formulated as a 5 mg/ml solution in phosphate buffered saline (PBS) at pH 6.2, was provided by Boehringer Ingelheim. PEG 3000, PEG 6000 and PEG 20000 were obtained from Clariant (Muttenz, Switzerland), sodium acetate, sodium chloride, sodium citrate, L-arginine monohydrochloride and L-histidine from Merck (Darmstadt, Germany), sodium phosphate from Riedel-de Haën (Seelze, Germany) and sodium succinate from Alfa Aesar (Karlsruhe, Germany).

### **2.2. Solubility determination by precipitation**

The PEG of interest was dissolved to a 40 % (w/v) solution in purified water. IgG1 solutions were prepared by dialysis with 14 kDa MWCO regenerated cellulose membranes (Karl Roth, Karlsruhe, Germany). The PEG solution was added to 500  $\mu$ l of protein solution to reach a final PEG concentration comprised between 12 % and 18 % and an end solution volume of 1 ml. After sample homogenization with a vortex mixer,

samples were incubated at room temperature during 12 h before being centrifuged (6000g, 20 min).

Protein concentrations were measured spectrophotometrically with an Agilent 8453 instrument (Agilent technology, Waldbronn, Germany) at 280 nm using as extinction coefficient  $1.44 \text{ ml}\cdot\text{mg}^{-1}\cdot\text{cm}^{-1}$ . All experiments were conducted in triplicate. The absorbance of PEG at 280 nm was minimal (e.g. 0.051 AU for 20 % PEG 6000) so that it did not disturb protein concentration measurements. The IgG1 quantification limit of the spectrophotometrical method was  $13 \text{ }\mu\text{g/ml}$ . The logarithm of the protein concentrations in the supernatant after centrifugation was plotted as a function of PEG concentration. Data in the linear region of  $\log [\text{IgG1}]$  versus  $[\text{PEG}]$  plots were fitted to straight lines.

## 3. RESULTS AND DISCUSSION

### 3.1. Method optimization

#### 3.1.1. Molecular weight of PEG

The influence of PEG molecular weight on IgG1 precipitation was first studied. The three different PEG grades (PEG 3000, PEG 6000 and PEG 20000) induced IgG1 precipitation, which became more pronounced with increasing PEG concentration (Fig. V-1). PEG 3000 required a concentration higher than 15 % to induce IgG1 precipitation, whereas a concentration higher than 12 % was sufficient for both PEG 6000 and 20000. Moreover, at the same PEG concentration, protein precipitation increased with PEG molecular weight from 3000 to 6000. However, the degree of polymerization of PEG did not infinitely enhance the protein precipitation, as the use of PEG having a molecular weight higher than 6000 did not improve the quantity of precipitated protein (Atha and Ingham, 1981, Ingham, 1990). Such observations reflected the theory of steric exclusion. Increasing the size of PEG induced an increase in the volume of the solution from which proteins have to be excluded, and the chemical potential of the protein was more enhanced in the presence of PEG of higher molecular weight (Kumar *et al.*, 2009). As described by Boncina and co-workers (2008) and contrary to Stevenson and Hageman (1995), the extrapolated protein solubility differed with the PEG molecular weight: 149 mg/ml, 900 mg/ml and 40 mg/ml with PEG 3000, PEG 6000 and PEG 20000 respectively. Even though both PEG 6000 and 20000 allowed a rapid reduction of the protein concentration in solution, PEG 6000 was chosen for the further studies because PEG 20000 solutions showed a high viscosity that made solution handling more difficult.

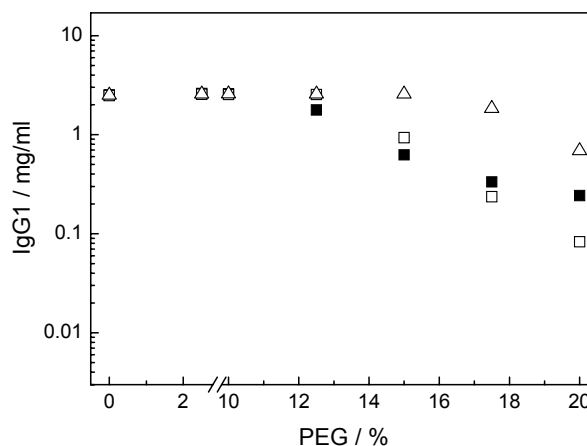


Fig. V-1: Effect of PEG molecular weight on IgG1 concentration in supernatant: PEG 3000 ( $\Delta$ ), PEG 6000 ( $\square$ ) and PEG 20000 ( $\blacksquare$ ) (IgG1 was formulated in PBS buffer pH 6.2 and had an initial concentration of 5 mg/ml).

### 3.1.2. IgG1 concentration

The influence of the initial IgG1 concentration was tested in the concentration range from 5 to 50 mg/ml. A higher protein concentration displaced the beginning of precipitation; the PEG concentration that induced IgG1 precipitation was smaller for the 50 mg/ml IgG1 solution as compared to the 20 and 5 mg/ml IgG1 solutions (Fig. V-2). However the slope of the three plotted straight lines was comparable, as no quantitative reaction takes place between PEG and protein (Hasko et al.; 1982; Ingham; 1978). Thus, initial protein concentration should have no or little effect on protein solubility determination.

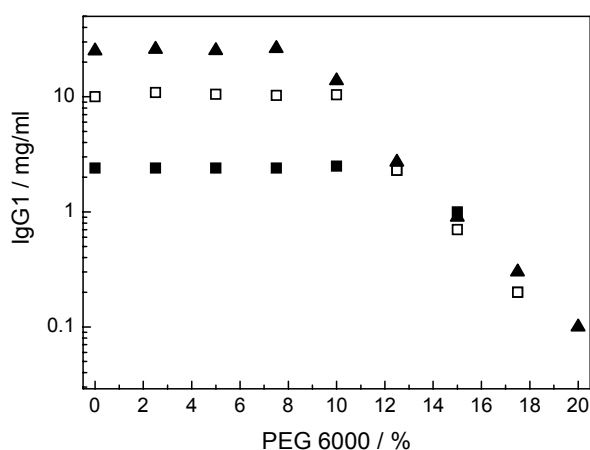


Fig. V-2: Effect of IgG1 initial concentration on IgG1 concentration in supernatant as a function of PEG 6000 concentration: 5 mg/ml ( $\blacksquare$ ), 20 mg/ml ( $\square$ ) and 50 mg/ml ( $\blacktriangle$ ).



## 3.2. Comparison of different IgG1 formulations with the precipitation method

### 3.2.1. Influence of pH

IgG1 was formulated in a buffer blend that comprised sodium acetate, sodium phosphate and sodium succinate at three different pH values: 4.0, 6.0 and 8.0. IgG1 precipitation was more effective at alkaline pH; less than 0.1 mg/ml IgG1 remained in solution after addition of 12 % PEG 6000 to protein formulated at pH 8.0 (Fig. V-3). On the other hand, the IgG1 did hardly precipitate at pH 4.0, even at 18 % PEG concentration. As the IgG1 has an alkaline isoelectric point of approximately 8.3, increasing pH reduced the protein net charge. Given that the protein solubility is approximately proportional to the square of the protein net charge, the protein solubility was lowered as the pH was near its pI (Shaw *et al.*, 2001). Moreover the osmotic second virial coefficient ( $B_{22}$ ) of IgG1 decreased by increasing the pH towards the protein pI (Table V-1), revealing a decrease in repulsive interactions between protein molecules and thus corresponding to a decrease in the IgG1 solubility. Consequently, the increase in IgG1 precipitation at higher pH was in agreement with the fact that protein precipitation should be enhanced by conditions that foster protein association because of the larger size of the complexes, whereas conditions that limit protein association would have the opposite effect (Ingham, 1990). The IgG1 solubility values that were obtained by extrapolation to zero PEG concentration were surprising, as the resulting IgG1 solubility was 19 mg/ml at pH 4 and 2370 mg/ml at pH 6 (Table V-1). There was no correlation between the extrapolated solubility values and the resistance to PEG precipitation and the theoretical reduction of net charges on protein.

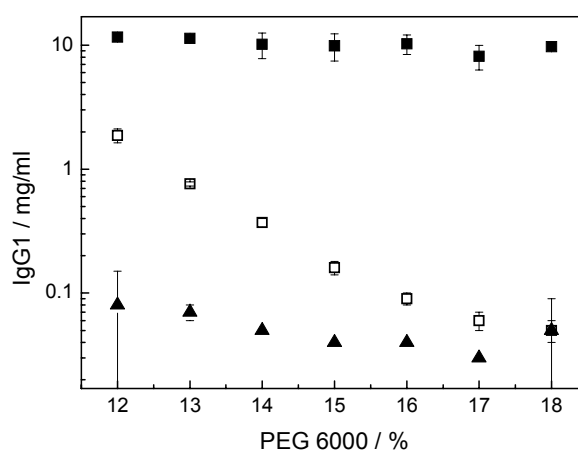


Fig. V-3: Effect of PEG 6000 on IgG1 concentration (initial concentration of 20 mg/ml) as a function of pH solution: pH 4 (■), pH 6 (□) and pH 8 (▲).

### 3.2.2. Influence of buffer composition

The buffer species influence was tested at pH 6.2 and two concentration levels (5 and 50 mM). At both concentrations, the sodium citrate buffer presented the lower IgG1 concentrations, whereas IgG1 did not precipitate in the presence of 5 and 50 mM histidine buffers (Fig. V-4A and V-4B). The IgG1 precipitation profile was concentration dependent for sodium phosphate and sodium succinate buffer. IgG1 began to precipitate by addition of 16 % PEG in the presence of 5 mM phosphate or succinate buffer, whereas its precipitation occurred already at 12 % in the presence of 50 mM of the same buffers. Increasing buffer concentration did not necessarily improve the IgG1 resistance to PEG precipitation but leveled the differences between the salt buffers. The  $B_{22}$  measurements underlined also that the 5 mM histidine formulation was superior and that higher buffer concentrations did not necessarily improve the repulsive interactions between protein molecules (Table V-1). However  $B_{22}$  differed with the histidine concentration, as increasing histidine concentration lowered  $B_{22}$  and thus repulsive interactions.

The extrapolation to zero PEG concentration was not applied to the determination of the solubility of IgG1 formulated with histidine, as insufficient precipitation was observed. Moreover extremely high protein solubility values were obtained in the presence of 5 mM phosphate and 5 mM succinate buffers with 71912 and 18655 mg/ml respectively, which raises the question about the plausibility of solubility values obtained by extrapolating the plotted straight lines. Discrepancies between extrapolated solubility values that overestimated protein solubility and theoretical excluded volume treatment of hemoglobin activities have been already reported (Middaugh *et al.*, 1979).

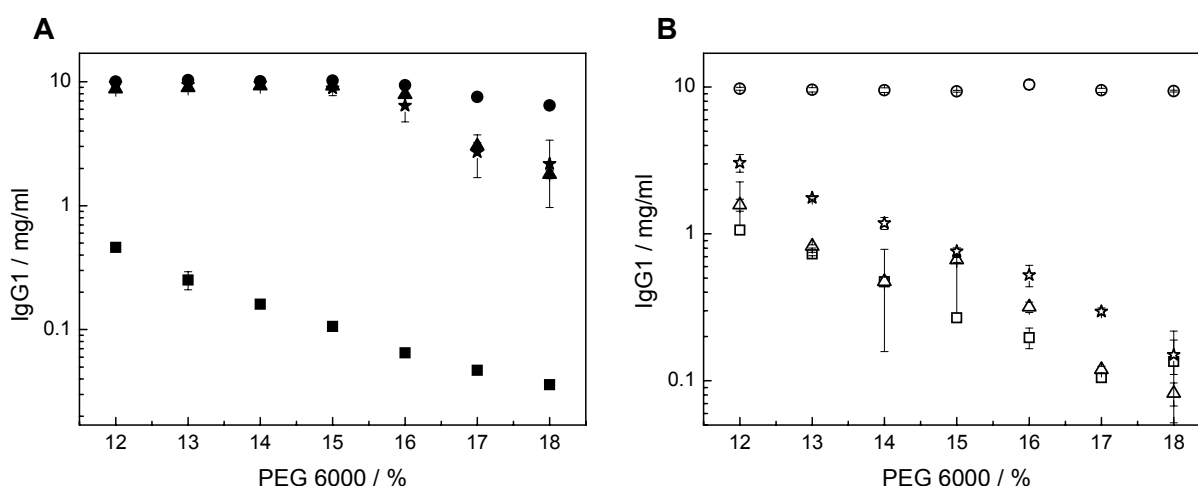


Fig. V-4: Effect of PEG 6000 on IgG1 concentration (initial concentration of 20 mg/ml) as a function of:

(A) Buffer species (5 mM concentration, pH 6.2): citrate (■), histidine (●), phosphate (▲), succinate (★).

(B) Buffer species (50 mM concentration, pH 6.2): citrate (□), histidine (○), phosphate (△), succinate (☆).

### 3.2.3. Influence of amino acids and salts

The influence of sodium chloride was tested as a function of its concentration in the presence of 5 mM sodium succinate buffer pH 6.2. Addition of salt favored IgG1 precipitation (Fig. V-5A), since salt screened protein charges. The two salt concentrations tested (25 and 150 mM) presented comparable solubility profiles.  $B_{22}$  measurements however showed that increasing salt concentration to 150 mM more significantly screened the protein charges as compared to the 25 mM NaCl containing protein solution and that consequently repulsive interactions were diminished (Table V-1). A decrease in solubility and an increase in IgG1 precipitation would be expected by increasing sodium chloride concentration.

The influence of arginine was tested similarly as a function of its concentration. Addition of arginine favored IgG1 precipitation in sodium succinate buffer (Fig. V-5B). The IgG1 precipitation was slightly more pronounced in the presence of 100 mM arginine than in the presence of 10 mM arginine at PEG concentrations between 12 % and 15 %. Arginine is an amino acid commonly used to stabilize protein (Arakawa *et al.*, 2007). Adding arginine to protein solution slightly penalized  $B_{22}$  at low concentration ( $0.66 \cdot 10^{-4}$  mol·ml·g<sup>-2</sup> at 10 mM) but increased it at higher concentration such as 100 mM ( $2.27 \cdot 10^{-4}$  mol·ml·g<sup>-2</sup>) (Table V-1). Its influence on protein interactions was not reflected in the PEG precipitation experiments as little differences were noticed. Extrapolating the slope to zero PEG concentration again did not result in plausible results in the presence of salt and arginine.

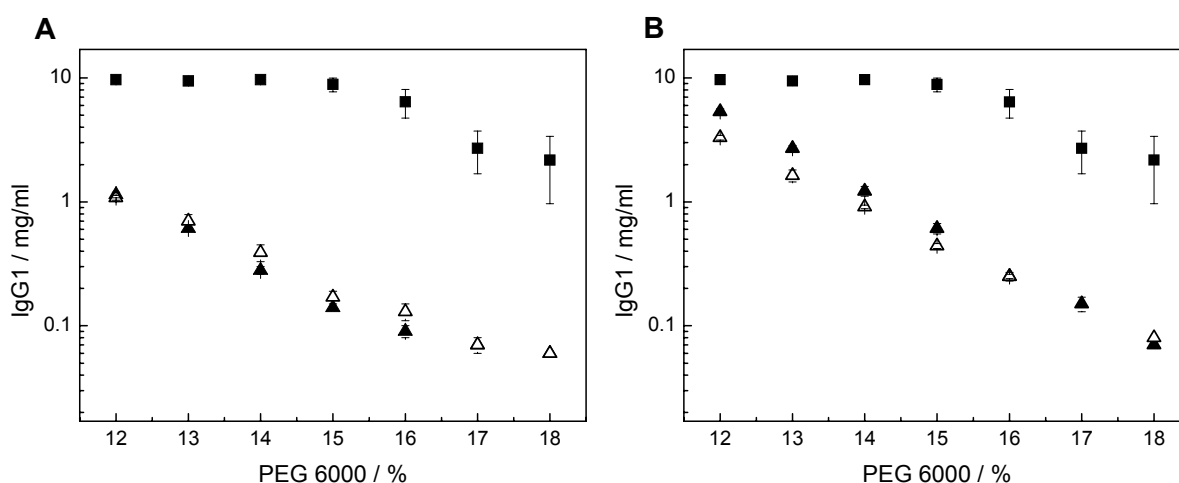


Fig. V-5: Effect of PEG 6000 on IgG1 concentration (initial concentration of 20 mg/ml) as a function of:

(A) NaCl concentration (5 mM succinate buffer pH 6.2): succinate buffer (■), 25 mM NaCl (▲), 150 mM NaCl (△).

(B) Arginine concentration (5 mM succinate buffer pH 6.2): succinate buffer (■), 10 mM arginine (▲) and 100 mM arginine (△).

	PEG precipitation method			$B_{22}$ value ( $10^{-4}$ mol·ml·g <sup>-2</sup> )
	extrapolated solubility value (mg/ml)	1 <sup>st</sup> solubility ranking	2 <sup>nd</sup> solubility ranking	
mixed buffer pH 4.0 *	19	A	A	2.35
mixed buffer pH 6.0 *	2370	D	C	2.00
mixed buffer pH 8.0 *	1	D	D	1.82
5 mM citrate pH 6.2	64	D	C	1.68
5 mM histidine pH 6.2	n/a	A	A	2.32
5 mM phosphate pH 6.2	71912	B	A	1.56
5 mM succinate pH 6.2	18655	B	A	1.87
50 mM citrate pH 6.2	109	D	B	1.84
50 mM histidine pH 6.2	n/a	A	A	1.88
50 mM phosphate pH 6.2	433	D	B	1.90
50 mM succinate pH 6.2	966	D	B	1.83
25 mM NaCl pH 6.2 **	418	D	C	2.06
150 mM NaCl pH 6.2 **	493	D	B	1.69
10 mM arginine pH 6.2 **	32893	D	B	0.66
100 mM arginine pH 6.2 **	5299	D	B	2.27

\* buffer composition: 10 mM sodium acetate, 10 mM sodium phosphate, 10 mM sodium succinate

\*\* formulation containing 5 mM succinate buffer

n/a insufficient precipitation

Table V-1: IgG1 solubility values and groups as a function of IgG1 formulations.

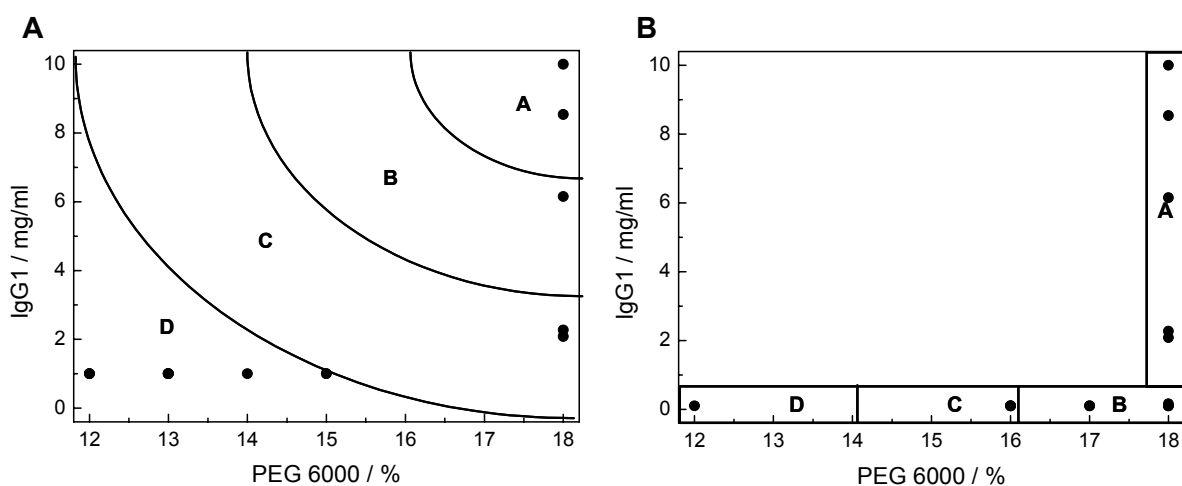


Fig. V-6: Ranking according to (A) the PEG 6000 concentration inducing IgG1 precipitation and the corresponding IgG1 concentration in the supernatant, (B) the PEG 6000 concentration necessary to reduce IgG1 solubility to 0.1 mg/ml or IgG1 concentration in the presence of 18 % PEG 6000 in the case of insufficient precipitation.

### 3.3. Method interpretation: extrapolation versus ranking

As extrapolated solubility values did not deliver reliable results, other interpretation methods were to be attempted. Because of the differences in precipitation slopes, a ranking approach could be useful to determine formulation parameters that favor the resistance of protein to precipitation. As described previously, formulations that presented a higher solubility required higher PEG concentration to start precipitating.

A first ranking was based on (i) the PEG 6000 concentration inducing first precipitation of the protein; and (ii) the corresponding IgG1 concentration (Fig. V-6A) - the less the tendency of the protein to precipitate in the presence of PEG, the higher its solubility. Four solubility classes could be distinguished: "A" for high solubility, "B" for good solubility, "C" for medium solubility and "D" for low solubility. Nevertheless, this approach did not allow differentiating clearly between the different formulations tested, as two groups were mainly represented. The first one included formulations presenting a good or high solubility and a second preponderant class presented formulations exhibiting low solubility. A second ranking approach was attempted based on (i) the PEG 6000 concentration required to reduce the concentration in solution to 0.1 mg/ml IgG1; and (ii) if a reduction to 0.1 mg/ml could not be reached, the IgG1 concentration in solution in the presence of 18 % PEG 6000 (Fig. V-6B). As for the previous ranking, the same four categories, A, B, C and D, could be differentiated.

This second method of ranking led to a different distribution of IgG1 formulations. The predominant group D of the first ranking was split into the three groups D, C and B. The second ranking allowed a better estimation and differentiation of the formulation contribution. With increasing the pH value from 4 to 6 to 8, the IgG1 formulations were attributed to groups A, C and D. Increasing the concentration of citrate, phosphate and succinate buffer also resulted in the assignment of different solubility categories. However no differences could be made with arginine containing formulations and no logical classification was obtained with NaCl containing formulations.

$B_{22}$  has been demonstrated theoretically (Haas *et al.*, 1999) as well as experimentally (George *et al.*, 1997) to correlate with protein solubility and the higher the  $B_{22}$  value, the better the solubility. In the case of the IgG1 tested the  $B_{22}$  values were all positive (Table V-1), revealing that all conditions tested favored repulsive interactions between protein molecules. No extremely unfavorable conditions were tested. Increasing pH reduced both  $B_{22}$  and protein precipitation. The role of the buffer species and concentration differed according to the analytical method used. For example,  $B_{22}$  was higher at 5 mM histidine as compared to 50 mM, but IgG1 hardly precipitated by addition of PEG at both histidine concentrations. In phosphate buffer the IgG1

presented a more positive  $B_{22}$  value at high than at low concentration, whereas the PEG precipitation indicated lower solubility at high concentration. Furthermore, for the addition of 150 mM NaCl a decrease in  $B_{22}$  pointed to a reduced solubility, whereas it appeared to be improved according to the PEG precipitation. In addition, arginine had the most important influence on  $B_{22}$ , whereas no notable difference appeared in PEG precipitation. Obviously, only few data gave comparable solubility trends. Thus, solubility differences could be better underscored by  $B_{22}$  than by PEG precipitation. Overall, this latter ranking method allowed a rough differentiation of the formulation effect on protein solubility, but only parameters having a strong influence could be reflected.

## 4. CONCLUSIONS

Depletion interaction occurred by addition of PEG to IgG1 solution, resulting in IgG1 precipitation. As described in the literature, the protein concentration remaining in solution was proportional to the PEG concentration. Increasing pH towards IgG1 pI enhanced protein precipitation as predicted by  $B_{22}$ . Increasing the solution ionic strength by varying the concentration of buffer or NaCl induced various IgG1 precipitations, whose variations could not be systematically correlated to  $B_{22}$ . In addition, an apparent protein solubility could not be determined by extrapolation to zero PEG concentration as the numerical solubility values were not reliable. An alternative interpretation method was established providing a ranking in four solubility classes according to the following parameters: (i) the PEG 6000 concentration required reducing the concentration in solution to 0.1 mg/ml IgG1; and (ii) if a reduction to 0.1 mg/ml could not be reached, the IgG1 concentration in solution in the presence of 18 % PEG 6000. This ranking method did not provide absolute solubility data but a meaningful interpretation of the formulation effects on protein solubility. Thus, in order to obtain solubility values, methods based on concentration processes appear to be more appropriated. The PEG precipitation method could be attractive as simple method, which requires reasonable amount of protein material, to quickly gain rough information on protein solubility affecting factors. However, the results obtained by the PEG precipitation method could not be correlated to  $B_{22}$ , as many discrepancies were observed. The predicative character of the ranking method remains uncertain.

## 5. REFERENCES

Arakawa, T., and Timasheff, S. N. Mechanism of poly(ethylene glycol) interaction with proteins. *Biochemistry*, 24, 6756-6762 (1985).

Arakawa, T., Tsumoto, K., Kita, Y., Chang, B., and Ejima, D. Biotechnology applications of amino acids in protein purification and formulations. *Amino Acids*, 33, 587-605 (2007).

Asakura, S., and Oosawa, F. Interaction between particles suspended in solutions of macromolecules. *Journal of Polymer Science*, 33, 183-192 (1958).

Atha, D. H., and Ingham, K. C. Mechanism of precipitation of proteins by polyethylene glycols. Analysis in terms of excluded volume. *Journal of Biological Chemistry*, 256, 12108-12117 (1981).

Bhat, R., and Timasheff, S. N. Steric exclusion is the principal source of the preferential hydration of proteins in the presence of polyethylene glycols. *Protein Science*, 1, 1133-1143 (1992).

Bloustine, J., Virmani, T., Thurston, G. M., and Fraden, S. Light scattering and phase behavior of lysozyme-poly(ethylene glycol) mixtures. *Physical Review Letters*, 96, 1-4 (2006).

Boncina, M., Rescic, J., and Vlachy, V. Solubility of lysozyme in polyethylene glycol-electrolyte mixtures: The depletion interaction and ion-specific effects. *Biophysical Journal*, 95, 1285-1294 (2008).

Cocke, D. L., Wang, H. J. and Chen, J. Interaction between poly(ethylene glycol) and human serum albumin. *Chemical Communications*, 2331-2332 (1997).

Dumetz, A. C., Lewus, R. A., Lenhoff, A. M. and Kaler, E. W. Effects of ammonium sulfate and sodium chloride concentration on PEG/protein liquid#liquid phase separation. *Langmuir*, 24 (18), 10345-10351 (2008).

Finet, S., Vivares, D., Bonnete, F., and Tardieu, A. Controlling biomolecular crystallization by understanding the distinct effects of PEGs and salts on solubility. *Methods in Enzymology*, 368, 105-129 (2003).

George, A., Chiang, Y., Guo, B., Arabshahi, A., Cai, Z., and Wilson, W. W. Second virial coefficient as predictor in protein crystal growth. *Macromolecular Crystallography*, 276, 100-110 (1997).

Haas, C., Drenth, J., and Wilson, W. W. Relation between the solubility of proteins in aqueous solutions and the second virial coefficient of the solution. *Journal of Physical Chemistry B*, 103, 2808-2811 (1999).

Hasko, F., Vaszileva, R., and Halasz, L. Solubility of plasma proteins in the presence of polyethylene glycol. *Biotechnology and Bioengineering*, 24, 1931-1939 (1982).

Ingham, K. C. Precipitation of proteins with polyethylene-glycol - characterization of albumin. *Archives of Biochemistry and Biophysics*, 186, 106-113 (1978).

Ingham, K. C. Precipitation of proteins with polyethylene glycol. *Methods in Enzymology*, 182, 301-306 (1990).

Kozer, N., Kuttner, Y. Y., Haran, G., and Schreiber, G. Protein-protein association in polymer solutions: from dilute to semidilute to concentrated. *Biophysical Journal*, 92, 2139-2149 (2007).

Kumar, V., Sharma, V. K. and Kalonia D. S. Effect of polyols on polyethylene glycol (PEG)-induced precipitation of proteins: Impact on solubility, stability and conformation. *International Journal of Pharmaceutics*, 366, 38-43 (2009).

Li, L., Kantor, A., and Warne, N. Prediction of relative polypeptide solubility by polyethylene glycol precipitation. 2007-US11818 (2007).

Mcperson, A. Current approaches to macromolecular crystallization. *European Journal of Biochemistry*, 189, 1-23 (1990).

Middaugh, C. R., Tisel, W. A., Haire, R. N., and Rosenberg, A. Determination of the apparent thermodynamic activities of saturated protein solutions. *Journal of Biological Chemistry*, 254, 367-370 (1979).

Polson, A., Potgieter, G. M., Largier, J. F., Joubert, F. J., and Mears, G. E. F. Fractionation of Protein Mixtures by Linear Polymers of High Molecular Weight. *Biochimica et Biophysica Acta*, 82, 463 (1964).

Schein, C. H. Solubility as a function of protein structure and solvent components. *Biotechnology* 8, 308-317 (1990).

Shaw, K. L., Grimsley, G. R., Yakovlev, G. I., Makarov, A. A., and Pace, C. N. The effect of net charge on the solubility, activity, and stability of ribonuclease Sa. *Protein Science*, 10, 1206-1215 (2001).

Shulgin, I. L., and Ruckenstein, E. Preferential hydration and solubility of proteins in aqueous solutions of polyethylene glycol. *Biophysical Chemistry*, 120, 188-198 (2006).

Stevenson, C. L., and Hageman, M. J. Estimation of recombinant bovine somatotropin solubility by excluded-volume interaction with polyethylene glycols. *Pharmaceutical Research*, 12, 1671-1676 (1995).

Trevino, S. R., Scholtz, J. M., and Pace, C. N. Measuring and increasing protein solubility. *Journal of Pharmaceutical Sciences*, 97, 4155-4166 (2008).



## CHAPTER 6

### EVALUATION OF FLUORESCENCE CORRELATION

### SPECTROSCOPY FOR PROTEIN FORMULATION DEVELOPMENT

#### 1. INTRODUCTION

Protein interactions, which vary according to the solution conditions and the protein concentration, result from two contributions: (i) the excluded volume, which depends only on the protein itself and corresponds to the repulsive interaction due to mutual impenetrability; and (ii) forces either attractive or repulsive between the molecules at distance greater than steric contact, which is conditional on the solutions conditions (Minton, 2006 and 2007). Excluded-volume represents a significant contribution to non-ideality in protein solution because of the large size of protein molecules. In addition, protein molecules are forced to exist in a considerably reduced volume fraction at high concentrations, as the behavior of a protein molecule is affected by the presence of the same other protein molecules. Protein molecules get closer with increasing concentration and the likelihood that a protein molecule interacts with more than one molecule increases.

Changes in protein interactions can be reflected by the formation of protein associates and aggregates. Protein associates differ from protein aggregates, as protein associates correspond to the reversible formation of higher molecular weight species in which monomers in their native conformation are held together by non covalent bonds, whereas protein aggregates refer to the formation of irreversible higher molecular weight species from the non-native monomer (Saluja and Kalonia, 2008). As simplification only the term aggregate will be further used to qualify both species, since they can not be differentiated by the described analytical methods.

An analytical method measuring the propensity of protein aggregation in concentrated protein solution without sample dilution is of interest. One approach could be Fluorescence Correlation Spectroscopy (FCS), which detects any fluctuation in fluorescence intensity in time that is caused by the diffusion of fluorescently labeled molecules in a very small detection volume (Grunwald *et al.*, 2005). It allows the study of molecule diffusion, molecule binding and molecular interactions. The measurement

of protein diffusion time gives information on the molecule size according to the equation 1, presuming that the molecule has a globular form:

$$D = \frac{k_B \cdot T}{6 \pi \cdot \eta \cdot r} \quad (1)$$

where  $k_B$  is Boltzmann's constant,  $T$  is the temperature,  $\eta$  is the intrinsic viscosity and  $r$  is the radius of the globular species. For a globular molecule diffusing in a three dimensional homogeneous liquid, the diffusion coefficient depends on the molecular weight  $M$  as  $M^{-1/3}$  (Elson, 2001). As changes in fluorescence intensity are dominated by uncorrelated noise at high concentrations of fluorescent molecules in the observation volume, FCS measurements are usually practiced in a small detection volume (1 fl) and at low fluorescent molecule concentration (nM or pM range).

The diffusion rate of macromolecules is usually studied with dynamic light scattering (DLS). FCS presents some advantages as compared to DLS: (i) the measurement is simple and fast; (ii) the background intensity is low given that the excitation light is filtered away from the measured fluorescence; (iii) the molecule concentration is reduced since the detection sensitivity is high; (iv) the detection is specific as molecules are fluorescently labeled; (v) two-color detection is possible; and (vi) the use of well-plate reader reduces the sample volume and allows the method automation (Elson, 2004). Given that oligomers are formed of several monomers, they present a higher diffusion time as compared to monomers, due to their larger size, but also a higher brightness per particle because of their higher fluorescent labeling. The relative brightness of particles is proportional to the number of fluorescent molecules in the oligomer, supposing the association of fluorescent molecules does not change their quantum yield.

Fluorescence Intensity Distribution Analysis (FIDA) is a method derived from FCS that just measures instantaneous intensity fluctuations and can provide the distribution of aggregate sizes in a polydisperse mixture. In addition, a dual color intensity analysis permits to increase the method specificity as a simultaneous increase in both fluorescent signals can be distinguished from the increase of only one fluorescent signal (Bieschke *et al.*, 2000), thus distinguishing associates formed due to the presence of a specific dye. Contrary to FCS, FIDA measurements do not depend on the solution viscosity. Moreover the relative brightness of two molecule species must differ theoretically by a factor of 2 to be differentiated by the FIDA method, while their molecular weight must differ by a factor of 5 to be distinguished by their diffusion rate with FCS (Elson, 2004).

Both FCS and FIDA techniques require the fluorescent labeling of protein. As bioconjugation should not disrupt the protein structure and activity,  $\alpha$ -amino and  $\epsilon$ -lysyl amino residues are the main targets in bioconjugation as only a few of these residues are involved in the protein active site (Veronese and Morpurgo, 1999). Alexa<sup>®</sup> dyes are commonly used as fluorescent dyes because of their properties. They show higher quantum yield and are more photostable than their commonly used spectral analogues (e.g. rhodamine 6G or texas red) but also insensitive to pH in the range of 4 to 10 (Panchuk-Voloshina *et al.*, 1999). Moreover, they are available as a succinimidyl form, which can be conjugated with protein primary amines. They are thus expected to bind to the  $\alpha$ -amino and  $\epsilon$ -lysyl amino residues and to preserve the protein structure and activity.

The aim of this work was to evaluate the FCS and FIDA techniques in measuring the formation of protein aggregates. The binding of Alexa<sup>®</sup> dyes and the spiking ratio of labeled to unlabeled proteins were first optimized. Secondly, the FIDA technique was compared to usual analytical methods of detection of protein aggregates.

## 2. MATERIALS AND METHODS

### 2.1. Materials

The humanized monoclonal IgG1 antibody, which was formulated as a 5 mg/ml solution in phosphate buffered saline (PBS), was provided by Boehringer Ingelheim. Alexa<sup>®</sup> succinimidyl ester 488 and Alexa<sup>®</sup> succinimidyl ester 647 were obtained from Molecular Probes (Invitrogen, Paisley, United Kingdom), dimethyl sulfoxide (DMSO), free of water, from Fluka (Buchs, Switzerland), potassium phosphate, sodium chloride and sodium carbonate from Merck (Darmstadt, Germany), sodium phosphate from Riedel-de-Haën (Seelze, Germany), potassium chloride from Caesar & Lorentz (Hilden, Germany) and sodium hydroxide 1N from Prolabo (Fontenay sous Bois, France).

### 2.2. Methods

#### 2.2.1. Binding to Alexa<sup>®</sup> dyes

The IgG1 was dialyzed overnight into PBS pH 7.4 at 4 °C using a 14 kDa MWCO regenerated cellulose dialysis membrane (Karl Roth, Karlsruhe, Germany). After dialysis, the protein concentration was determined spectrophotometrically with an Agilent 8453 instrument (Agilent technology, Waldbronn, Germany) at 280 nm using as extinction coefficient  $1.44 \text{ ml}\cdot\text{mg}^{-1}\cdot\text{cm}^{-1}$  and the IgG1 concentration was adjusted to 1 mg/ml. Alexa<sup>®</sup> 488 and Alexa<sup>®</sup> 647 were dissolved in DMSO to reach a concentration

of 2 mg/ml. For coupling reaction, 2 ml protein solution (1 mg/ml) were added to 200  $\mu$ l 1M sodium carbonate and 10  $\mu$ l dye solution. The sample was incubated 1 h at room temperature (200 rpm on a horizontal shaker). At the end of the incubation, the sample was purified with a PD-10 column (Sephadex<sup>TM</sup> G-25M, GE Healthcare, Buckinghamshire, United Kingdom). The column was equilibrated with 25 ml PBS before adding the sample that was collected in 7 fractions of 500  $\mu$ l. Only the fractions 2 to 6 that contained labeled protein were retained and combined. The degree of labeling was determined spectrophotometrically at 280 nm and 494 nm for Alexa<sup>®</sup> 488 (equations 2 and 3) and 280 nm and 650 nm for Alexa<sup>®</sup> 647 (equations 4 and 5) (Molecular Probes, 2007).

$$[\text{IgG1}] = \frac{(A_{280} - 0.11 \cdot A_{494}) \cdot \text{dilution factor}}{203000} \quad (2)$$

$$\text{Degree of labeling} = \frac{A_{494} \cdot \text{dilution factor}}{71000 \cdot [\text{IgG1}]} \quad (3)$$

$$[\text{IgG1}] = \frac{(A_{280} - 0.03 \cdot A_{650}) \cdot \text{dilution factor}}{203000} \quad (4)$$

$$\text{Degree of labeling} = \frac{A_{650} \cdot \text{dilution factor}}{239000 \cdot [\text{IgG1}]} \quad (5)$$

### 2.2.2. FCS and FIDA measurements and analysis

FCS and FIDA measurements were carried out on an Insight Reader (Evotec Technologies, Düsseldorf, Germany) with dual-color excitation at 488 nm and 633 nm, using a 40X 1.2 NA microscope objective (Olympus, Japan) and a pinhole diameter of 70  $\mu$ m at FIDA setting. Excitation power was 100  $\mu$ W at 488 nm and 150  $\mu$ W at 633 nm. Each sample was measured 5 times during 10 s at room temperature. The fluorescence data were analyzed by autocorrelation analysis using the FCSPPEvaluation software version 2.0 from Evotec technologies whereas fluorescence intensity data were acquired and summed over time intervals of constant length (bins) of 40  $\mu$ s using the Insight Reader software. The frequency of specific combinations of resulting photon counts per bin of Alexa<sup>®</sup> 488 and Alexa<sup>®</sup> 647 was recorded in a 2 dimensional intensity distribution histogram with intensity values from 0 to 255 photons/ bin (Giese *et al.*, 2005).

### **2.2.3. Size exclusion high performance liquid chromatography (SE-HPLC)**

SE-HPLC was performed on a HP 1100 instrument (Agilent Technology, Waldbronn, Germany) in connection with a SWXL guardcolumn and a TSK3000SWXL column (Tosoh Bioscience, Stuttgart, Germany). The mobile phase consisted of 0.05 M sodium dihydrogen phosphate dihydrate and 0.6 M sodium chloride and was adjusted to pH 7.0 with NaOH 2N. The flow rate was 0.5 ml/min, the injection volume 10  $\mu$ l and the UV signal was detected at 280 nm.

### **2.2.4. Turbidity**

Turbidity was measured as photometric absorbance at 350 nm against WFI as blank value in triplicate with a Fluostar Omega microplate reader (BMG Labtech, Offenburg, Germany).

### **2.2.5. Dynamic light scattering**

DLS was performed with a Zetasizer Nano S (Malvern, Herrenberg, Germany) in a non-invasive-backscatter technique at an angle of 173° and at a constant temperature of 25°C with a solution viscosity of 1.2 mPa·s in triplicate.

### **2.2.6. Light obscuration**

Light obscuration measurements were conducted with a PAMAS-SVSS-C Sensor HCB-LD 25/25 (Partikelmess- und Analysensysteme GmbH, Rutesheim, Germany) to quantify particles  $\geq 1 \mu$ m. Three aliquots of 0.3 ml of each sample were analyzed.

## **3. RESULTS AND DISCUSSION**

### **3.1. Optimization of protein binding to Alexa<sup>®</sup> dyes**

The number of fluorescent dye molecules bound per protein molecule influences the protein diffusion behavior and its fluorescent property, modifying its molecular weight and its fluorescent brightness respectively. As FCS is a highly sensitive method, a low binding ratio is required to detect fluorescent protein molecules. Moreover, to better discriminate between low and high molecular weight protein species a low binding ratio is more appropriate. However, considering the relative brightness proportional to the number of fluorescent molecules, the maximum sensitivity of detection is reached less easy. Therefore, the labeling procedure had to be optimized.

The quantity of free dye remaining in solution was assessed by FCS. After determination of the diffusion time of each dye alone, the diffusion time of the labeled IgG1 was fitted with a 2 component model of the fluorescence fluctuation autocorrelation function. Alexa<sup>®</sup> 488 and Alexa<sup>®</sup> 647 had a diffusion time of 190 and 290  $\mu$ s respectively in PBS whereas IgG1-Alexa<sup>®</sup> 488 and IgG1-Alexa<sup>®</sup> 647 had a diffusion time of 1150 and 1400  $\mu$ s. After two purification steps with a PD-10 column, less than 10 % of free dye Alexa<sup>®</sup> 488 and Alexa<sup>®</sup> 647 remained in solution, which was an acceptable quantity to realize FCS measurements. Increasing the number of purification steps did not further remove free dye but diminished the protein recovery because of the sample dilution.

Alexa <sup>®</sup>	Dye Quantity ( $\mu$ g)	Degree of Labeling
647	200	4.1
	50	1.7
	20	0.6
	20	0.7
488	200	4.4
	20	0.8
	20	0.6
	20	0.6

Table VI-1: Degree of labeling of IgG1 as a function of the Alexa<sup>®</sup> quantity used for the binding reaction.

The degree of protein labeling was determined spectrophotometrically after purification. Only 20  $\mu$ g dye were needed to reach a labeling ratio of one protein molecule to one dye molecule (Table VI-1), which was reproducible for both dyes. This ratio was considered optimal for the FIDA studies as the measured intensity was about 25 photons / bin with a 10 nM IgG1 solution. As the maximum intensity was 250 photons / bin, a 10 fold increase in intensity could be measured. Thus, based on a signal intensity proportional to the number of fluorescent dyes, oligomers containing up to 10 monomers could be detected.

## 3.2. Evaluation of the FIDA method for the screening of protein formulations

### 3.2.1. Optimization of the spiking ratio

Since only fluorescent molecules in the pM or nM concentration range can be detected with the FCS techniques, concentrated solution of labeled IgG1 molecules can not be analyzed. Instead, labeled IgG1 is spiked to unlabeled IgG1. The spiking ratio between unlabeled and labeled molecules should be adjusted to reach a good signal intensity of the initial monomer species but also to detect aggregates of high intensity. Thus, to optimize the spiking ratio, a 20 mg/ml IgG1 solution in 5 mM sodium phosphate buffer at pH 6.2 that was spiked with the two differently labeled IgG1 at a molar ratio of 5000:1 (unlabeled: labeled) was stressed 30 min at 65 °C. The initial and stressed solutions were measured directly with the FIDA method (i) at the spiking ratio of 5000:1; and (ii) after dilution with the initial IgG1 solution having a 20 mg/ml concentration to achieve a final ratio of 25000:1.

The intensity of both dyes was measured simultaneously and was represented on the x axis of the fluorescence histogram for Alexa<sup>®</sup> 488 and on the y axis for Alexa<sup>®</sup> 647. The maximal intensity that could be detected was 250 photons / bin. According to the spiking ratio the initial intensity level varied. At a spiking ratio of 5000:1 (IgG1: IgG1-Alexa) Alexa<sup>®</sup> 488 showed an intensity of 50 photons / bin, while Alexa<sup>®</sup> 647 had a higher intensity of about 75 photons / bin (Fig. VI-1A). The Alexa<sup>®</sup> 647 intensity distribution presented some spots in the intensity range of 75 to 250 photons / bin, indicating the presence of aggregates between IgG1-Alexa<sup>®</sup> 647 molecules. Based on an intensity level proportional to the number of fluorescent molecules, only aggregates composed of up to 5 monomers of IgG1-Alexa<sup>®</sup> 488 and 3 monomers of IgG1-Alexa<sup>®</sup> 647 could be detected under those experimental conditions. After the thermal stress, the formation of aggregates could be seen since intensity spots close to the diagonal in the middle field of the diagram reflected the presence of both labeled proteins in a newly formed aggregate (Fig. VI-1B). The intensity of Alexa<sup>®</sup> 488 increased and was distributed between 50 and 200 photons / bin, revealing the formation of higher molecular weight species composed of 2 up to 4 IgG1-Alexa<sup>®</sup> 488 monomers, whereas the intensity of Alexa<sup>®</sup> 647 was focused between 75 and 150 photons / bin, corresponding to the presence of 1 to 2 IgG1-Alexa<sup>®</sup> 647 monomers.

More diluted sample to 25000:1 exhibited an initial intensity level for both dyes of 25 photons / bin (Fig. VI-1C). Although a higher dilution of the samples theoretically might allow for a more sensitive detection of brighter species, no higher molecular weight aggregates containing both labels in the diagonal area could be found after thermal

stress and dilution (Fig. VI-1D). But the formation of aggregates became evident by the displacement of the Alexa<sup>®</sup> 647 intensity towards the middle field of the diagram. Nevertheless, increasing the spiking ratio decreased the labeled protein concentration and reduced the likelihood that labeled molecules meet. The interpretation of the molecular composition became more difficult as the displacement to higher Alexa<sup>®</sup> 488 intensity was small. Overall, both dilution levels the formation of associates / aggregates could be shown. Even though the spiking ratio of 25000:1 offered theoretically a better discrimination in associate/ aggregate size, the data interpretation was more difficult and gave less information than at the spiking ratio of 5000:1.

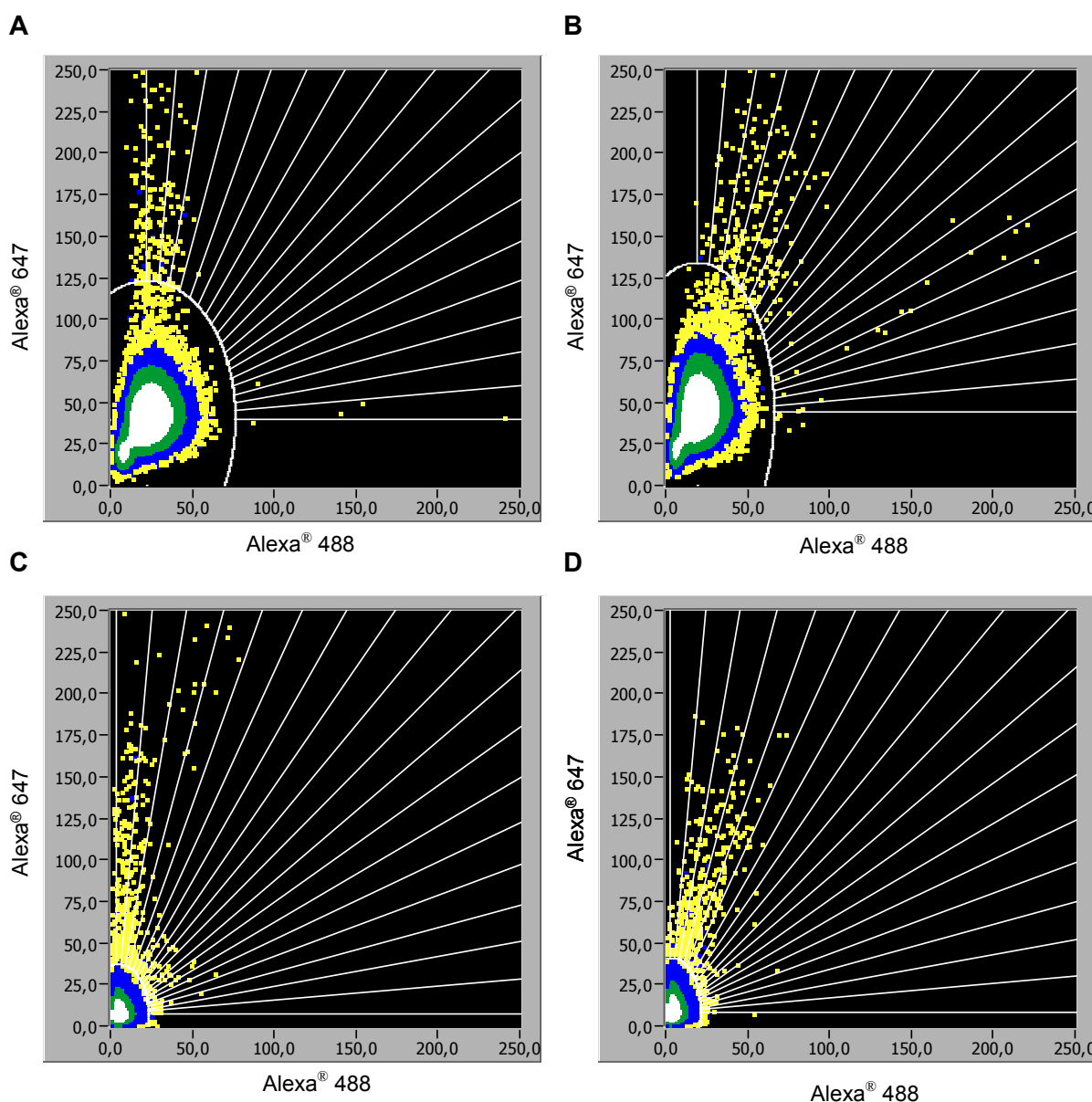


Fig. VI-1: Dual-color fluorescence histograms of IgG1-Alexa<sup>®</sup> 488 and IgG1-Alexa<sup>®</sup> 647 at a spiking ratio of 5000:1 in the initial IgG1 solution (A) and in the stressed IgG1 solution (B), and at a spiking ratio of 25000:1 in the initial IgG1 solution (C) and in the stressed IgG1 solution (D). The fluorescence intensity (photons / bin) of Alexa<sup>®</sup> 488 and Alexa<sup>®</sup> 647 was represented on the x axis and on the y axis respectively.



### 3.2.2. Comparison of FCS to other analytical methods

After the thermal stress at 65 °C during 30 min applied for the FCS tests, the solution turbidity increased from 54 mOD to 341 mOD revealing substantial formation of insoluble aggregates (Table VI-2). This turbidity increase was reflected by a raise in cumulative particle amount in light obscuration (Fig. VI-2). In addition, SE-HPLC revealed the formation of soluble aggregates, dimers and small oligomers, corresponding to 23 % of the total soluble protein species. DLS confirmed the formation of aggregates, as after thermal stress IgG1 monomer, which presented a diameter of 8 nm, represented only 94 % of the volume. The typical hydrodynamic diameter ( $d_H$ ) of an IgG1 is approximately 11 nm (Bermudez and Forciniti, 2004). However, the  $d_H$  of an IgG2, that was measured at low ionic strength (4 mM), varied between 4 to 14 nm according to solution pH (4.0 to 9.0) and protein concentration (4 to 12 mg/ml) (Saluja *et al.*, 2007). Below the protein's pI,  $d_H$  decreased with increasing protein concentration, reaching e.g. 9 nm at a concentration of 12 mg/ml. Thus, the small  $d_H$  of IgG1 measured was related to the protein concentration and protein charge. A second protein species having an average diameter of 44 nm appeared, corresponding to IgG1 aggregates. This aggregate population was heterogeneous as its peak had a width of 16 nm.

	A350 (mOD)	Aggregates (%)
initial solution	54 ± 3	0.7 ± 0.0
stressed solution (65 °C/ 30 min)	341 ± 4	22.8 ± 1.7

Table VI-2: Turbidity and soluble aggregate content of IgG1 solutions before and after thermal stress (65 °C/ 30 min).

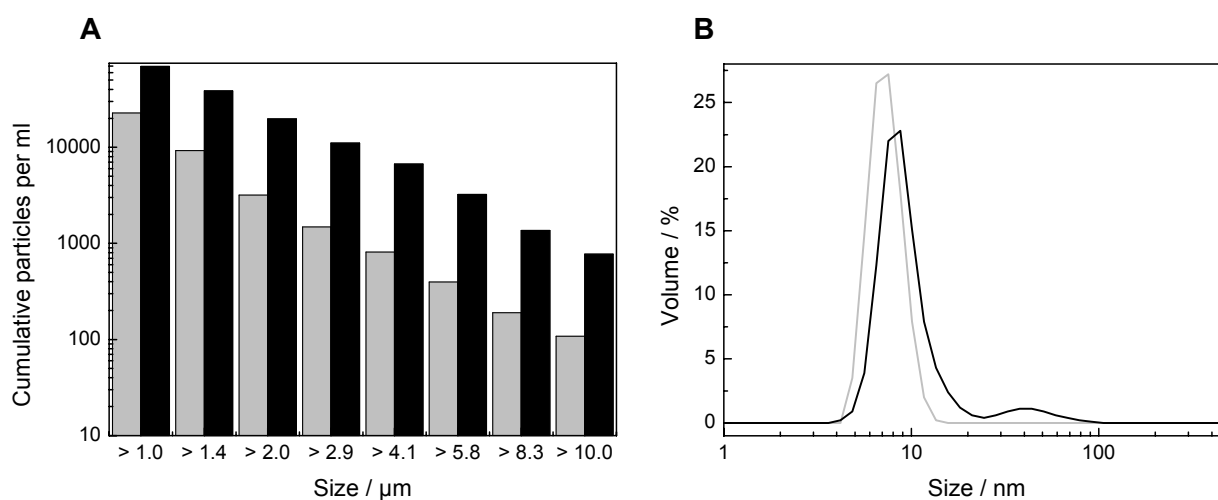


Fig. VI-2: Particle size distribution of IgG1 solutions before (grey) and after (black) thermal stress (65 °C/ 30 min) measured by light obscuration (A) and DLS (B).

Thus, those results obtained by turbidity, SE-HPLC, light obscuration and DLS confirmed the results seen by FIDA. The thermal stress induced formation of soluble and insoluble protein aggregates. The insoluble aggregates that had a bigger size than the soluble ones could be detected by turbidity and light scattering, whereas the heterogeneous soluble protein aggregates could be analyzed by FIDA, SE-HPLC and DLS. Obviously, the FIDA method did not improve the detection of aggregates as compared to the other analytical methods, but allowed analysis in a small sample volume.

## 4. CONCLUSIONS

FCS was developed for analysis of solutions containing low protein concentration, but the detection of soluble protein aggregates in concentrated protein solution was feasible. Studying protein solution having a concentration of 20 mg/ml, species containing 2 to 6 IgG1 oligomers were detectable with the FIDA technique. The major difficulty of the method lied in the adjustment of the spiking ratio between unlabeled and labeled proteins that conditioned the detection limit of oligomers. FIDA presented some advantages as compared to SE-HPLC and DLS as the sample volume was reduced to 20  $\mu$ l and measurement did not need any sample dilution, was quick and automatable. Furthermore changes in solution viscosity did not interfere with the FIDA measurements, contrary to FCS and DLS, and the molecule size could be estimated even if it was in a limited area. Nevertheless, FIDA required labeling as preliminary experimental step and could not differentiate protein associates from protein aggregates. Moreover, the FCS / FIDA instrumentation remains expensive. This evaluation was based on the use of a 20 mg/ml protein solution. The study of highly concentrated protein solution remains a challenge.

## 5. REFERENCES

Bermudez, O., and Forciniti, D. Aggregation and denaturation of antibodies: a capillary electrophoresis, dynamic light scattering, and aqueous two-phase partitioning study. *Journal of Chromatography B*, 807, 17-24 (2004).

Bieschke, J., Giese, A., Schulz-Schaeffer, W., Zerr, I., Poser, S., Eigen, M., and Kretzschmar, H. Ultrasensitive detection of pathological prion protein aggregates by dual-color scanning for intensely fluorescent targets. *Proceedings of the National Academy of Sciences*, 97, 5468-5473 (2000).

Elson, E. L. Fluorescence correlation spectroscopy measures molecular transport in cells. *Traffic*, 2, 789-796 (2001).

Elson, E. L. Quick tour of fluorescence correlation spectroscopy from its inception. *Journal of Biomedical Optics*, 9, 857-864 (2004).

Giese, A., Bader, B., Bieschke, J., Schaffar, G., Odoy, S., Kahle, P. J., Haass, C., and Kretzschmar, H. Single particle detection and characterization of synuclein co-aggregation. *Biochemical and Biophysical Research Communications*, 333, 1202-1210 (2005).

Grunwald, D., Cardoso, M. C., Leonhardt, H., and Buschmann, V. Diffusion and binding properties investigated by Fluorescence Correlation Spectroscopy (FCS). *Current Pharmaceutical Biotechnology*, 6, 381-386 (2005).

Minton, A. P. Macromolecular crowding. *Current Biology*, 16, R269-R271 (2006).

Minton, A. P. Static light scattering from concentrated protein solutions, I: General theory for protein mixtures and application to self-associating proteins. *Biophysical Journal*, 93, 1321-1328 (2007).

Molecular Probes. Amine reactive Probes, Technical note MP 00143 (2007).

Panchuk-Voloshina, N., Haugland, R. P., Bishop-Stewart, J., Bhalgat, M. K., Millard, P. J., Mao, F., Leung, W. Y., and Haugland, R. P. Alexa dyes, a series of new fluorescent dyes that yield exceptionally bright, photostable conjugates. *Journal of Histochemistry & Cytochemistry*, 47, 1179-1188 (1999).

Saluja, A., Badkar, A., Zeng, D. L., Nema, S., and Kalonia, D. S. Ultrasonic storage modulus as a novel parameter for analyzing protein-protein interactions in high protein concentration solutions: correlation with static and dynamic light scattering measurements. *Biophysical Journal*, 92, 234-244 (2007).

Saluja, A., and Kalonia, D. S. Nature and consequences of protein-protein interactions in high protein concentration solutions. *International Journal of Pharmaceutics*, 358, 1-15 (2008).

Veronese, F. M., and Morpurgo, M. Bioconjugation in pharmaceutical chemistry. *Il Farmaco*, 54, 497-516 (1999).

## CHAPTER 7

### SUMMARY

Protein-protein interactions control the physical properties of proteins in solution such as solubility, association / aggregation and solution viscosity. The interactions are mainly governed by weak forces comprising the excluded volume, solvation and electrostatic interactions. The individual contribution varies with the protein concentration and the solute composition. Various analytical methods can be used to test the parameters. According to the literature, measuring the osmotic second virial coefficient ( $B_{22}$ ) enables the evaluation of protein crystallization, solubility, colloidal stability and viscosity.  $B_{22}$  characterizes the strength and the direction of the interactions between two protein molecules of the same kind in solution. One of the most promising methods to analyze those interactions consists of self-interaction chromatography (SIC) as it combines a rapid measurement and a reduction of protein consumption.

The  $B_{22}$  profile of two proteins was determined via SIC. Lysozyme was chosen as protein of reference because of its broad utilization in literature, whereas an IgG1 was studied as therapeutic protein model. SIC measures the interactions between native proteins in solution and native like immobilized protein, since no modification of the structure of both protein models was detected after their immobilization on chromatography particles. SIC was successfully implemented as screening method of lysozyme formulations. Variations of  $B_{22}$  were reported by changing pH or ionic strength as well as by addition of sugars or polyols. Those variations reflected changes in protein interactions, especially electrostatic and solvation forces. Moreover, variations in  $B_{22}$  were correlated to changes in protein solubility. Thus,  $B_{22}$  was predictive of solution solubility.

The formation of protein aggregates frequently involves partially unfolded protein species. Measuring the interactions between unfolded lysozyme species online at 80 °C via SIC demonstrated high attractive interactions, probably due to an increase of hydrophobic interactions and electrostatic screening. The increase in attractive lysozyme interactions under folded and unfolded states corresponded to a decrease in formulation stability assessed by thermal stress as well as by stirring stress.

The SIC method was further successfully adapted to the therapeutic protein model. Small variations in  $B_{22}$  values were measurable under different physiologically relevant formulation parameters. At all the tested conditions,  $B_{22}$  remained positive indicating that repulsive interactions were favored in all the formulation systems tested. Formulation parameters having the most impact on  $B_{22}$  of IgG1 were pH and ionic strength. The buffer species exhibited an influence only at low ionic strength whereas salt and amino acid addition played a role at higher concentration. High NaCl concentration screened the repulsive interactions, whereas high amino acid concentrations maintained or increased repulsive interactions.

Increasing  $B_{22}$  values corresponded to an eased IgG1 concentration process for the different buffer formulations tested. Moreover, increasing  $B_{22}$  values reflected a decrease of solution viscosity. IgG1 stability was tested at two different concentrations by thermal stress at 40 °C. At low protein concentrations (20 mg/ml), the 5 mM histidine formulation presenting the best  $B_{22}$  value showed the best stability, once its chemical instability was controlled by EDTA addition. Regarding the protein stability at high concentration (170 mg/ml), all the tested formulations showed comparable stability. Only pH had a significant influence on protein stability. The high protein stability could result from the self-buffering action of monoclonal antibodies and the macromolecular crowding effect at high protein concentration. Obviously, IgG1 stability was protein concentration dependent, reflecting the impact of concentration on the strength and the nature of protein-protein interactions in solution.

The protein precipitation method by PEG was tested as an alternative method to determine or rank protein solubility. Depletion interaction occurred by addition of PEG to IgG1 solution, resulting in IgG1 precipitation. As described in the literature, the protein concentration remaining in solution was proportional to the PEG concentration. Extrapolation of protein solubility to zero PEG concentration could not provide meaningful apparent solubility values as the resulting numbers were in various cases implausibly high and in others not meaningful. An alternative interpretation method was established providing a ranking in four solubility classes according to the following parameters: (i) the PEG 6000 concentration required to reduce the IgG1 concentration in solution to 0.1 mg/ml; and (ii) if a reduction to 0.1 mg/ml could not be reached, the IgG1 concentration in solution in the presence of 18 % PEG 6000.

Furthermore, fluorescence correlation spectroscopy (FCS) / fluorescence intensity distribution analysis (FIDA) was tested to determine protein associate/ aggregate formation. This method required protein labeling as first experimental step. Protein soluble aggregates were detected in concentrated protein solution. The major difficulty of the method lied in the adjustment of the spiking ratio between

unlabeled and labeled proteins that conditioned the detection limit of oligomers. Although the FIDA technique presented some advantages such as low sample volume, viscosity independence and high speed measurement, the method did not show enough sensitivity. Moreover, FIDA could not differentiate protein associates from protein aggregates.

Hence,  $B_{22}$  was shown to be a promising screening method of protein formulation parameters. This method evaluates the strength of protein-protein interactions in solution, which condition protein solubility, protein colloidal stability as well as solution viscosity. Moreover, SIC allows rapid determination of  $B_{22}$  under high throughput conditions using automated systems. However,  $B_{22}$  can only be used to compare different formulation conditions, since it does not allow a direct quantification of protein solubility, viscosity or aggregate formation. The alternative analytical methods, PEG precipitation and FCS for the determination of protein solubility and protein association/aggregation respectively, did not significantly improve formulation screening as compared to  $B_{22}$  via SIC.

## **POSTERS AND PUBLICATIONS ASSOCIATED WITH THIS WORK**

### **Posters**

Le Brun, V., Schultz-Fademrecht, T., Muehlau, S., Garidel, P., Friess, W. Protein formulation screening using self-interaction chromatography. 6<sup>th</sup> World Meeting on Pharmaceutics, Biopharmaceutics and Pharmaceutical technology, Barcelona, Spain (2008).

Le Brun, V., Schultz-Fademrecht, T., Muehlau, S., Garidel, P., Friess, W. Evaluation of a SIC method to measure protein self-interactions in protein formulation. Colorado Protein Stability Conference, Breckenridge, USA (2007).

### **Articles**

Le Brun, V., Friess, W., Schultz-Fademrecht, T., Muehlau, S., Garidel, P. Insights in lysozyme - lysozyme self-interactions as assessed by the osmotic second virial coefficient: impact for physical protein stabilization. *Biotechnology Journal*, 4 (9), 1305-1319 (2009).

Le Brun, V., Friess, W., Bassarab, S., Muehlau, S., Garidel, P. A critical evaluation of self-interaction chromatography as a predictive tool for the assessment of protein-protein interactions in protein formulation development: a case study of a monoclonal antibody, *European Journal of Pharmaceutics and Biopharmaceutics* (submitted).

Le Brun, V., Friess, W., Bassarab, S., Garidel, P. Correlation of protein-protein interactions as assessed by affinity chromatography with colloidal protein stability: A case study with lysozyme. *Pharmaceutical Development and Technology*, DOI: 10.1080/10837450903262074 (2009)

# CURRICULUM VITAE

## Virginie Le Brun

### Personal Data

---

Date of Birth	November 7, 1978
Place of Birth	Le Mans, France
Nationality	French

### Education

---

Since 11/2005	PhD thesis, Department of Pharmaceutical Technology and Biopharmaceutics, Ludwig-Maximilians-University, Munich, Germany
2004-2005	Master of science in "Innovation en pharmacotechnie et biopharmacie", Châtenay-Malabry University, France
2002-2003	Master of science in "Qualité totale et biotechnologies", Angers University, France
1996-2004	Graduation in Pharmacy, industrial specialization, Angers University, France
1993-1996	High School, Lycée Bellevue, Le Mans, France

### Professional and additional experience

---

Since 02/2009	Post-doc, Process Science / Pharma Development, Boehringer Ingelheim Pharma GmbH & Co. KG, Biberach, Germany
12/2004-07/2005	Practical training, Department of Pharmaceutical Technology - INSERM U646 "Ingénierie de la vectorisation particulaire", Angers University, France
03/2003-11/2003	Internship, Department of Pharmaceutical Development, Schering AG, Berlin, Germany
07/2002-09/2002	Practical training, Pharmacy, Charité Hospital, Berlin, Germany
05/2001-07/2001	Erasmus exchange program, Department of Pharmaceutical Technology, Freie Universität Berlin, Germany